

AD-A023 537

PROPAGATION MODELING AND ANALYSIS FOR HIGH ENERGY
LASERS

Science Applications,
Incorporated

Prepared for:

Naval Surface Weapons Center

April 1975

DISTRIBUTED BY:

NTIS

National Technical Information Service
U. S. DEPARTMENT OF COMMERCE

KEEP UP TO DATE

Between the time you ordered this report—which is only one of the hundreds of thousands in the NTIS information collection available to you—and the time you are reading this message, several *new* reports relevant to your interests probably have entered the collection.

Subscribe to the **Weekly Government Abstracts** series that will bring you summaries of new reports as soon as they are received by NTIS from the originators of the research. The WGAs are an NTIS weekly newsletter service covering the most recent research findings in 25 areas of industrial, technological, and sociological interest—invaluable information for executives and professionals who must keep up to date.

The executive and professional information service provided by NTIS in the **Weekly Government Abstracts** newsletters will give you thorough and comprehensive coverage of government-conducted or sponsored re-

search activities. And you'll get this important information within two weeks of the time it's released by originating agencies.

WGA newsletters are computer produced and electronically photocomposed to slash the time gap between the release of a report and its availability. You can learn about technical innovations immediately—and use them in the most meaningful and productive ways possible for your organization. Please request NTIS-PR-205/PCW for more information.

The weekly newsletter series will keep you current. But *learn what you have missed in the past* by ordering a computer **NTISearch** of all the research reports in your area of interest, dating as far back as 1964, if you wish. Please request NTIS-PR-186/PCN for more information.

WRITE: Managing Editor
5285 Port Royal Road
Springfield, VA 22161

Keep Up To Date With SRIM

SRIM (Selected Research in Microfiche) provides you with regular, automatic distribution of the complete texts of NTIS research reports *only* in the subject areas you select. SRIM covers almost all Government research reports by subject area and/or the originating Federal or local government agency. You may subscribe by any category or subcategory of our WGA (**Weekly Government Abstracts**) or **Government Reports Announcements and Index** categories, or to the reports issued by a particular agency such as the Department of Defense, Federal Energy Administration, or Environmental Protection Agency. Other options that will give you greater selectivity are available on request.

The cost of SRIM service is only 45¢ domestic (60¢ foreign) for each complete

microfiched report. Your SRIM service begins as soon as your order is received and processed and you will receive biweekly shipments thereafter. If you wish, your service will be backdated to furnish you microfiche of reports issued earlier.

Because of contractual arrangements with several Special Technology Groups, not all NTIS reports are distributed in the SRIM program. You will receive a notice in your microfiche shipments identifying the exceptionally priced reports not available through SRIM.

A deposit account with NTIS is required before this service can be initiated. If you have specific questions concerning this service, please call (703) 451-1558, or write NTIS, attention SRIM Product Manager.

This information product distributed by

NTIS

U.S. DEPARTMENT OF COMMERCE
National Technical Information Service
5285 Port Royal Road
Springfield, Virginia 22161

UNCLASSIFIED

SECURITY CLASSIFICATION OF THIS REPORT (If different from that of the report)

REPORT DOCUMENTATION PAGE

READ INSTRUCTIONS
BEFORE COMPLETING FORM

1. REPORT NUMBER

2. GOVT. ACCESSION NO.

3. DOCUMENT CATALOG NUMBER

ADA023537

4. TITLE (and Subtitle)

Propagation Modeling and Analysis for High Energy Lasers

5. TYPE OF REPORT & PERIOD COVERED

Final Report
July 1974 - March 1975

6. PERFORMING ORG. REPORT NUMBER

SAI-74-629-WA

8. CONTRACT OR GRANT NUMBER(s)

N60921-75-C-0007

7. AUTHOR(s)

L. N. Peckham
P. R. Carlson

R. T. Liner
C. W. Wilson

9. PERFORMING ORGANIZATION NAME AND ADDRESS

Science Applications, Inc.
1911 North Myer Drive
Arlington, Virginia 22209

10. PROGRAM ELEMENT, PROJECT, TASK AREA & WORK UNIT NUMBERS

11. CONTROLLING OFFICE NAME AND ADDRESS

Naval Surface Weapons Center
White Oak Laboratory
White Oak, Silver Spring, Maryland 20910

12. REPORT DATE

April 1975

13. NUMBER OF PAGES

14. MONITORING AGENCY NAME & ADDRESS (if different from Controlling Office)

15. SECURITY CLASS. (of this report)

Unclassified

15a. DECLASSIFICATION/DOWNGRADING SCHEDULE

16. DISTRIBUTION STATEMENT (of this Report)

Approved for public release; distribution unlimited.

17. DISTRIBUTION STATEMENT (of the abstract entered in Block 20, if different from Report)

IS SUBJECT TO CHANGE

18. SUPPLEMENTARY NOTES

REPRODUCED BY
NATIONAL TECHNICAL
INFORMATION SERVICE
U.S. DEPARTMENT OF COMMERCE
SPRINGFIELD, VA. 22161

19. KEY WORDS (Continue on reverse side if necessary and identify by block number)

High energy lasers
Lower beams
Propagation codes
Continuous wave

20. ABSTRACT (Continue on reverse side if necessary and identify by block number)

This report analyzes simplified propagation codes and recommends improved models for characterizing the propagation of high energy CW laser beams.

DD FORM 13/3

EDITION OF 1 NOV 65 IS OBSOLETE
(11-71-11-214-50)

UNCLASSIFIED

DECLASSIFICATION OF THIS PAGE (If different from that of the report)

①

PROPAGATION MODELING AND ANALYSIS
FOR HIGH ENERGY LASERS

FINAL REPORT

SAI-74-629-WA

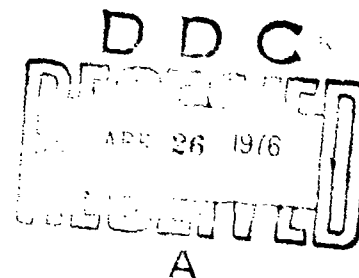
Mr. L.N. Peckham
Mr. P.R. Carlson
Dr. R.T. Liner
Dr. C.W. Wilson

This work was performed under Contract
No. N60921-75-C-0007, July 1974 through
March 1975.

April 1975

SCIENCE APPLICATIONS, INCORPORATED

1911 North Fort Myer Drive, Suite 1200, Arlington, Virginia 22209
(703) 527-7571



DISTRIBUTION STATEMENT A

Approved for public release;
Distribution Unlimited

FOREWORD

This is the final report covering work performed for the Naval Surface Weapons Center under contract N60921-75-C-0007. The purpose of the contract was to analyze simplified propagation codes and recommend improved models for characterizing the propagation of high energy CW laser beams. The work was performed under the direction of Mr. Larry Jobson of NSWC.

This report documents the work performed during the period January-March 1975. It also provides a review of the earlier work (July 1974-January 1975). The earlier work was described in detail in interim reports SAI-74-587-WA (October 1974) and SAI-74-622-WA (January 1975).

The authors wish to express their appreciation to Dr. Tom Tuer of the SAI Ann Arbor office for his development of the multi-line absorption coefficients. We also thank Mrs. T. Peckham for implementing the numerous code modifications.

APPROVED BY	
THIS	DATE
10	10/10/75
BY	
DISTRIBUTION	
DISC	
A	

TABLE OF CONTENTS

<u>SECTION</u>	<u>PAGE</u>
1 INTRODUCTION	1-1
2 A SIMPLIFIED OPTICAL TRAIN MODEL	2-1
2.1 MODEL FORMULATION	2-3
2.1.1 Input Beam	2-3
2.1.2 Aerodynamic Window	2-7
2.1.3 Beam Clipper	2-10
2.1.4 High Power Mirrors	2-14
2.1.5 Beam Expander	2-18
2.1.6 Exit Aperture	2-20
2.2 ASSESSMENT OF OVERALL PERFORMANCE	2-24
2.2.1 Transmitted Power	2-24
2.2.2 Beam Quality	2-26
2.2.3 Beam Jitter	2-29
2.2.4 Beam Divergence	2-29
2.3 SAMPLE CALCULATIONS	2-33
3 CREATION OF SAICOM	3-1
3.1 MODIFICATIONS OF COMBO	3-1
3.1.1 Improvements to Computational Speed and Accuracy	3-2
3.1.2 Beam Quality	3-5
3.1.3 The Optical Train Model	3-6
3.1.4 Multi-Line Propagation	3-8
3.1.5 Modification of Turbulence and Jitter to Include Short and Long Term Effects	3-10
3.1.6 Far-Field Intensity Distribution	3-15
3.1.7 Calculation of Optimum Power	3-16
3.1.8 Miscellaneous Modifications	3-17

TABLE OF CONTENTS (CONT'D)

<u>Section</u>	<u>Page</u>
3.1.8.1 Variable Turbulence in Blooming Computations	3-17
3.1.8.2 Extinction Calculations in Blooming Integral	3-18
3.1.8.3 Power Variation	3-18
3.1.8.4 Deletion of Weight and Volume Calculations	3-18
3.1.9 Summary of Equations	3-19
3.2 A USER'S GUIDE TO SAICOM	3-20
3.2.1 OPTRAIN	3-22
3.2.2 ATM	3-25
3.2.3 BB	3-27
3.2.4 Input Data	3-27
4 SUMMARY OF TASKS I-IV	4-1
4.1 REVIEW OF TASK I. CODE COMPARISONS	4-1
4.2 REVIEW OF TASK II. BEAM SHAPE AND DISPLACEMENT	4-4
4.3 REVIEW OF TASK III. BEAM QUALITY	4-5
4.4 REVIEW OF TASK IV. BEAM TRUNCATION AND OBSCURATION	4-6
5 CONCLUSIONS	5-1
APPENDIX A Molecular Absorption of DF Laser Radiation	A-1
APPENDIX B SAICOM	B-1
REFERENCES	R-1

LIST OF FIGURES

<u>FIGURE</u>		<u>PAGE</u>
2.1	Typical Optical Train	2-4
2.2	Comparison of Input Beam Quality Specifications	2-8
2.3	Diffraction Spillover Losses	2-11
2.4	Beam Quality Loss Due to Central Obscuration in Terms of θ and W_t/l_0	2-21
2.5	Effects of Exit Aperture Temperature Fluctuations on Beam Jitter	2-25
2.6	Simplified Optical Train Employed in Defocus Calculations	2-31
2.7	Schematic of Optical Train for Sample Calculations	2-34
2.8	Results of Sample Calculations	2-39
3.1	Variations in Elements of the Blooming Calculations	3-4
3.2	α_1 as a Function of Altitude	3-11
3.3	α_2 as a Function of Altitude	3-12
3.4	α_3 as a Function of Altitude	3-13
3.5	$\alpha_{\text{RESULTANT}}$ as a Function of Altitude	3-14
3.6	SAICOM Flow Diagram	3-21
3.7	OPTRAIN Flow Diagram	3-24
3.8	ATM Flow Diagram	3-25
3.9	BB Flow Diagram	3-28
A-1	Water Concentration Profiles for Five Model Atmospheres and Analytic Fit	A-5
A-2	Demonstration of the Effect of Scaling to Account for Various Atmospheric Water Concentrations - P ₂ (8) DF Laser (a) No Scaling (b) With Scaling	A-6
A-3	Laser Propagation-Altitude Function Type A: Dominated by Water at Low Altitudes but with Underlying Absorption Lines which become Important at High Altitudes	A-8

LIST OF FIGURES

<u>FIGURE</u>		<u>PAGE</u>
A-4	Laser Propagation-Altitude Function Type B: Dominated by Water at Low Altitudes but with Underlying Absorption Lines which become Important at High Altitudes	A-9
A-5	Laser Propagation-Altitude Function Type C: Dominated by Water at Low Altitudes but with Underlying Absorption Lines which become Important at High Altitudes	A-10
A-6	Contributors to the Molecular Absorption of the $P_2(8)$ DF Line (Midlatitude Summer, Sea Level).	A-11
A-7	Contributors to the Molecular Absorption of the $P_2(9)$ DF Line (Midlatitude Summer Sea Level)	A-12
A-8	Contributors to the Molecular Absorption of the $P_3(8)$ DF Line (Midlatitude Summer, Sea Level)	A-13
A-9	Least Squares Fit to Type A Laser Lines	A-15
A-10	Least Squares Fit to Type B Laser Lines	A-16
A-11	Least Squares Fit to Type C Laser Lines	A-17

LIST OF TABLES

<u>TABLE</u>		<u>PAGE</u>
2.1	Summary of Beam Expander Transmissions and Obscuration Calculations	2-19
3.1	Beam Quality Parameters	3-7
3.2	SAICON Subroutines	3-23
3.3	Input Parameters	3-29
3.4	Sample Input Form with Default Values	3-34
3.5	Flags	3-36
A-1	List of DF-BDL Lines	A-2
A-2	Coefficients of Least Square Fit	A-14

Section 1

INTRODUCTION

In support of the Systems Analysis Team of the Naval Surface Weapons Center, Science Applications, Inc. (SAI), performed a series of tasks designed to develop a better understanding of the modeling alternatives available to laser systems analysts and to assist in the continual improvement of the NGL Engagement Code (NOLEC). Emphasis was placed on the resolution of propagation issues of interest to systems analysts. The tasks involved quantitative comparison of simplified HEL propagation codes used by DOD analysts, clarification of the beam quality problem, development of beam distortion and displacement models, development of a simplified optical train model, and expansion and improvement of the AFHL COMBO code.

The work was divided into six tasks. The first four tasks are reviewed in this report (Section 4), but are covered more extensively in interim reports (References 1 and 2):

First Interim Report - July-September 1974,

SAI-74-587-WA, October 1974 (Reference 1)

Task 1. Quantitative Comparison of
Simplified Propagation Codes

Task 3. Beam Quality Modeling.

Second Interim Report - September 1975-

January 1975, SAI-74-622-WA, January 1975
(Reference 2)

Task 2. Beam Shape and Displacement
Due to Thermal Lensing.

Task 4. Effect of Truncation and
Obscuration on the Far-Field Beam Profile.

Task 5 required the development of a simplified optical train model. This work is described in Section 2 of this report. Task 6 involved modification and extension of the AFWL COMBO code and included the incorporation of models developed in the earlier tasks. The new version of the code was named SAICON. Section 3 describes the modifications and provides a user's guide to SAICON.

Section 2

A SIMPLIFIED OPTICAL TRAIN MODEL

When performing laser application studies, the system analyst all too frequently assumes that the characteristics of the beam leaving the transmitting optic are the same as the characteristics of the beam leaving the laser device without regard for any changes induced by the optical elements and/or components required to get the beam from the laser device to the transmitting optic, i.e., the optical train. It is known, however, that significant changes to the characteristics of the beam do occur as it propagates through the optical train (see for example References 3 and 4). The finite absorptivity of the high power mirrors, clipping and blockage of a portion of the high power beam, and diffraction effects all reduce the available power in the beam at the transmitting optic. In addition the optical quality of the beam is affected by nearly every component or element through changes in the phase and amplitude distribution of the beam. Therefore, if realistic estimates of the performance of candidate laser systems are to be obtained during these application studies, it is important to include the effect of the optical train on the characteristics of the laser beam.

An accurate assessment of the impact of the optical train is a tedious and difficult calculation requiring a wave optics approach and sophisticated analytical tools for modeling each of the elements in the optical train. Obviously these are not very practical for use in systems analysis

application studies in which a large parameter space must be investigated. Therefore, if the effect of the optical train is to be included in such analyses, the development of simple but reasonably accurate models is required.

One such model has been developed by the AFWL (Reference 5) which is used in their simplified propagation code (COMBO). However, its use is somewhat restrictive in that most of the component effects are left for the user to specify. Prescriptions for scaling these effects in terms of system parameters are not given. In addition, the impact of the optical train on the beam quality is assessed in terms of peak intensity reduction. Based on work under this contract, it is felt that an assessment in terms of the far-field power distribution provides a better characterization of the beam quality (see Reference 1 and Section 4.3 of this report).

We have developed a more comprehensive "simplified" optical train model which can be used to estimate the degradation in system performance caused by the optical components required to direct the beam from the laser device to the transmitting optic (i.e., aerodynamic window, mirrors, beam expander, etc.). The intent of the model is not to provide detailed engineering design data but rather to provide the systems analyst with a rapid assessment capability which will allow him to perform more realistic systems analyses of candidate HEL systems. Hence, emphasis is placed on formulating simple but reasonably accurate models for the various factors influencing the performance of the laser system. The approach is similar to that taken by the AFWL in their simplified model but with new additions and modifications to make the model more flexible. The model has been implemented in a subroutine called OPTRAIN and is included in the SAICOM code as described in Section 3 below.

2.1 MODEL FORMULATION

Conceptually, the optical train may be viewed as a "black box" located between the laser device and the transmitting optic. The input to the box is the output beam from the laser. The model operates on this beam according to the number and type of elements in the train, and its output, in the form of certain performance parameters, provides the input to an atmospheric propagation model. The performance parameters are: (1) the power available at the transmitting optic, (2) beam quality, (3) beam divergence, and (4) beam jitter. In addition, the actual diameter of the beam at the exit aperture is computed for use in the propagation model.

The essential features of the model are illustrated in Figure 2.1. The optical elements and components include (1) an aerodynamic window, (2) a beam clipper, (3) several high power mirrors, (4) a beam expander, (5) an exit aperture, and (6) a focusing element for transmitting the beam to the target plane. In most practical cases the beam expander and focusing element are combined into a single telescope. However, it is convenient for the present analysis to separate them into an ideal beam expander which simply expands the beam and a separate element which applies the curvature to the beam phase front for focusing purposes.

2.1.1 Input Beam

Although it is not an optical element or component, the input beam is necessarily an integral part of the model since it has strong influence on the behavior of the rest of the optical train. In order to simplify the analysis of the components in the optical train, it is assumed that the beam from the laser is circular. However, because of

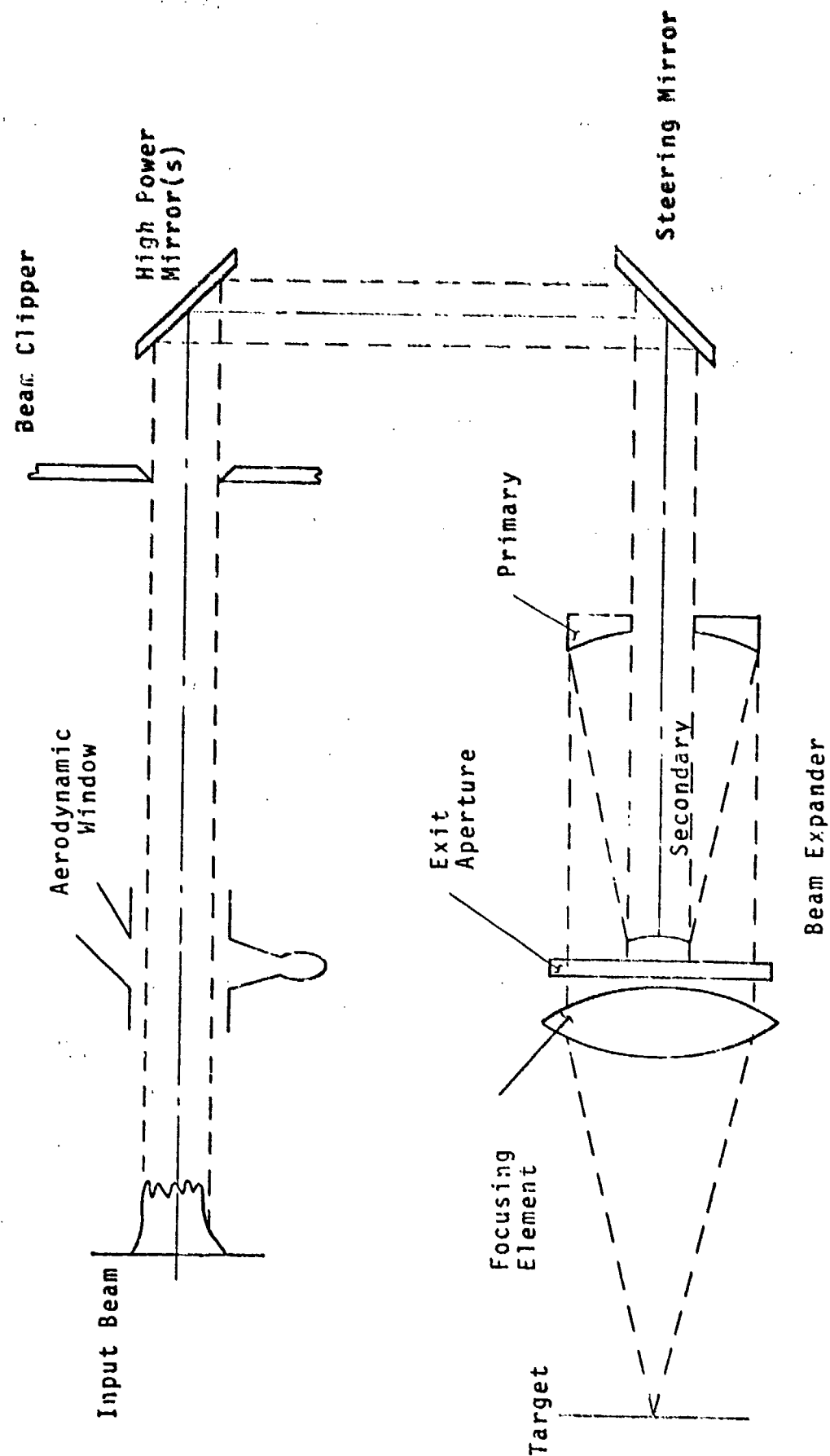


Figure 2.1 Typical Optical Train

the widespread use of unstable resonator configurations to extract power from high power devices, the possibility of a central obscuration in the input beam is incorporated into the model. The inner and outer diameters of the input beam are ϵD_B and D_B respectively. An unobscured input beam profile can be realized by defining $\epsilon = 0$. Other parameters required to specify the input beam are (1) the power in the beam, P_L , (2) the pulse length, Δt , (3) the curvature of the phase front, R_L , and the beam jitter, θ_L .

In order to evaluate the effect the beam has on the high power mirrors in the optical train, it is also necessary to characterize the intensity profile entering the optical train. This is achieved by specifying both the magnitude and scale size of the intensity fluctuations, the magnitude being specified as a fraction of the average intensity ($\Delta I/I_{ave}$) and the scale size as a fraction of the beam diameter (ℓ_I/D_B). Thus the input beam profile may be visualized as having a uniform intensity I_{ave} with fluctuations ΔI superimposed upon this level.

The optical quality of the input beam is specified by a wavelength scaling factor, n_L . Unfortunately, this definition of beam quality does not allow one to easily incorporate the other beam quality degrading factors induced by the various elements of the optical train. Therefore this parameter is converted by the model into an equivalent root-mean-square phase distortion, σ_L .

Two alternative approaches for this conversion were investigated for use in the model. The first approach is to define the equivalent phase distortion so as to match the reduction in the peak intensity, I_p . According to the analysis presented in Reference 6, the peak intensity reduction is (for a gaussian beam containing small scale random phase variations)

$$I_p/I_g = \exp(-\sigma_L^2)$$

where I_g is the ideal on-axis intensity. According to the wavelength scaling definition of beam quality

$$\frac{I_p}{I_g} = \frac{1}{n_L^2}$$

so that

$$\sigma_L = \sqrt{2 \ln(n_L)} \quad (1)$$

It should be noted that this approach is equivalent to the power scaling definition of beam quality and is also the approach taken by the AFWL in their optical system model (Reference 5).

The second approach investigated was to define the equivalent phase distortion to match the power in the "bucket" ($R\lambda/D = 1$) predicted by wavelength scaling. This is given by (Reference 1):

$$P(R\lambda/D) = P_0 \{1 - \exp(-\pi^2/2n_L^2)\}.$$

Again, following the analysis of Reference 4, the power in the bucket for a non-diffraction-limited gaussian beam is given by

$$P(R\lambda/D) = P_0 \exp(-\sigma_L^2) \{1 - \exp(-\pi^2/2)\}$$

assuming all of the quality degradation can be characterized as a scattering loss. Equating these expressions and solving for σ_L yields,

$$\sigma_L = \left\{ -\ln \left[\frac{1 - \exp(-\pi^2/2n_L)}{1 - \exp(-\pi^2/2)} \right] \right\}^{1/2} \quad (2)$$

Intuitively it would seem that both of these approaches should yield approximately equivalent results. Quantitatively however, substantial differences were found. These are illustrated in Figure 2.2 which compares the phase distortion computed from Equations (1) and (2). The phase distortion based on matching the peak intensity reduction is always considerably higher than that based on matching the power-in-the-bucket, e.g., over a factor of 2.5 for a 1.5 times diffraction-limited input beam. The reasons for these differences are not clear. One possible explanation is the equivalence of wavelength and power scaling methods of defining peak intensity reduction. It was found during previous work under this contract (Reference 1) that power scaling was always more pessimistic in its predictions of the beam quality than wavelength scaling. Therefore, matching the peak intensity based on a method that is equivalent to power scaling might be expected to produce more pessimistic results (i.e., higher σ_L) than matching the power-in-the-bucket based on wavelength scaling.

Whatever the reasons for the differences, we recommend the use of Equation (2) because the power-in-the-bucket is a more meaningful measure of laser performance than peak intensity reduction. The latter suffers from its sensitivity to defocusing errors and difficulty in experimental measurement.

2.1.2 Aerodynamic Window

The first component in the optical train is the aerodynamic window isolating the optical cavity of the laser

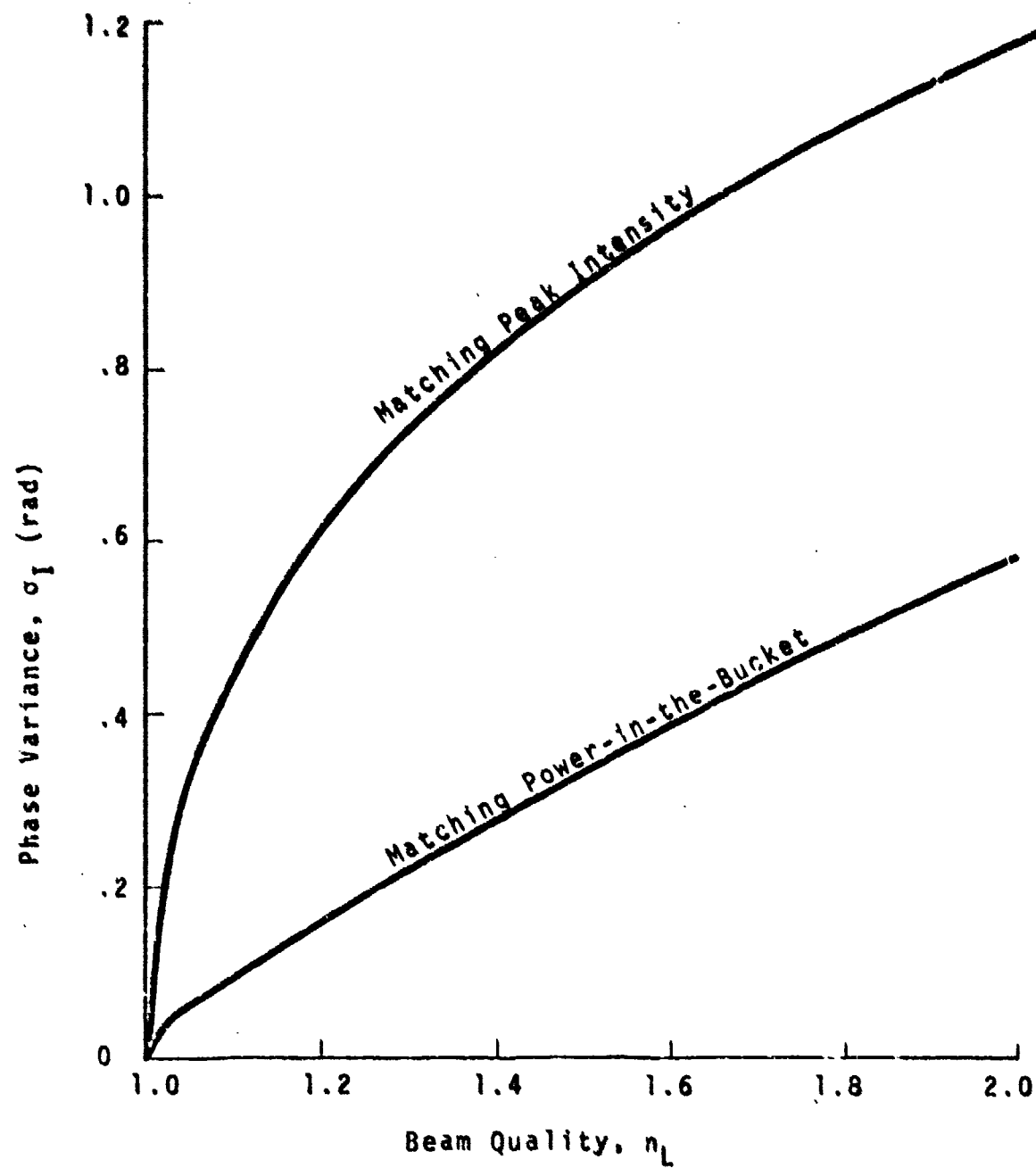


Figure 2.2. Comparison of Input Beam Quality Specifications

from the atmosphere. Basically there are two types of aerodynamic windows currently being considered for HEL applications: (1) focused and (2) unfocused. In both cases, if the window is properly designed, there should be little or no power loss when the beam passes through it. In addition, it is also assumed that no spherical distortion to the phase front will be induced by the aerodynamic window. The shock waves supporting the pressure rise and the turbulence generated by the aerodynamic window will, however, induce a loss in the beam quality. An expression for this loss is given by (Reference 4)

$$\Delta I/I = 2.84 \times 10^{-10} \left(\frac{\Delta \rho}{\rho_s} \frac{D_B}{\lambda} \right)^2$$

where $\Delta \rho$ is density change across the shear layer and ρ_s is a reference density at STP. Again this formulation of beam quality degradation is not convenient for use in the model and is converted into an equivalent phase distortion, σ_{aw}^2 by use of the Strehl formula (Reference 4):

$$\Delta I/I = \sigma_{aw}^2.$$

Solving for the phase distortion yields

$$\sigma_{aw} = 1.69 \times 10^{-5} \left(\frac{D_B}{\lambda} \frac{\Delta \rho}{\rho_s} \right).$$

A typical value of σ_{aw} for a 10 cm beam from a chemical laser ($\lambda = 3.8 \mu\text{m}$), assuming $\Delta \rho/\rho_s = 0.25$ for the density variations, is $\sigma_{aw} = 0.11$ radians. This corresponds to an intensity reduction of $\Delta I/I \approx 1.2\%$.

For the focused aerodynamic window, the beam diameter will typically be very small (<0.1 cm) so that the phase distortion can be neglected, i.e., $\sigma_{aw} \approx 0$.

2.1.3 Beam Clipper

For NEL systems in which the laser device and the pointer/tracker are not closely coupled, a beam clipper or scraper will probably be employed near the pointer/tracker to control the size of the high power beam entering the transmitter. The beam clipper will influence both the power available at the transmitting optic and the beam quality; the latter by limiting the maximum diameter at the transmitting optic.

The loss in power at the beam clipper is due primarily to diffractive spreading of the beam as it propagates between the aerodynamic window and the beam clipper. In general, the diffractive spreading will depend upon the phase and amplitude aberrations in the input beam profile. An accurate assessment of the actual losses requires a detailed calculation involving numerical solutions of the Fresnel diffraction integral or spatial frequency approaches to optical propagation (i.e., Fourier Optics). These techniques are very time consuming and were not considered as viable candidates for the "simplified" model. Instead, an empirical approach based on curve fits of available data in the literature was taken. Unfortunately very little data were available for examination. Only two sources were found (References 4 and 7). The data obtained from these sources are illustrated in Figure 2.3 which shows the variation in power diffracted into the geometric shadow of a uniformly illuminated aperture as a function of the propagation distance from the aperture. The AFWL data were calculated for a one-dimensional beam profile while the HAC (Hughes

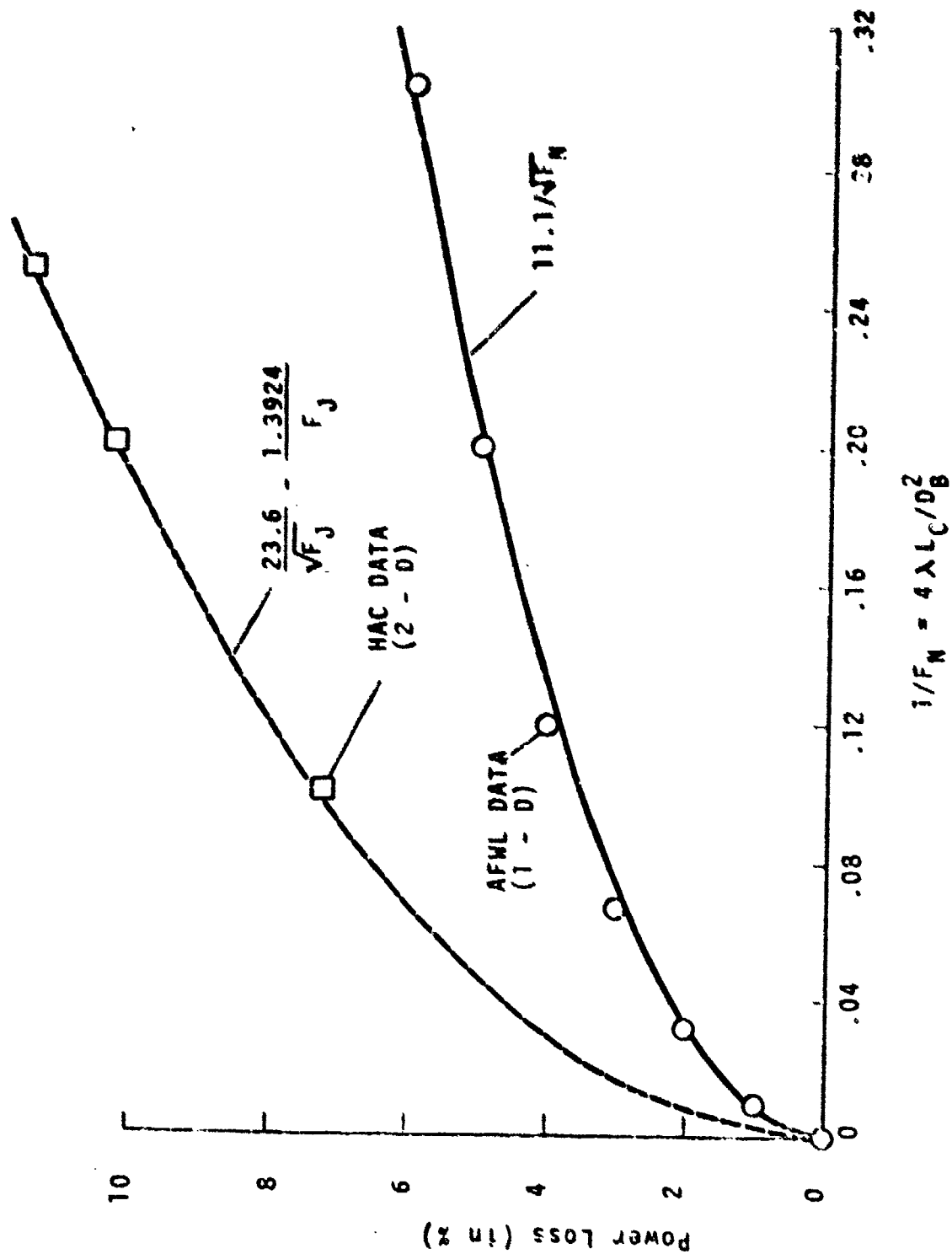


Figure 2.3. Diffractive Spillover Losses

Aircraft Company) calculations were performed for a round beam. Therefore, the data must be adjusted for these differences before a direct comparison can be made.

Intuitively one would expect a factor of two difference between the data based on simple geometrical arguments. For example, a square beam profile would have twice the loss of a one-dimensional profile because of the two additional edges. For a round beam, however, the ratio is not quite as straightforward. Assuming circular symmetry, the fractional power loss is

$$\Delta_{2-0} = \frac{2\pi \int_a^\infty I(\sigma) \sigma d\sigma}{\pi a^2 I_0}$$

where a is the radius of the aperture and I_0 is the initial intensity. The major contribution to the integral occurs near the edge of the aperture. Thus over this region the radius can be taken as being approximately constant ($= a$) and removed from the integral without affecting its value, i.e.,

$$\Delta_{2-0} = \frac{2}{a I_0} \int_a^\infty I(\sigma) d\sigma.$$

For the one-dimensional beam profile the fractional power loss is given by

$$\Delta_{1-0} = \frac{\int_a^\infty I(x) dx (1)}{a I_0 (1)}$$

so that if one further assumes that the intensity profiles at the aperture plane are the same in either case, i.e., $I(r) = I(x)$, then one again gets a factor of two difference between the power losses.

The actual ratio indicated by the data was somewhat higher than a factor of 2 as shown by the corresponding curve fits of the data. Both sets of data correlated very well as a function of the reciprocal of the square root of the Fresnel number. However, the proportionality constant for the HAC data was found to be 23.6 versus 11.1 for the AFWL data.

In order to use these results in the optical train model, the power loss was assumed to be related to an effective increase in the beam diameter at the aperture plane, i.e.,

$$\frac{D_B}{D_{B_0}} = (1 - \text{loss})^{1/2} = 1 - \frac{0.112}{\sqrt{F_N}}$$

where D_{B_0} is the new diameter of the beam at the beam clipper station and $F_N = D_B^2 / 4\lambda L_C$ is the propagation Fresnel number. It was also assumed, for the case of an obscured beam, that the hole in the beam filled in as much as the diameter of the hole would grow were it a uniformly illuminated aperture (i.e., Babinet's Principle). Thus the inner diameter of the obscured beam, D_{B_i} , is computed by

$$D_{B_i} = \epsilon D_B (1 - 0.112 / \epsilon \sqrt{F_N}).$$

If D_c is the diameter of the beam clipper, then the power transmission through the aperture is

$$T_c = \begin{cases} 1.0 & \text{if } D_{B_0} \leq D_c \\ (D_c/D_{B_0}) & \text{if } D_{B_0} > D_c \end{cases}$$

In the latter case, the beam diameter is set equal to the clipper diameter for the remaining calculations in the model.

2.1.4 High Power Mirrors

The mirrors in the optical train will affect all the performance parameters. Although it is not necessary we assume that all of the mirrors are identical in order to reduce the number of inputs.

A mirror alters the amplitude of the beam by absorbing a fraction of the incident radiation. For a series of N mirrors each having a surface reflectivity R , the transmission factor is

$$T_M = R^N.$$

It should be noted that in the present analysis N includes all of the mirrors in the optical train, i.e., relay, steering, secondary and primary.

The beam quality degradation is due to (1) surface roughness and manufacturing errors in the mirror figure, and (2) surface distortions due to absorption of power from the incident beam. The former are independent of the power in the beam while the latter is a function of both the power and the irradiance distribution. In addition, if

cooled mirrors are used, there will also be distortions induced by the pressure variations inside the coolant passages. However, these distortions will depend upon the details of the mirror construction and their characterization is felt to be beyond the scope of this model. Therefore, for this analysis, distortions of this type will be included in (1) above.

The beam quality degradation induced by the mirrors is incorporated into the optical train model through an equivalent phase variance, σ_M where

$$\sigma_M^2 = N\sigma_f^2 + [(N - 1)\sigma_I + \sigma_I/M^2]^2.$$

The first term on the right hand side of the above expression represents the uncorrelated sum of the phase distortion due to fabrication errors such as surface roughness, figure error, coolant passage distortion, etc. The remaining terms represent the correlated sum of the irradiance mapping phase distortion. The distortion of the primary mirror is reduced by the square of the magnification of the beam expander to account for its reduced thermal loading.

In practice, σ_f is not known but is instead specified as a tolerance on the manufacturing process. Therefore, for modeling purposes this parameter was left to the user to specify.

The approach taken to model σ_I was to assume that the distortions scale directly with the irradiance fluctuations. That is,

$$\sigma_I = KI_{rms}$$

where K is a constant which depends upon the physical parameters of the mirror, the cooling scheme, etc. If we assume that the peak to peak intensity fluctuations specified in the input beam description are uniformly distributed and random in character, then

$$I_{rms} = \frac{I_{ave}}{\sqrt{12}} \left(\frac{\Delta I}{I_{ave}} \right)$$

where, for a circular beam,

$$I_{ave} = \frac{4 P_L}{\pi D_B^2}$$

Expressions for the evaluation of K depend upon whether the mirror is water cooled or not, i.e., for cooled optics

$$K(m^2/watt) = 5 \times 10^{-14} (1 - R) (2\pi/\lambda)$$

whereas, for uncooled optics

$$K = 4\pi (1 - R) \alpha \Delta t / \lambda C \rho$$

where

α = the thermal expansion coefficient of the mirror material

C = the specific heat of the mirror material

ρ = density of the mirror material.

The expression for cooled optics is based on the NPT/Chemical Laser Compatibility Study conducted by Hughes Aircraft Company for NSWC (Reference 8) in which similar expressions were employed to compute the phase distortion caused by the NACL irradiance profile. The expression for uncooled optics is based on a simplified one-dimensional heat transfer analysis (Reference 9).

Local surface distortion is not the only performance degrading factor caused by the finite absorptivity of the mirrors. A bending distortion is also induced by the differential growth of the front and rear mirror surfaces. For properly designed, cooled mirror configurations, this distortion can be kept small. However, for uncooled mirrors, it may be important.

To first order, the bending distortion is primarily a function of the total beam power and not the irradiance distribution. In addition it produces mostly a spherical phase front distortion. Thus in the optical train model, we compute this distortion mode as a beam divergence instead of a quality loss since, in theory, it could be corrected by the focusing optic (if detected).

For an uncooled mirror that was initially flat, the change in the focal length with time can be approximated as (see Reference 9)

$$f = \frac{D_B^2 \ell \cos \theta}{2.44 P_L (1 - R) \alpha} \left(\frac{D \rho K}{\Delta t} \right)^{1/2}$$

where

ℓ is the mirror thickness

θ is the beam angle of incidence on mirror

K is the thermal conductivity of the mirror material

f is the focal length of the distorted mirror.

The mechanism by which the defocusing errors induced by the individual mirrors are accumulated throughout the optical train is explained later.

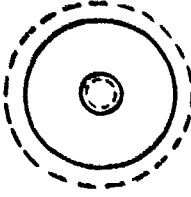
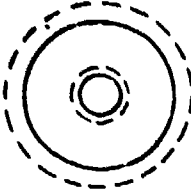
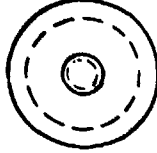
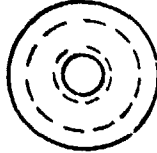
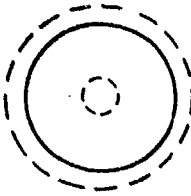
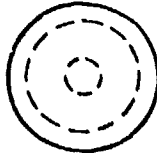
2.1.5 Beam Expander

In the formulation of the beam expander model, we allow for two types: (1) an on-axis or (2) an off-axis system. Either type system affects the available power at the transmitter, the beam quality, beam jitter and beam divergence. A discussion of the methodology for computing the transmission factor and beam quality is given below. The beam jitter and divergence are discussed in a later section.

The power transmission through the beam expander is computed by projecting the exit aperture (defined by the user) onto the plane of the beam clipper station. Simple geometry then allows one to compute the power lost due to a mismatch between the beam diameters and exit aperture diameters. The formulas are illustrated in Table 2.1 for both the on-axis and off-axis cases.

The beam quality is not affected by the off-axis system except to the extent that the limiting diameter is $MD_{B_0} \leq D_t$ for spot size calculations at the target plane. This is also true of the on-axis case. However, the on-axis system also introduces a central obscuration ϵ , which reduces the beam quality. The expressions used in the model to compute the final obscuration of the beam leaving the optical train are also given in Table 2.1.

Table 2.1. Summary of Beam Expander Transmissions and Obscuration Calculations

TYPE	GEOMETRY	TRANSMISSION	OBSCURATION
ON AXIS		$\frac{D_o^2 - D_i^2}{D_{B_o}^2 - D_{B_i}^2}$	D_i/D_o
		$\frac{D_o^2 - D_{B_i}^2}{D_{B_o}^2 - D_{B_i}^2}$	D_{B_i}/D_o
		$\frac{D_{B_o}^2 - D_i^2}{D_{B_o}^2 - D_{B_i}^2}$	D_i/D_{B_o}
		1.0	D_{B_i}/D_{B_o}
OFF AXIS		$(D_o/D_{B_o})^2$	D_{B_i}/D_o
		1.0	D_{B_i}/D_{B_o}

The effect of the obscuration on the beam quality is again computed by relating it to an equivalent phase distortion. This relationship was derived empirically based on the results of the previous work under this contract (Reference 2), and is illustrated graphically in Figure 2.4. Within the computer code, this relationship is represented by a third order polynomial developed from a "least-squares" regression analysis of the data presented in Figure 2.4. Also shown on the figure is the effective scale size of the phase distortion. Its use in the model will be explained below.

2.1.6 Exit Aperture

Provisions were also made in the optical train model for an exit aperture downbeam of the pointer/tracker. It can be either a material window or open port, with an aerodynamic curtain protecting the optics from the environment, based on user specified option parameters.

In either case the loss in power through this exit aperture will be

$$T_E = e^{-\beta L_W} (1 - A_S/A_B)$$

where

β = absorption coefficient of material window

L_W = thickness of material window

A_S = area of struts supporting window or secondary mirror in the case of an on-axis beam expander

A_B = beam area ($\pi M^2 D_{B_0}^2 / 4$).

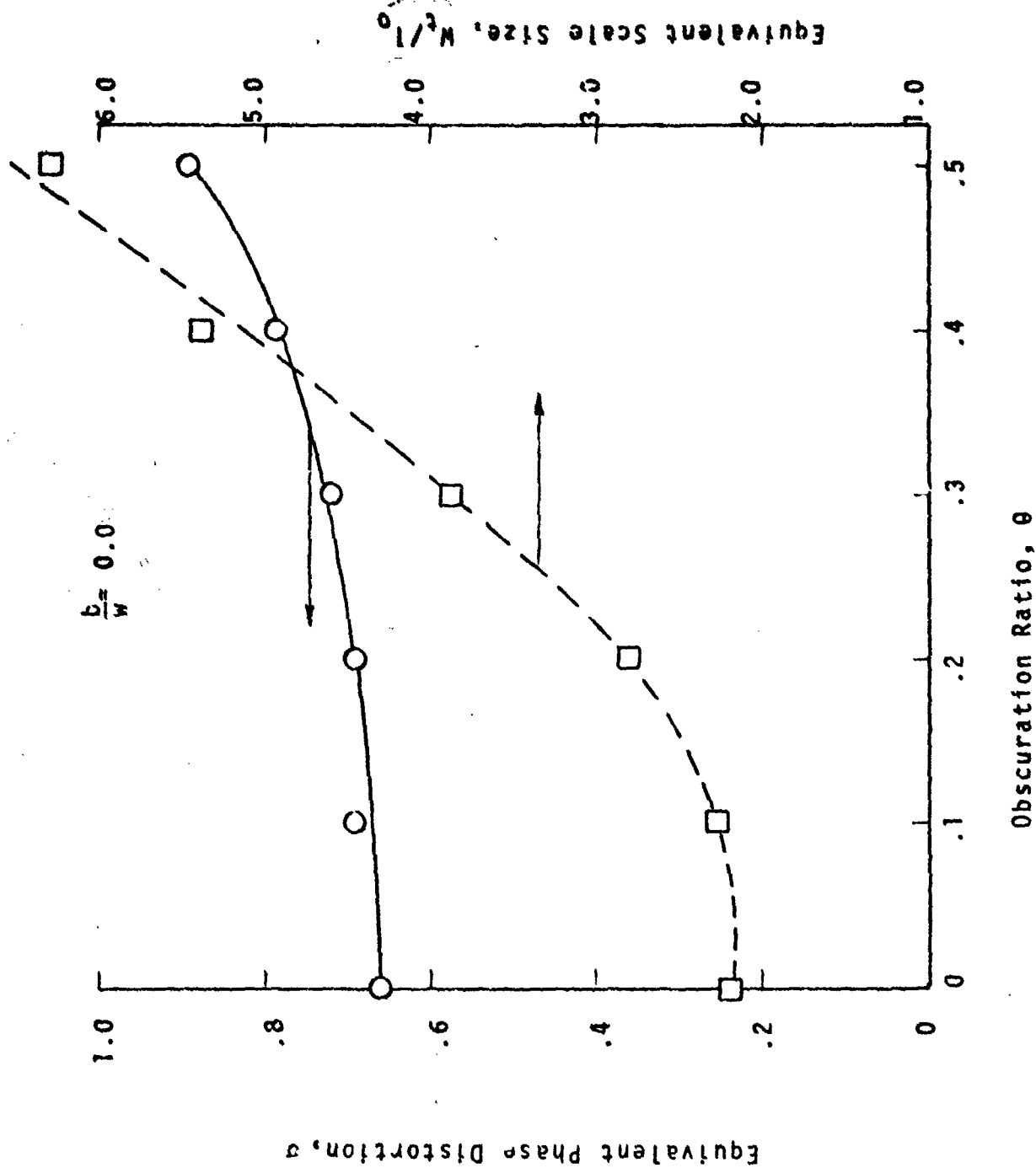


Figure 2.4. Beam Quality Loss Due to Central Obscuration in Terms of θ and W_t/l_0

Note that an open port can be simulated by setting $\beta = 0$.

For simplicity, the phase distortion induced by the material window is assumed to be proportional to the local intensity fluctuations in the beam profile. That is

$$\sigma_w = \left(\frac{2\pi}{\lambda} \right) \frac{\beta \Delta t L_w}{\rho c} \left[(n - 1) \alpha + \frac{\partial n}{\partial T} \right] \frac{I_{rms}}{M^2}$$

where (in addition to those parameters previously defined) n is the refractive index and T is the temperature. The magnification appears because of the assumed location of the window downstream of the beam expander. In order to minimize the number of inputs to the model, the material constants were lumped into a single parameter defined as

$$\gamma = \frac{1}{\rho c} \left[(n - 1) \alpha + \frac{\partial n}{\partial T} \right]$$

which varies between $4 \times 10^{-12} \text{ m}^3/\text{j}$ for the fluoride windows (CaF_2 , MgF_2 , SrF_2) to $15 \times 10^{-12} \text{ m}^3/\text{j}$ for the salt windows (NaCl , KCl). A value of $5 \times 10^{-12} \text{ m}^3/\text{j}$ was hard-wired into the model as being representative of current window technology.

The presence of struts in the beampath will also cause a reduction in the beam quality. To first order, this loss will be directly proportional to the area of the beam blocked by the struts. Consider, for example, the on-axis intensity which, in the context of scalar diffraction theory, is given by the integral of the complex field leaving the transmitting aperture, i.e.,

$$I(0) \sim \left[\iint u(x,y) dx dy \right]^2.$$

Thus, for a constant field aperture strength, the integral is simply the area of the clear aperture. That is

$$I(o) \sim (A_B - A_s)^2$$

so that the intensity reduction relative to no struts is simply

$$\frac{I(o)}{I_0} = \left(1 - \frac{A_s}{A_B}\right)^2 = T_s (1 - A_s/A_B).$$

For modeling purposes, this intensity reduction was considered to be separable into (1) a power loss due to the transmission of the aperture, T_s , and (2) a beam quality loss characterized by wide angle scattering, $(1 - A_s/A_B)$. The latter can be related to an equivalent phase distortion via the Strehl equation

$$\sigma_s = (A_s/A_B)^{1/4}.$$

The phase distortion induced by an open port is not intensity dependent but instead a function of the turbulence level inside the beam expander and aerodynamic curtain. Because of the presence of turbulence, this effect is treated as an additional source of beam jitter in the model. The magnitude of the jitter is estimated from (Reference 8)

$$\theta_J = 2.14 \times 10^{-7} \left[\frac{L_e^3 \Delta T^6}{\lambda D_t^2} \right]^{1/5}$$

where L_e is the path length through the beam expander and ΔT is the magnitude of the temperature fluctuations within the beam expander. Some representative values of the jitter are illustrated in Figure 2.5 for a 0.7 meter transmitter diameter. For example, a 1°C temperature fluctuation produces approximately $4.5 \mu\text{rad}$ of beam jitter for a $3.8 \mu\text{m}$ wavelength beam.

2.2 ASSESSMENT OF OVERALL PERFORMANCE

The previous discussion was primarily concerned with the influence each of the elements has on the characteristics of the laser beam as it traverses the optical train. In the following section we show how these individual effects are accumulated to arrive at an overall assessment of system performance.

2.2.1 Transmitted Power

The power available at the transmitting optic is simply the input power from the laser device modified to account for all of the power losses that have occurred along the optical train. That is

$$P_t = T P_L$$

where T is an overall transmission factor. Since the power losses are multiplicative, the overall transmission factor is

$$T = (T_C) (T_M) (T_{BE}) (T_E)$$

Diameter = 0.7 m
Length = 2.0 m

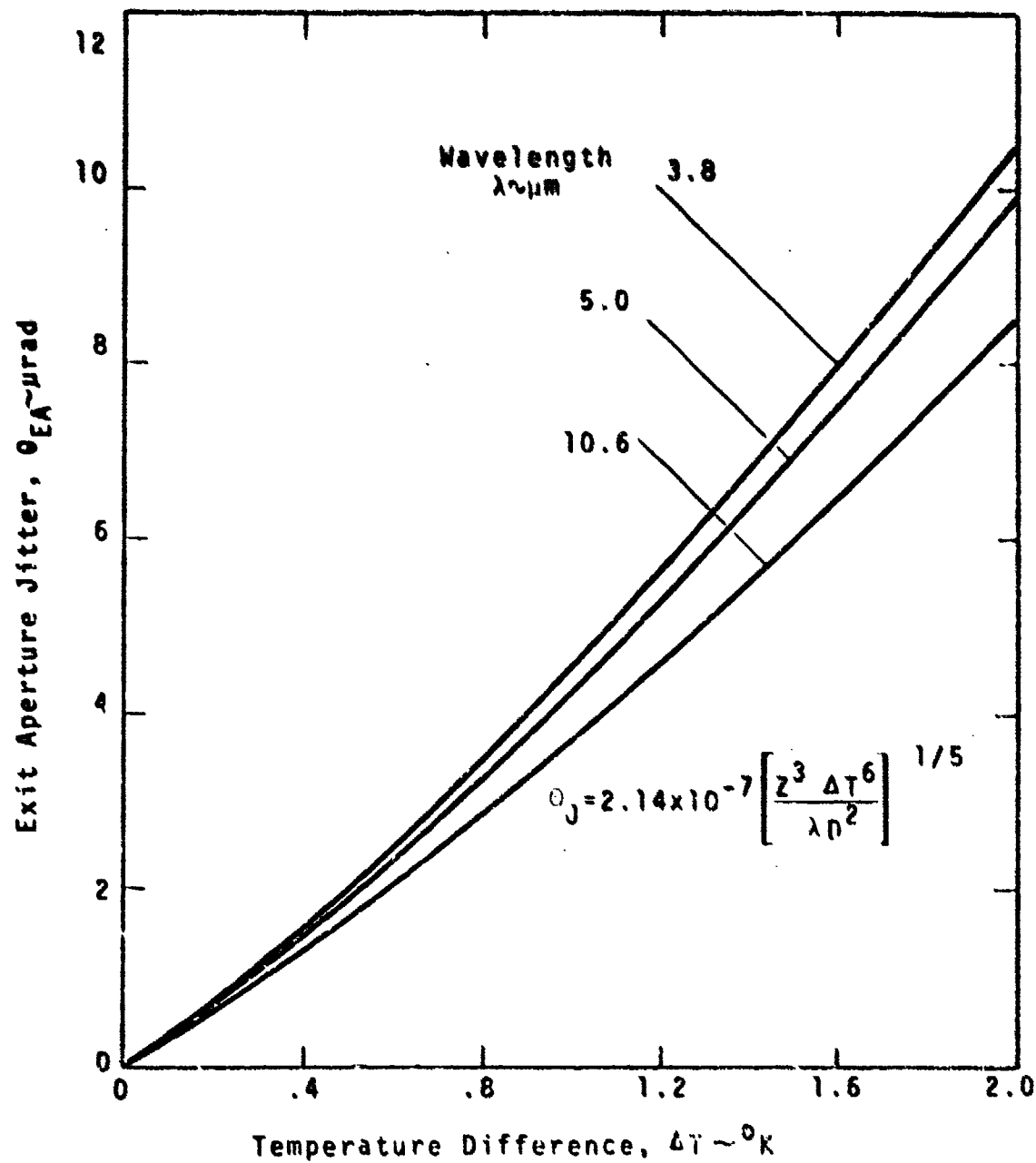


Figure 2.5. Effects of Exit Aperture Temperature Fluctuations on Beam Jitter

where T_c is the transmission factor of the beam clipper, T_M is the transmission factor of all the high power mirrors, T_{BE} is the transmission factor of the beam expander, and T_E is the transmission factor of the exit aperture. Formulas for all of these factors were given previously.

2.2.2 Beam Quality

The quality of the beam at the transmitting optic is characterized by the two beam quality parameters, m_1 and m_2 (see Reference 1 and Section 4.3 of this report). Unfortunately, the calculation of m_1 and m_2 is not simple. The basic problem is to combine the effect of all the quality degrading factors occurring within the optical train. This is somewhat complicated because the phase distortions induced by the individual components do not add up in a straightforward manner but instead depend, in a complicated manner, upon the distribution as well as the magnitude of the phase distortion. For example, a "smooth" distortion behaves differently than a very "rough" distortion even though their magnitudes are the same.

To circumvent this problem, a statistical approach is used within the model to accumulate the phase distortions. This approach is somewhat loosely based on the theoretical investigations of nondiffraction-limited gaussian beams by B. Hogge at the AFWL. Briefly, the approach is to consider the overall beam profile at the focal plane as being composed of two gaussian beam profiles of different relative amplitudes and widths. That is, a certain fraction of the energy in the beam is propagated completely unaffected by the phase distortion, i.e.,

$$I_u(r) = e^{-\sigma^2} \exp \left(-\frac{2r^2}{w_f^2} \right) I_0$$

where w_f is the diffraction limited waist parameter, I_0 is the on-axis intensity and σ^2 is the variance of the phase distortion (assumed to a gaussian random variable). The remaining energy is smeared or spread by the phase distortion into a somewhat larger beam profile, i.e.,

$$I_s(r) = (1 - e^{-\sigma^2}) \left(\frac{w_f^2}{w_f^2 + 2\sigma^2 f^2} \right) \exp \left(\frac{-2r^2}{w_f^2 + 2\sigma^2 f^2} \right) I_0$$

where Θ is the angular spread of the scattered beam.

The problem thus reduces to characterizing the overall phase variance, σ , and beam spread parameters, Θ , that "best" model the summation of all of the phase distortions in the optical train.

A true characterization of σ and Θ is, in reality, not possible. Some theoretical arguments can be made for isolated phase distributions such as the random gaussian noise model investigated by Hogge. In the real world, however, optical systems do not produce such amiable distortions. Nevertheless, using these results as being at least qualitatively correct, we compute the total phase distortion as simply the uncorrected sum of each of the individual distortions, i.e.,

$$\sigma^2 = \sigma_L^2 + \sigma_{AW}^2 + \sigma_M^2 + \sigma_{BE}^2 + \sigma_S^2 + \sigma_W^2.$$

Instead of computing the beam spread, Θ , it is more convenient to compute an effective scale size or correlation length of the overall phase distortion, L . This scale size is related to the beam spread via $\Theta^2 = (\lambda/\pi L)^2$. In the

aforementioned work of Hogge, it was noted that the effective correlation length for a number of sources of phase distortion was found to be an average of the correlation lengths of the individual sources, each weighted by its respective variance. Again, taking the inductive leap, we compute L from

$$L = \frac{1}{\sigma^2} \left[\epsilon_L \sigma_L^2 + \epsilon_{AW} \sigma_{AW}^2 + \epsilon_M \sigma_M^2 + \epsilon_{BE} \sigma_{BE}^2 + \epsilon_S \sigma_S^2 + \epsilon_W \sigma_W^2 \right].$$

In practice very little is known about the magnitude of the scale sizes characterizing the individual components. Therefore, for the present model, we have made some additional assumptions regarding their respective sizes. For example, the irradiance mapping phase distortions such as σ_I and σ_W are assumed to have the same scale size as the intensity fluctuations in the input beam profile. For other components, such as the laser device, the aerodynamic window and the struts, we assume that the scale size is zero. In effect this is assuming that each of these components scatters the energy in the beam beyond a usable radius in the focal plane and therefore is somewhat conservative. The scale size of the beam expander was determined empirically since the effect of obscuration on the near-field beam profile was readily calculated (see Figure 2.4). Within the model this relationship is represented by a third order polynomial.

The computed values of the phase variance and scale size are used to evaluate the power distribution at two radial positions in the far-field, namely $r = w_f$ and $r_2 = 2w_f$. These power points are then used to generate the beam quality parameters m_1 and m_2 . The procedure for doing this is outlined in Reference 1.

2.2.3 Beam Jitter

The beam jitter is accumulated throughout the optical train by assuming that the sources of beam jitter are independent of each other. Thus they may be root-sum-squared to get the total jitter. The primary consideration for the beam jitter calculation is whether or not the source of the jitter is upbeam or downbeam of the beam expander. The beam expander reduces the jitter by a factor of $1/M^2$ where M is the magnification.

The sources of beam jitter considered by the model are

- Tracking jitter, θ_{TR}
- Boresight jitter, θ_{BS}
- Autoalignment system jitter, θ_{AA}
- Servo jitter, θ_S
- Device jitter, θ_L
- Exit aperture induced jitter, θ_E .

The jitter of the input beam and the jitter induced by the beam steering mirror in the autoalignment system are assumed to occur before the beam expander. The remaining jitter sources are assumed to occur after the beam expander. Thus the total jitter leaving the optical train is given by:

$$\sigma_J = \{\theta_{TR}^2 + \theta_{BS}^2 + \theta_S^2 + \theta_E^2 + (\theta_L^2 + \theta_{AA}^2)/M^2\}^{1/2}.$$

2.2.4 Beam Divergence

The beam divergence represents the spherical phase curvature in the beam as it enters the transmitting optic and results in a larger spot size at the target than one

would expect had the beam been collimated when it entered the transmitting optic. As an example, consider a collimated ideal gaussian beam which has been focused to produce a spot size of w_f (actually a radius to the e^{-2} intensity point) at a target. If the beam is instead diverging (or converging) with a radius of curvature $-R_B$ ($+R_B$) as it is reflected from the same transmitting optic, the new spot size w'_f is larger than the original by

$$\left(\frac{w'_f}{w_f}\right)^2 = 1 + \left(\frac{\pi D_B^2}{4\lambda R_B}\right)^2$$

where D_B is the (e^{-2}) diameter of the ideal gaussian beam and λ is the wavelength. For example, 0.1λ spherical phase error will increase the spot size approximately 20% for a 100 cm diameter optic transmitting at $\lambda = 3.8 \mu$. For the present study we assume that any phase curvature in the output beam from the optical train behaves in a similar manner.

The change in the curvature of the phase front of the beam as it propagates through the optical train is computed by employing a simplified geometric optics calculation through the optical elements preceding the beam expander. The usual simplifying assumptions, i.e., paraxial rays, thick lenses, etc., are made in order to make the calculation tractable.

Following the ray matrix approach of Reference 10 we first obtain the equivalent ray matrix of the optical train illustrated in Figure 2.6 by multiplying together the individual ray matrices of the individual elements, i.e.,

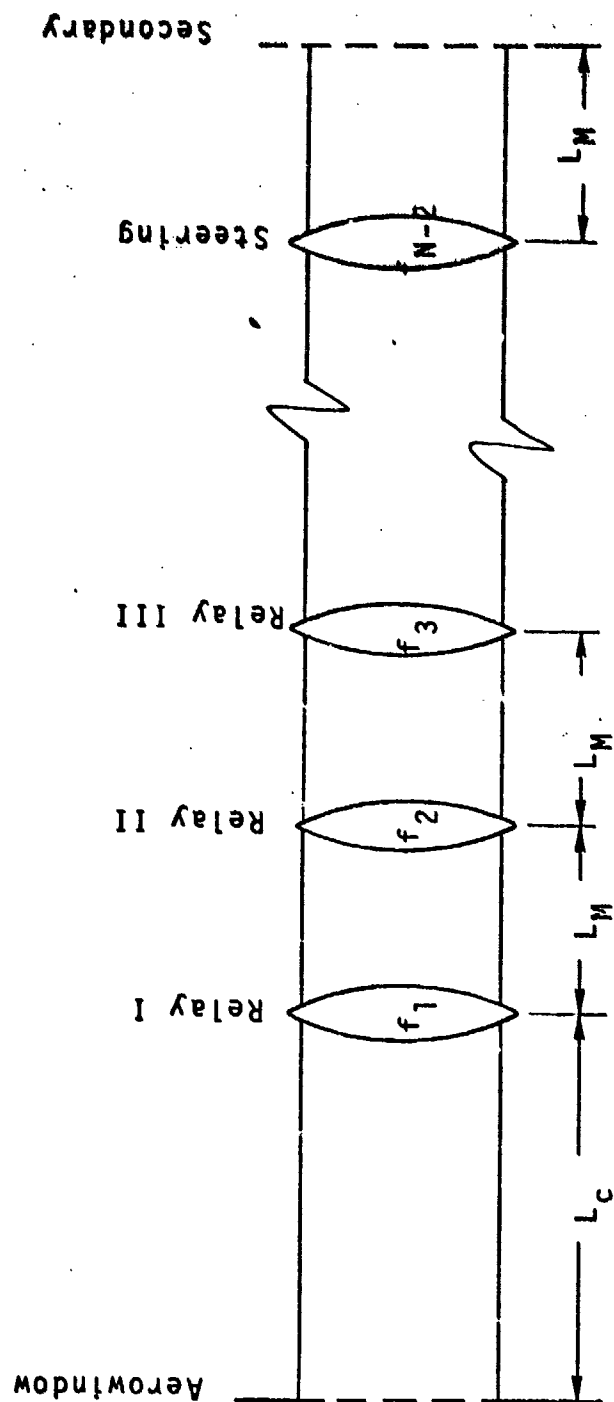


Figure 2.6. Simplified Optical Train Employed in Defocus Calculations

$$\begin{bmatrix} A & B \\ C & D \end{bmatrix} = \begin{bmatrix} 1 & L_M \\ 0 & 1 \end{bmatrix} \begin{bmatrix} 1 & 0 \\ -1/f_{N-2} & 1 \end{bmatrix} \cdots \begin{bmatrix} 1 & 0 \\ -1/f_2 & 1 \end{bmatrix} \begin{bmatrix} 1 & L_M \\ 0 & 1 \end{bmatrix} \begin{bmatrix} 1 & 0 \\ -1/f_1 & 1 \end{bmatrix} \begin{bmatrix} 1 & L_C \\ 0 & 1 \end{bmatrix}$$

where (going from right to left) the first matrix represents the propagation distance between the aerodynamic window and the beam clipper, the second matrix represents the reflection of the beam from the first relay mirror in the optical train, the third matrix represents the propagation distance between the first relay mirror and the second relay mirror, the fourth matrix represents the reflection of the beam from the second relay mirror, and so on until the beam is incident upon the secondary mirror. At this point we assume that the beam expander simply expands the beam by the specified magnification. The curvature of the phase front at this point, R_B , is related to the phase front curvature of the input beam, R_L , by

$$R_B = M \left(\frac{AR_L + B}{CR_L + D} \right).$$

The computed value of R_B is then used to compute the new spot size of the focused beam. In order to transfer this information to the propagation model, the beam quality parameter, m_2 , which characterizes the spread of the beam profile in the absence of other effects, such as thermal blooming, turbulence and beam jitter, is internally adjusted by the model to reflect the increased beam spread, i.e.,

$$(m_2)_{\text{final}} = \sqrt{1 + \left(\frac{\pi D_B^2}{4\lambda R_B} \right)^2} (m_2).$$

2.3 SAMPLE CALCULATIONS

As an illustration of how the optical train influences the performance of a laser system, we present below a sample calculation for the optical train schematically illustrated in Figure 2.7.

The laser device is assumed to be operating in an unstable confocal resonator mode with the power coupled out of the device via a scraper mirror located in front of the convex optic of the resonator. Accordingly, the output beam contains a central obscuration. The parameters assumed for this beam are:

Beam Diameter = 0.1 meters
Power = 400 kw
Wavelength = 3.8 microns
Obscuration = 0.5

In addition, it is assumed that the beam is essentially collimated ($R_L = \infty$) and contains peak-to-peak intensity fluctuations that are 50 percent of the average intensity ($\Delta I/I_{ave} = 0.5$). The scale size of these fluctuations is taken to be 1 cm or $\lambda_L/D_B = 0.1$. We also assume that the quality of the beam leaving the device is characterized as being 1.2 times diffraction-limited ($n_L = 1.2$). This corresponds to an equivalent rms phase distortion in the beam of $\sigma_L = 0.16$ radians or about $\lambda/40$ (see Figure 2.2).

The output beam from the laser device is focused through an aerodynamic window to a collimating mirror. Since the beam size is very small (typically < 0.1 cm) at the aerodynamic window, we neglect any phase distortion induced by the aerodynamic window (i.e., $\sigma_{aw} = 0$).

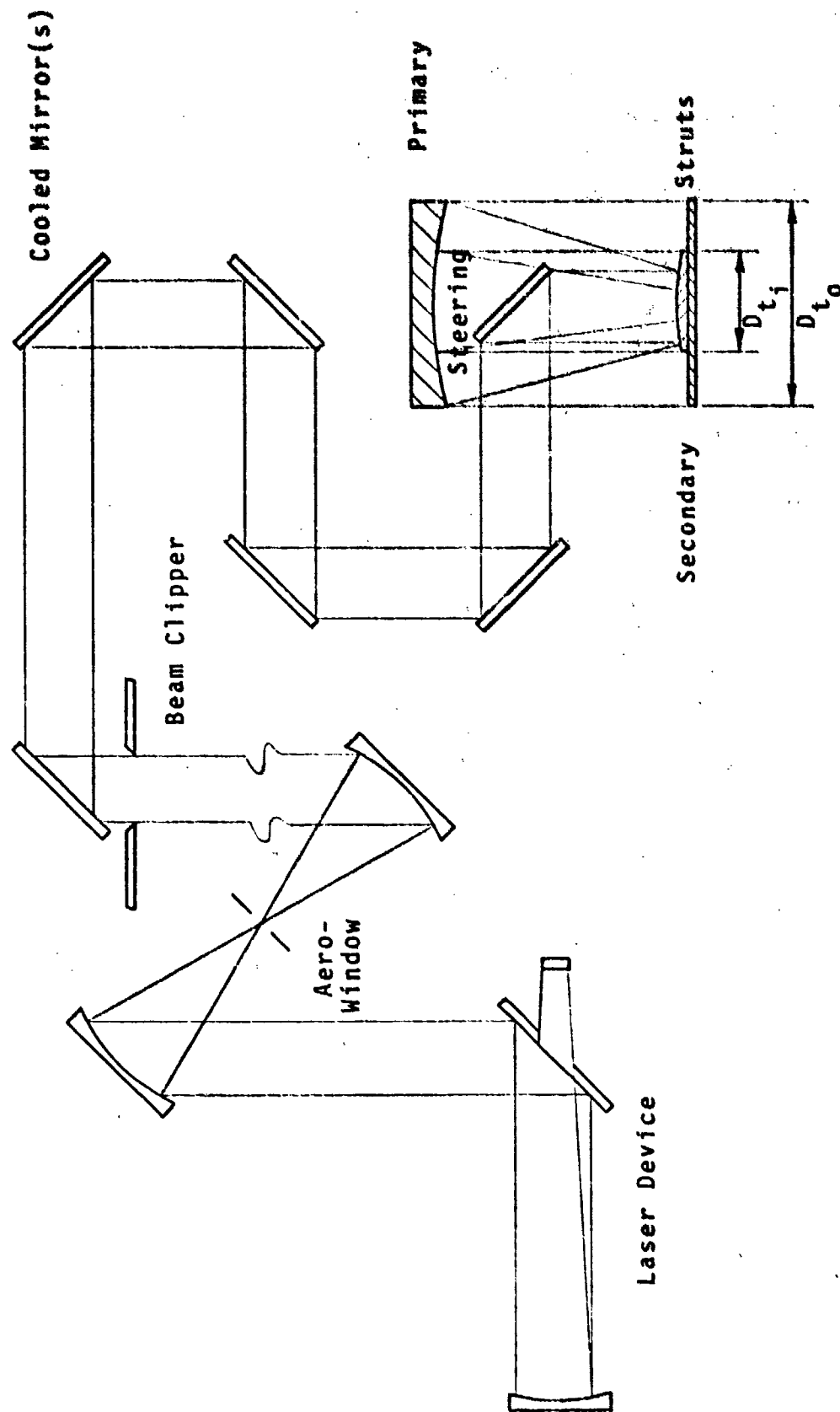


Figure 2.7. Schematic of Optical Train for Sample Calculations

For the example, we assume that the beam expander is located 50 meters from the aerodynamic window. Over this distance, diffraction effects cause the beam to expand somewhat. The Fresnel number for this propagation distance is

$$F_N = \frac{4D_B^2}{\lambda L_c} = 13.16$$

so that the beam diameters at the entrance to the beam expander are

$$D_{B_0} = \frac{D_B}{1 - 0.112/\sqrt{F_N}} = 0.103 \text{ m}$$

and

$$D_{B_i} = \left(\epsilon - \frac{0.112}{\sqrt{F_N}} \right) D_B = 0.047 \text{ m.}$$

In this example, we have assumed that the diameter of the beam clipper is 16 cm so that no power loss due to clipping occurs, i.e., $T_c = 1.0$.

The nine (9) mirrors employed in the optical train are assumed to be water cooled with a reflectivity of $R_i = 0.986$. We also take the fabrication error as being $\lambda_v/8$ where λ_v is 0.564 microns. Accordingly, the power lost to the beam due to the finite absorptivity of the mirrors is

$$T_M = (0.986)^9 = 0.88.$$

The phase distortion induced by each mirror depends upon the rms intensity fluctuations, which for the case being considered are

$$I_{rms} = \frac{4P_L}{\pi D_H^2} \frac{\Delta I/I_{ave}}{12} = 7.35 \times 10^6 \text{ w/m}^2$$

so that

$$\sigma_I = 5 \times 10^{-14} (1 - R)(2\pi/\lambda) I_{rms} = 0.0085 \text{ radians.}$$

Combining this with the fabrication error yields (for all of the mirrors in the optical train)

$$\sigma_M = 9\sigma_f^2 + [8\sigma_I + \sigma_I/M^2]^2 = 0.3454 \text{ radians.}$$

The beam expander is an on-axis system of magnification $M = 4.375$. The inner and outer diameters of the clear output aperture are $D_{t_0} = 0.7$ and $D_{t_i} = 0.252$ meters respectively. Since the beam entering the expander is not perfectly matched to the reduced clear aperture dimensions (i.e., $D_{t_0} = 0.16$ and $D_{t_i} = 0.576$), there is a power loss induced by the beam expander. From the geometry of the case being considered, this loss is computed to be approximately 13 percent or $T_{BE} \approx 0.87$. In addition, the beam expander has altered the obscuration of the input beam because of clipping. final obscuration of the beam leaving the beam expander is $\epsilon = 0.0576/10.3 = 0.558$. Note that the final obscuration is not the observation of the

telescope ($D_{t_1}/D_{t_0} = 0.36$) because the input beam was not large enough to fill the transmitting optic. The effective phase distortion of the actual beam is therefore much larger than one would compute based on the obscuration of the telescope. For the example being considered, this equivalent phase distortion is $\sigma_{BE} = 0.72$ radians.

The exit aperture was assumed to be an open port so that the only power loss is that due to blockage by the struts required to support the secondary mirror of the beam expander. Thus, $T_E = 0.95$. The quality loss due to the struts is

$$\sigma_s = (A_s/A_B)^{1/2} = 0.2236 \text{ radians.}$$

Within the model, the open port would also induce jitter into the beam. However, for the purposes of this example, we have ignored any performance loss caused by beam jitter.

Combining the above losses, we get for the overall transmission factor

$$T = T_C \cdot T_{BE} \cdot T_E = 0.727.$$

Thus, the power from the device that is available for propagation to the target is

$$P_t = 0.727 P_L = 290 \text{ kw.}$$

The total distortion is

$$\sigma = \left(\sigma_m^2 + \sigma_{BE}^2 + \sigma_s^2 + 0.433 \right)^{1/2} = 1.06 \text{ rads.}$$

This phase distortion is characterized by a scale size

$$\frac{\lambda}{D_B} = \frac{1}{\sigma^2} \left\{ \frac{\lambda_{BE}}{D_B} \sigma_{BE}^2 + \frac{\lambda_1}{D_B} \left[(N-1)\sigma_1 + \frac{\sigma}{M^2} \right]^2 + 0.196 \right\} = 0.114$$

in terms of the two parameter descriptions of the beam quality employed by the model $m_1 = 0.3536$ and $m_2 = 1.1076$. For this example, there were no defocusing errors induced by any of the components in the optical train so that no adjustment was made to the beam spread parameter m_2 . Note that the constraints in the last two equations (0.433 and 0.196) are needed to ensure the proper conversion of σ and $\frac{\lambda}{D_B}$ to m_1 and m_2 .

In order to quantify the impact of the optical train, we evaluate the power delivered to a particular spot in the focal plane, namely $r^* = f\lambda/D_{t_0}$. In the absence of atmospheric effects and beam jitter, this power is simply

$$P(r^*) = P_{t_0} \left\{ 1 - \exp \left[- \frac{\pi^2}{m_2^2} \left(\frac{D_B}{D_{t_0}} \right)^2 \right] \right\}$$

where D_B is the actual diameter of the beam on the transmitting optic, i.e., $D_B = M D_{B_0} \leq D_{t_0}$.

The results of this calculation for the example being considered is shown in Figure 2.8 along with some additional calculations made for various input beam diameters. For the conditions described above, only 83 kw of the initial 400 kw are delivered to the target. Note, however, that by expanding the input beam a significant increase in power can be achieved. The initial beam size of 10 cm was too small to effectively use the entire diameter of the transmitting optic. Hence, the beam profile at the target was

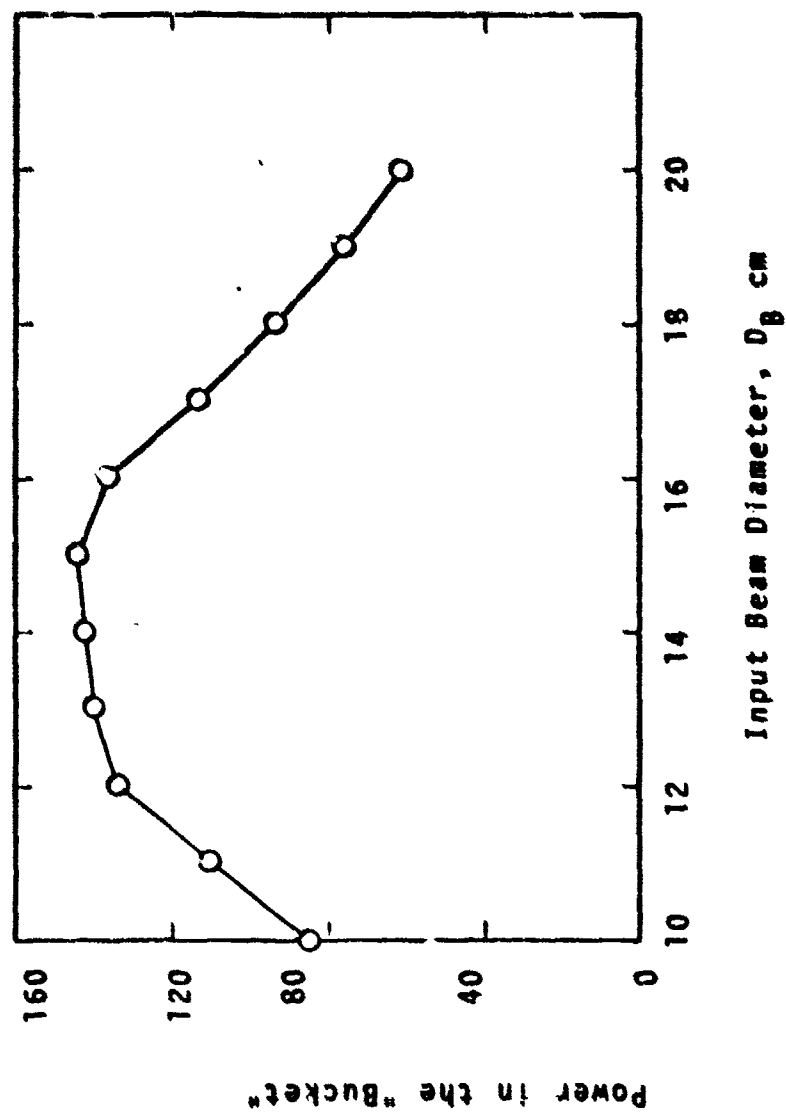


Figure 2.8. Results of Sample Calculations

larger than it should have been. In addition, because of the mismatch of device output beam and beam expander clear aperture, a significant power loss occurred. As the beam diameter is allowed to increase, both of these effects are reduced. Of course, at the point where the beam begins to spill-over onto the beam clipper, the near-field power is again reduced resulting in the performance fall-off shown in the figure.

It is recognized that a true performance evaluation cannot be made without including the propagation effects between the transmitter and target plane. However, the example does point out the necessity of including the effects of the optical train in any application study, since it indeed has a substantial impact on the near-field characteristics of the beam. In addition, the model also should provide some insight into the problems of integrating lasers and pointer/tracker systems. It is interesting to note that a detailed study of a similar system using a wave optics code resulted in an additional beam expander ($M = 1.3$) being placed in the optical train.

The simplified optical train model has been developed using state-of-the-art knowledge of the contribution of each element (windows, mirrors, etc.). It should be noted, however, that the model has not been verified using the more detailed wave optics codes. Such comparisons would be useful to not only verify, but also to improve, these simplified models.

Section 3

CREATION OF SAICOM

One of the High Energy Laser (HEL) propagation codes commonly used by the laser systems analysts is the COMBO (or ATM) code developed by the Air Force Weapons Laboratory (Reference 11). ATM is the propagation model documented in Reference 11. COMBO is a code which combines ATM with the Air Force HEL weight and volume projections (Reference 12). COMBO also includes some additional features such as the ability to perform reverse calculations in which the user specifies a desired intensity and the code determines the range at which the intensity can be delivered (given the power) or the power required (given the range). The primary asset of COMBO (or ATM) is its ability to make variable altitude calculations, including propagation paths extending to or from space.

One of the tasks performed under the present contract was devoted to modifying COMBO. The objectives were to reduce execution time, improve computational accuracy and to incorporate several of the newer developments resulting from the other tasks of this contract. A number of other minor additions, corrections and deletions were also made.

All of the primary modifications are discussed in Section 3.1. Collectively, they are sufficient to warrant a new code name -- SAICOM. A brief user's guide to SAICOM is provided by Section 3.2.

3.1 MODIFICATIONS OF COMBO

The primary modifications are dealt with in individual subsections below. The basic structure and organization

of the code remain essentially the same as in the original version (Reference 11). A summary of the more important equations is given in Section 3.1.9.

3.1.1 Improvements to Computational Speed and Accuracy

A substantial part of the COMBO modification effort was devoted to improving the speed of the calculations. Several modifications simply involved improvements in coding techniques. These included: (1) reducing the number of calls to MEGAIR (the subroutine which provides altitude dependent parameters such as temperature, pressure, etc.); (2) lumping several blooming parameters (viz., n , $\partial n / \partial T$, and C_p) into a single curvefit (GALTIN); (3) using a better search algorithm in the reverse calculations; and (4) reducing the subroutine calls.

Most of the improvement in both speed and accuracy was obtained by developing a completely new algorithm for performing the double integration required to compute the blooming parameter, NI. The expression for NI is of the form

$$NI = C \int_0^L \frac{1}{r(z')} \int_0^{z'} G(z'') dz'' dz'$$

where C is fixed for a given set of conditions (Reference 13). The integration paths are along the beam. In the original code, the double integral was evaluated by assuming the integrals to be constant between uniformly spaced points along the beam. The evaluation was successively repeated with reduced spacing until the results for consecutive evaluations agreed with 10 percent. This procedure

was found to be inefficient and often inaccurate. This should be readily apparent from Figure 3.1, which shows the important elements of the integral for a particular case of a highly focused beam. Note that the value of NI is dominated by the conditions within the last few percent of the range.

The new algorithm examines the local behavior of the integrand and chooses an efficient scheme and mesh spacing dynamically. It selects either a locally quadratic or locally exponential representation of the integrand. If neither is satisfactory, it reduces the mesh spacing and tries again. On the other hand, if the local convergence exceeds the accuracy requirements, it increases the mesh size to increase speed. Both integrations as well as a third implicit in G are performed in a single loop.

When the new algorithm was used for the severe example illustrated in Figure 3.1, the calculation required 1.49 seconds; the original COMBO exceeded a time limit of 200 seconds without completing the calculation!

As mentioned earlier, an additional improvement in computation time was obtained by modifying the convergence algorithm used in the reverse propagation calculation where the range is successively adjusted to obtain a desired target plane intensity. The range R' for one iteration is determined by modifying the previous range, R , viz.,

$$R' = KR \sqrt{I/OI}$$

where OI and I are the desired and computed intensities, respectively. In the original COMBO, the constant K was always 1.0, whereas in SAICOM, it varies between 0.7 and 1.0 to accelerate convergence. In addition, the convergence criterion was relaxed from 1% to 5%.

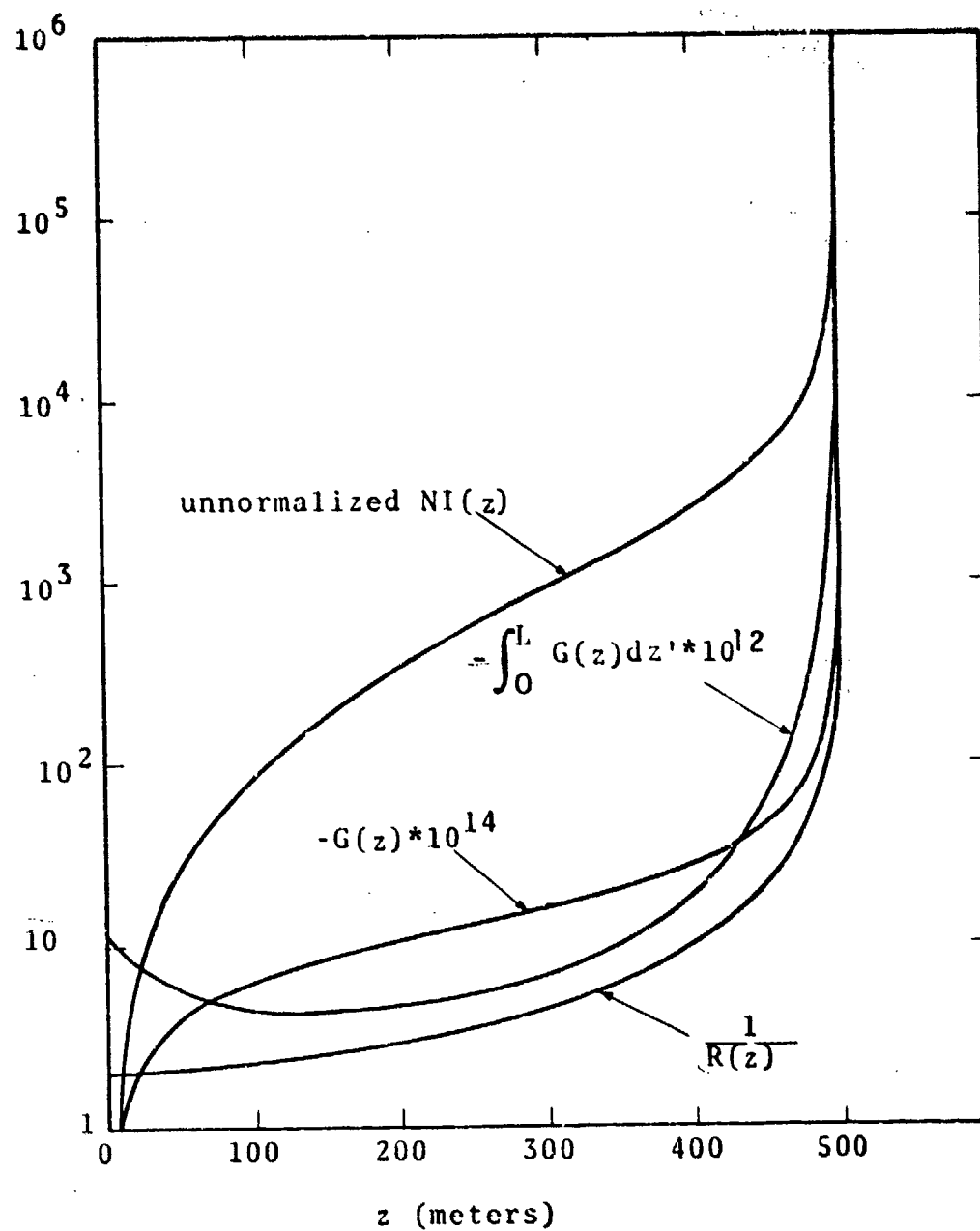


Figure 3.1 Variations in Elements of the Blooming Calculation

3.1.2 Beam Quality

The SAICOM code includes a significant innovation in the treatment of beam quality. It essentially replaces the usual one parameter concept of an "m x diffraction limited" beam by a two parameter representation. The two parameters, designated m_1 and m_2 , are used to specify a gaussian representation of the focal plane intensity profile so as to approximate the actual integrated power distribution. The two parameter model is inherently capable of including effects leading both to beam spreading (m_2) and to power loss due to wide angle scattering (m_1).

The origin and interpretation of m_1 and m_2 are discussed in some detail in Reference 1 and in Section 4.3 of this report. Their use in characterizing the effects of beam truncation and obscuration is discussed in Reference 2. In general, they are calculated in the new optical train model which is an integral part of SAICOM (see Section 2).

SAICOM incorporates the two parameter approach even though the user is only required to stipulate a single parameter, m . If the device power (P_D) and beam quality (m) are stipulated, the optical train portion of the code converts them to the appropriate aperture or transmitted power (P_T) and beam quality (m_1 , and m_2). If the optical train calculations are bypassed because the user specifies P_T , the specified beam quality is assumed to be pure beamspread.

The SAICOM intensity expression for a focused beam is of the form

$$I = \frac{[1 - (1 - 0.865 m_1 z/L)] P_T e^{-\alpha z}}{\pi r^2(z)}$$

where

$$r^2(z) = \frac{D}{4L^2} |L - z|^2 + 4z^2 \left[\left(\frac{0.3183 m_2 \lambda}{D} \right)^2 + \sigma_T^2 + \sigma_J^2 \right]$$

The term in the numerator that decreases as z increases represents the power losses that may be thought of as wide angle scattering. The 0.865 factor is present because the basic propagation equation used in the code is based on the $1/e^2$ radiance of an infinite Gaussian beam. Since m_1 and m_2 are used to account for the effect of different beam profiles as well as phase perturbation, these terms may be not the unity even for perfect beams. This situation is clarified in Table 3.1. In this table the $M1$ and $M2$ terms are the parameters computed in the optical train subroutine while m is the user specified beam quality for the total system. Note that if the optical train is bypassed (the user specifies P_T) and $m=1$, m_1 and m_2 are 0.89 and 1.29 respectively for a uniform beam and not unity because the basic propagation equation is based on an infinite gaussian model. But if the optical train is not bypassed, $m_1 = M1=0.89$ and $m_2 = M2=1.29$ because the basic profile used in the optical train subroutine is uniform.

3.1.3 The Optical Train Model

The development of an improved optical train model was the prime objective of Task 5 and is discussed in detail in Section 2 of this report. The model has been incorporated into SAICOM as subroutine OPTRAIN. It computes power losses, jitter, and beam quality degradation associated with transmission of the beam from the laser through

Table 3.1 Beam Quality Parameters

Aperture	Intensity Profile	Infinite Gaussian	$1/e^2$ Gaussian	Uniform
OPTRAIN BYPASSED	m_1	1	1	0.89
	m_2	1	1.41 m	1.29 m
OPTRAIN USED	m_1	0.89 M1	0.89 M1	M1
	m_2	0.775 M2	1.092 M2	M2

the final transmitting optic. It accepts a quite general specification of the optical train through a list of input parameters. OPTRAIN accounts for beam truncation and obscuration and for various contributions to phase perturbations. The output includes the two beam quality parameters m_1 and m_2 described above.

OPTRAIN can be bypassed simply by specifying the transmitted power, P_T , rather than the device power in the input. In this case, beam quality is based on wavelength scaling as usual.

3.1.4 Multi-Line Propagation

Since many of the lasers of interest for high energy applications emit several lines simultaneously, it is desirable to include these multi-line characteristics in the simplified propagation codes.

The approach used in SAICOM is to compute the amount of energy absorbed by the air on a line-by-line basis. This means that $\exp \left\{ - \int_0^R \alpha(z''') dz''' \right\}$

$$\sum_i \frac{P_i}{P_T} \exp \left\{ - \int_0^R \alpha_i(z''') dz''' \right\}$$

and $\alpha(z'') \exp \left\{ - \int_0^{z''} \alpha(z'') dz'' \right\}$ in the integrand of the

expression for the blooming parameter becomes

$$\sum_i \frac{P_i}{P_T} \alpha_{ai}(z'') \exp \left\{ - \int_0^{z''} \alpha_{ei}(z''') dz''' \right\}$$

where

α_{ai} = absorption coefficient of the i^{th} line

α_{ei} = extinction coefficient of the i^{th} line.

In SAICOM, the 3.8 μm DF propagation has been extended to include three distinct families of lines. These encompass ten lines of the DF laser, and represent 80% of the output of the BDL device. With the basic modification having now been made, it is straightforward to include multi-line HF or CO propagation.

The derivation of the DF absorption coefficients is given in Appendix A and is based on the BDL spectral data. The resulting SAICOM equations are

$$\alpha_i = A_0 e^{-A_1 + h(-A_2 + A_3 h)}$$

$$\text{where } A_0 = 1 + (0.9446 RH - 1)e^{-h(6.738 \times 10^{-5} + 9.61 \times 10^{-9} h)},$$

for groups 1 and 2

= 1, for group 3

A_1 = 10.047, 10.082, and 9.948 for group 1, 2 and 3, respectively

A_2 = 6.388×10^{-4} , 6.952×10^{-4} , and 2.199×10^{-4}

A_3 = 2.25×10^{-8} , 1.55×10^{-8} , and -1.96×10^{-8}

h = altitude in meters.

These equations imply that at sea level α varies between 0 and 0.0409 km^{-1} as relative humidity varies between 0 and 100%, α_2 between 0 and 0.0395 km^{-1} , and α_3 is a constant 0.0478 km^{-1} .

The above equations are only valid to around $h=13$ km; for the higher altitude the original COMBO coefficients are used. Unfortunately, a discontinuity existed at the 13 km altitude; so transition equations were created to connect the multi-line data below 13 km with the single-line data above that point. Figures 3.2, 3.3, 3.4, and 3.5 plot the α_1 , α_2 , α_3 , and $\alpha_{\text{resultant}}$ equations where

$$\alpha_{\text{resultant}} = \frac{\alpha_1 + \alpha_2 + \alpha_3}{3}$$

The scattering equations are the same as those used in the original COMBO (Reference 11).

3.1.5 Modification of Turbulence and Jitter to Include Short and Long Term Effects

During the code comparison work in Task 1 of this contract, it was noted that one of the useful features of ESP was the flexibility of including beam jitter in the blooming calculation if the frequency were high enough and excluding it otherwise (References 1 and 14). This feature has been included in SAICOM. The output jitter factors in SAICOM are high-frequency jitter (σ_{JHF}) and low-frequency jitter (σ_{JLF}). The former is used in the calculation of the blooming parameter and both are combined to give the total beamspread due to jitter. Similarly, the turbulence calculations are expanded to include the total, long-term turbulence (σ_{TLT}) and the high-frequency, short-term turbulence (σ_{TST}). The turbulence equations in SAICOM are based on work of Yura (References 15 and 16) whereas the COMBO code was based on Fried's work (Reference 17), but the results differ only slightly in the regions of interest. The equations used are

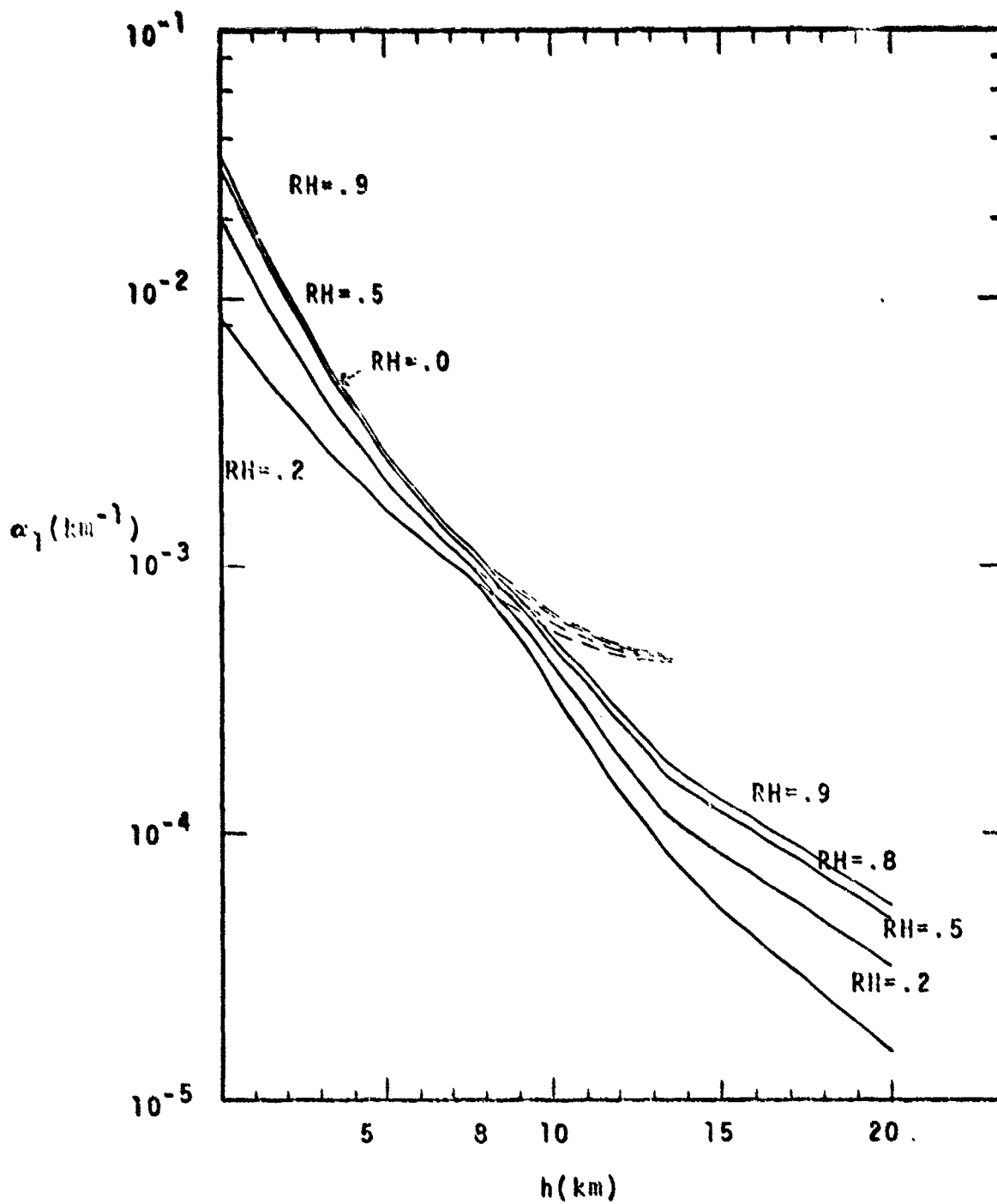


Figure 3.2. α_1 as a Function of Altitude

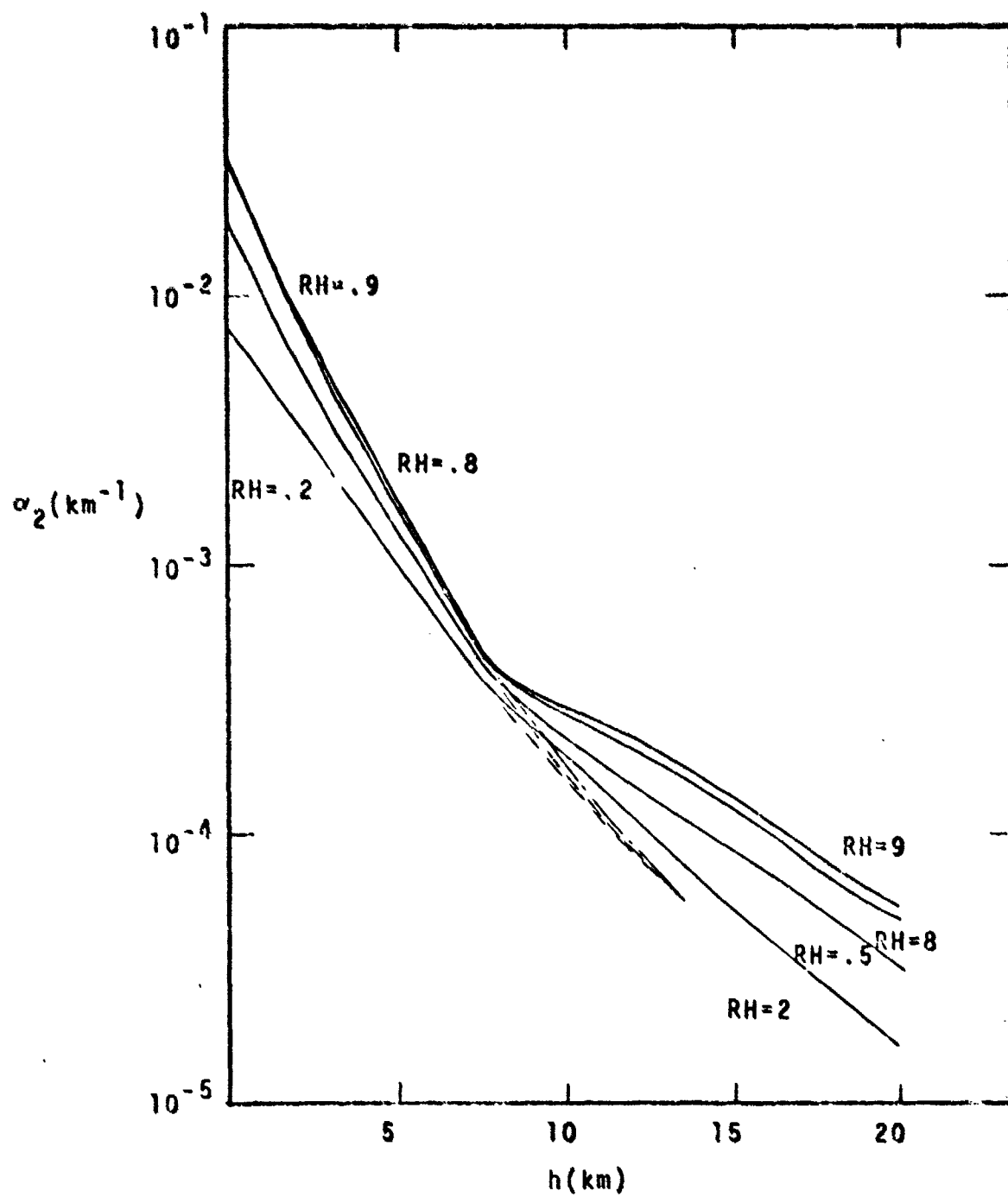


Figure 3.3. α_2 as a Function of Altitude

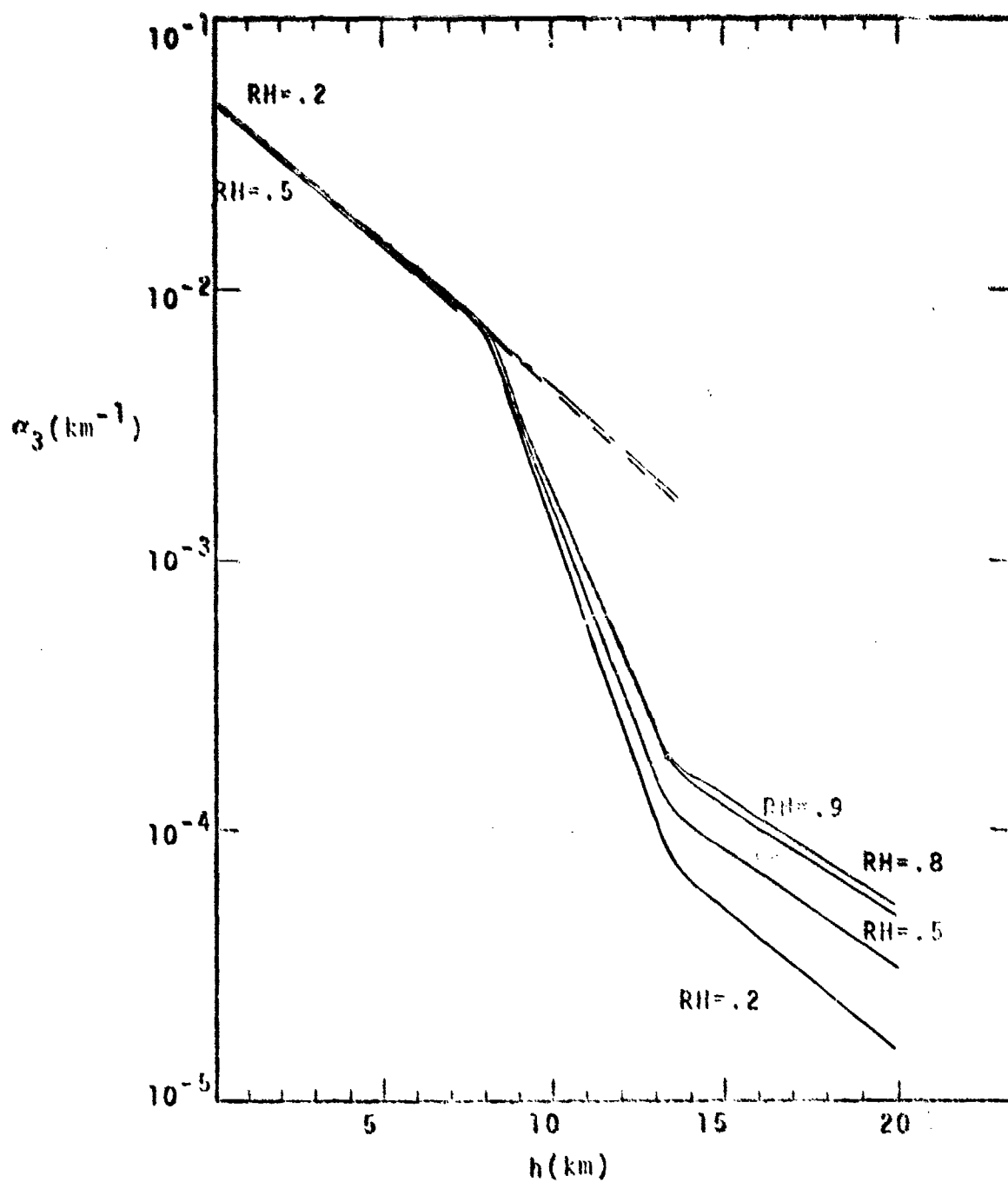


Figure 3.4. α_3 as a Function of Altitude

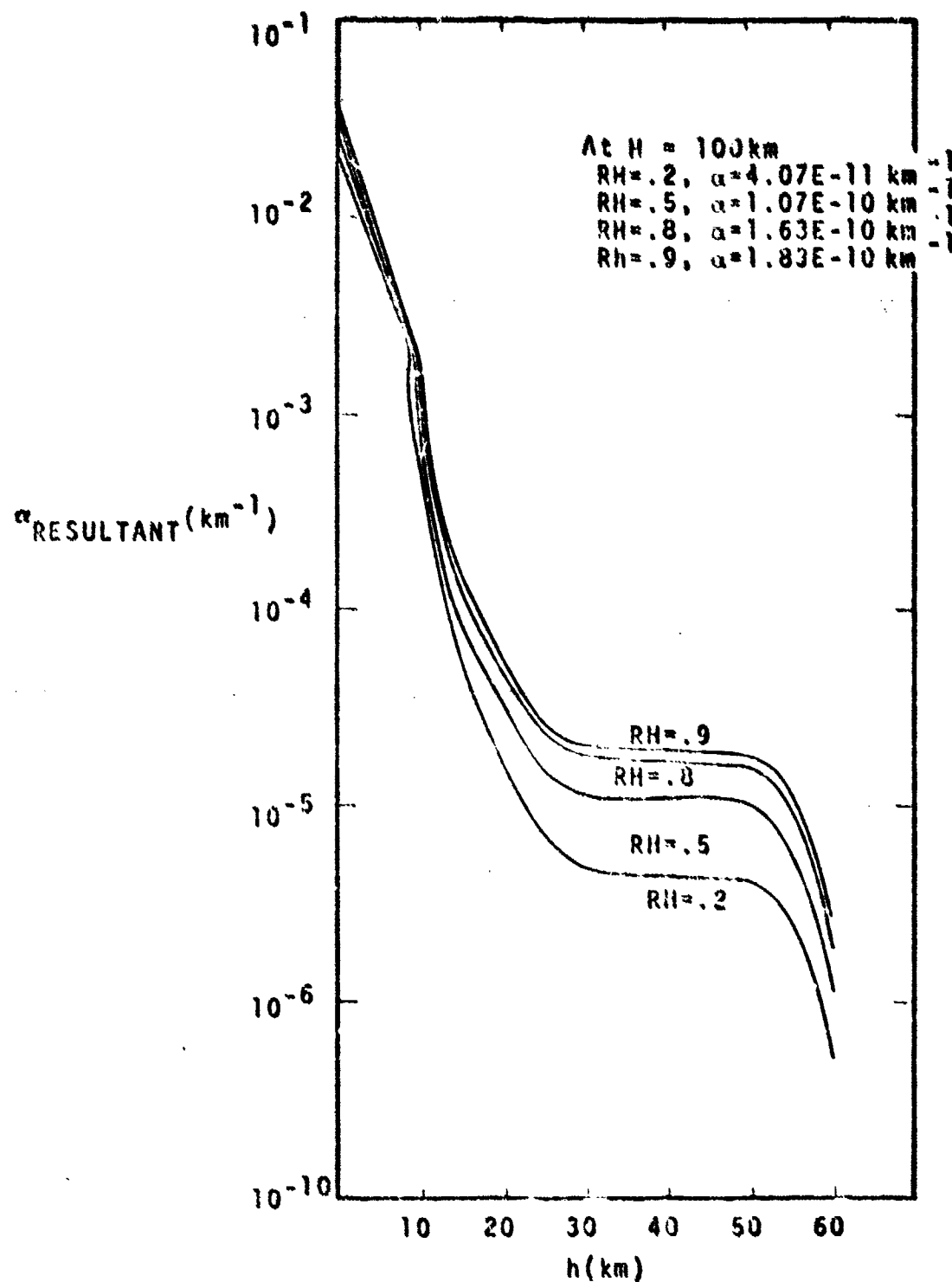


Figure 3.5. $\alpha_{\text{RESULTANT}}$ as a Function of Altitude

$$\sigma_{TLT} = \frac{2.549}{\lambda^{1/5}} \left[\int_0^L C_N^2(z) \left(\frac{L-z}{L} \right)^{5/3} dz \right]^{3/5}$$

and $\sigma_{TST} = \left[1 - 0.37 \left(\frac{\rho_0}{D} \right)^{1/3} \right] \sigma_{TLT}$

where $\rho_0 = \frac{1.439}{k^{1.2}} \left[\int_0^L C_N^2(z) dz \right]^{3/5}$

$$k = 2\pi/\lambda$$

D = diameter of the exit aperture.

These equations are generalizations of the co-altitude expression developed in Reference 16. In the blooming calculation σ_{TST} is used instead of the long-term expression, but it should be noted that some research indicates that no turbulence should be included in the beamspread before the blooming calculation (Reference 18).

3.1.6 Far-Field Intensity Distribution

In COMBO the standard calculation of the average intensity is based on the $1/e^2$ intensity radius in the far-field with a few other radii available for user specification (e.g., $1/e$ and $1/2$ intensity points). Since SAICOM is based on a gaussian approximation to the actual far-field distribution, it is a simple matter to use the $1/e^2$ results to describe the complete far-field profile. In addition to $I(1/e^2)$, the peak intensity $I_p = 2.312 \times I(1/e^2)$, is printed along with contour data. These contour data assume a

bivariant normal profile of the beam due to blooming distortion as developed in Reference 2. For each 10% contour ($I = \gamma I_p$, $\gamma = 0.9, 0.8, \dots, 0.1$) the area within that contour,

$$A(I > \gamma I_p) = \frac{\pi r^2 \ln(1/\gamma)}{2 KIP}$$

the total power within that area,

$$P(I > I_p) = P(1 - \gamma)$$

and the corresponding average intensity are printed. In addition, the beam displacement due to non-linear bending into the wind and the eccentricity of the resulting elliptical profile are computed and printed.

3.1.7 Calculation of Optimum Power

One of the more useful bits of information that comes from laser effectiveness studies is specification of optimum power based on maximizing energy on the target (Reference 19). Using the Gebhardt and Smith curve-fit for the intensity reduction due to blooming (Reference 20), the far-field intensity is related to transmitted power, P_T , by

$$I = a P_T I_{REL}(N)$$

where $N = b P_T$ and a and b are constants (independent of power). Setting $\partial I / \partial P_T = 0$ leads to

$$\partial \ln(I_{REL}) = -\partial \ln N$$

as the optimum condition. For the Gebhardt and Smith curve,

this condition is satisfied when $N=5.54$. Therefore, the optimum power is given by

$$P_{\text{optimum}} = \frac{5.5^4 P_T}{N}$$

where N is the value of the blooming parameter corresponding to the power P_T . The corresponding maximum intensity is

$$I_{\text{optimum}} = \frac{1.205 I}{N \text{ KIP}}$$

(KIP is the computer variable representing I_{REL}). It should be noted that the optimization does not include the possible effects associated with the optical train, i.e., it does not involve an iterative recall of OPTRAIN.

SAICOM prints the optimum power as derived above unless the corresponding intensity exceeds the air breakdown threshold. In that case, it prints the power at which breakdown would occur as the optimum power. The breakdown power level is estimated on the basis of peak intensity without blooming.

3.1.8 Miscellaneous Modifications

Several relatively minor additions, deletions and corrections are described below.

3.1.8.1 Variable Turbulence in Blooming Computations

In COMBO the turbulence is not varied as the blooming along the beampath is computed; instead only the final value is used. In SAICOM the distributive nature of turbulence is included in the integral calculation of the blooming parameter.

3.1.8.2 Extinction Calculations in Blooming Integral

In COMBO the linear power losses due to absorption and scattering are computed using $\exp[-\alpha_e(h)z]$ in the integrand whereas the expression should have been

$$\exp\left[-\int_0^z \alpha_e(h)dz\right].$$

This error causes an over-estimate of the extinction losses when firing downward and an under-estimate when firing upward. The appropriate correction has been made in SAICOM.

3.1.1.3 Power Variation

The reverse calculation option in COMBO involving calculation of the required power to deliver a desired intensity at a given range has been replaced in SAICOM. Now, whenever the intensity is calculated in a normal propagation run, the power is automatically varied between one-tenth the specified value and twice the original power. The output then lists the average intensity within the $1/e^2$ intensity area, the area over which the intensity is above a specified minimum value, and the total power available within that area. The equations used in these computations were discussed in Section 3.1.6. The user is allowed to stipulate the minimum intensity of interest through the input parameter OI. If the user does not specify the desired minimum intensity contour, the program automatically selects 10 kw/cm^2 .

3.1.8.4 Deletion of Weight and Volume Calculations

The technology projection portion of COMBO is an interesting but seldom used facet of the code. Therefore, it has been eliminated.

3.1.9 Summary of Equations

The basic equations used in SAICOM are as follows:

Average intensity in the $1/e^2$ intensity radius

$$I(Z) = \frac{\left[1 - (1 - 0.865 m_1 \frac{Z}{L})\right] P_T k_B e^{-\sum_i \int_0^Z \alpha_{ci}(Z') dZ'}}{\pi r^2(Z)}$$

where k_B = intensity reduction due to blooming
(sometimes written as KIP)
= $f(N)$

$$r^2(Z) = k_2 r_0^2 + k_3 \frac{r_0^2}{L^2} |L - Z|^2 + 4Z^2 \left[\left(\frac{0.3183 m_2 \lambda}{D} \right)^2 + \sigma_{TLT}^2 + \sigma_J^2 \right]$$

$$\sigma_J^2 = \sigma_{JHF}^2 + \sigma_{JLF}^2$$

$$\sigma_{TLT} = \frac{2.549}{\lambda^{1/5}} \left[\int_0^L c_H^2(Z) \left(\frac{L-Z}{L} \right)^{5/3} dZ \right]^{3/5}$$

The blooming parameter, N , is computed by

$$N = \frac{6.54}{\pi} \int_0^L \frac{1}{r(Z')} \int_0^{Z'} \frac{\left[1 - (1.865 m_1 \frac{Z}{L})\right] F(Z'') G(Z'') dZ'' dZ}{v(Z'') r^2(Z'')}$$

where

$$F(Z'') = P_T \sum_i \frac{P_i}{P_T} \alpha_{Ai}(Z'') e^{-\int_0^{Z''} \alpha_{ei}(Z'') dZ''}$$

$$r^2(Z'') = k_2 r_0^2 + k_3 \frac{r_0^2}{L^2} |L-Z|^2 + 4Z^2 \left[\left(\frac{0.318 m_2 \lambda}{D} \right)^2 + \sigma_{TST}^2 + \sigma_{JHF}^2 \right]$$

$$\sigma_{TST} = \left[1 - 0.37 \left(\frac{\ell_0}{D} \right)^{1/3} \right] \sigma_{TLT}$$

$$\ell_0 = \frac{1.439}{k^{1.2}} \left[\int_0^L C_N^2(Z) dz \right]^{3/5}$$

$$k = 2\pi/\lambda$$

$$G(Z'') = \frac{\frac{\partial \eta}{\partial T}(Z'')}{n(Z'') \rho(Z'') c_p(Z'')}$$

3.2 A USER'S GUIDE TO SAICOM

A brief description of the key features of the SAICOM code is given along with a discussion of how to operate the code. Users familiar with COMBO (Reference 11) should have little trouble with SAICOM since many of the subroutines are unchanged and the same modular format has

been retained. The basic structure of the executive routine (SAICOM) is shown in Figure 3.6. A substantial portion of this routine is devoted to initializing the input variables. As with COMBO, most of the input parameters are defined through a default namelist which requires the user to specify only those parameters which will differ from the default values. However, it should be noted that even if the propagation and optical train namelists are not used, namelist cards are required which read \$INPUT \$ and \$CASES \$, respectively. The optical train is called if the user specified PD; if PT is given, this subroutine is bypassed. A subtle point worthy of note is that when PD is given, SIGNF is assumed to refer to the device jitter only, and this term is combined with the four 10 jitters (THIR, THES, THAA, and THSV) given in namelist CASE to determine the high-frequency jitter of the total system.

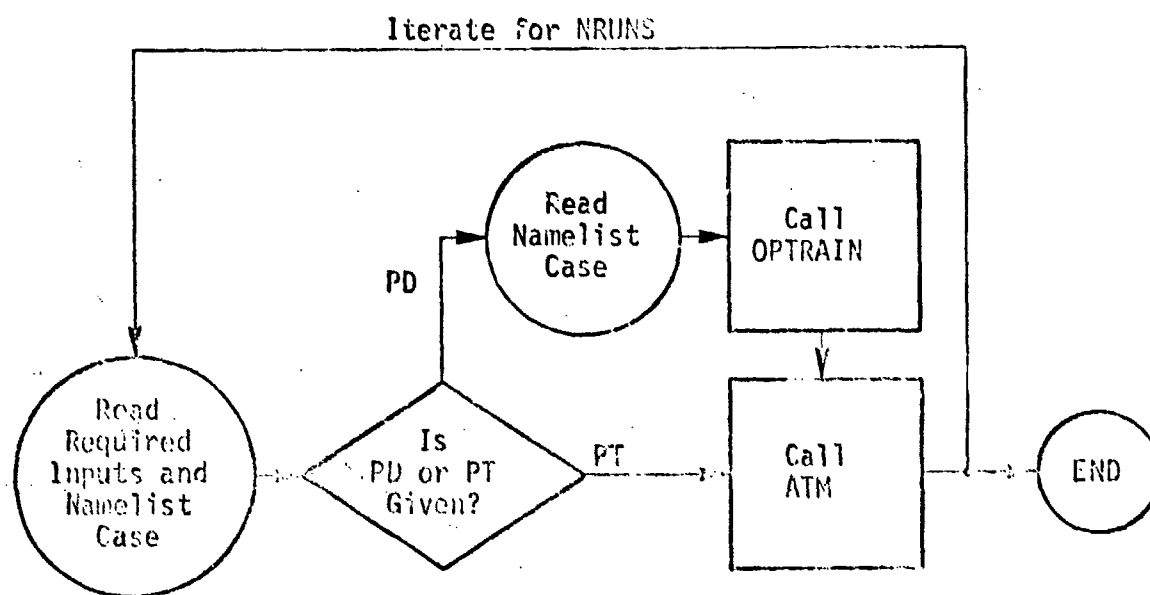


Figure 3.6 SAICOM Flow Diagram

Following these initialization activities, control is transferred to ATM, which handles the propagation calculations; control returns to SAICOM only after the calculations are completed and the results printed. Then SAICOM cycles through the same process until all of the specified cases have been completed.

In Table 3.2 a complete list of the SAICOM subroutines is given along with brief descriptions of their functions. Three of the subroutines, OPTRAIN, ATM, and BB, are discussed in further detail since they are the more important and complex portions of the program.

3.2.1 OPTRAIN

The calculation procedure within the Optical Train Model (OPTRAIN) is schematically shown in Figure 3.7. All inputs to the subroutine are passed through a labeled COMMON/OPTIN/statement and must be defined by the user prior to calling the subroutine. Following some initial calculations characterizing the input beam, the effect that each component within the optical train has on the transmitted power and beam quality is evaluated in a step by step manner. Although the specific elements within the optical train are fixed, i.e., aerodynamic window, beam clipper, mirrors, beam expander, and exit aperture, the user is allowed to specify, through the input parameters, different types of individual components such as cooled or uncooled mirrors, on-axis or off-axis beam expanders, and open port or material window exit apertures.

The output from the model is returned to the calling program via the labeled COMMON/OPTOUT/ and consists of (1) the diameter of the laser beam at the exit aperture, (2) the power in the beam, (3) the total beam jitter and (4)

Table 3.2 SAICOM Subroutines

<u>NAME</u>	<u>DESCRIPTION</u>
OPTRAIN	Calculation of Power Loss and Beam Degradations in the Optical Train.
ATM	Initialization of Propagation Parameters and Iteration of Reverse Calculations.
AA	Calculations for Laser and Target Above 100 km.
AB	Calculation for Laser Above 100 km and Target Below 100 km.
BA	Calculation for Laser Below 100 km and Target Above 100 km.
BB	Calculations for Laser and Target Below 100 km.
ALFSET	Sets Power Ratios for Multi-Line Propagation.
ALFFAC	Calculations of $\alpha_A e^{-\alpha_e z}$ and $e^{-\alpha_e z}$.
ALFAAB	Single Line Absorption Coefficients.
ALFAEX	Single Line Scattering Calculation.
CNSQ	Atmospheric Structure Constant.
KI	Computer Reduction in Intensity Due to Blooming.
GALTIN	Altitude Dependent Parameters Used in Blooming Integral.
MEGAIR	Pressure, Density and Temperature as a Function of Altitude.
VX	Calculation of Total Crosswind.

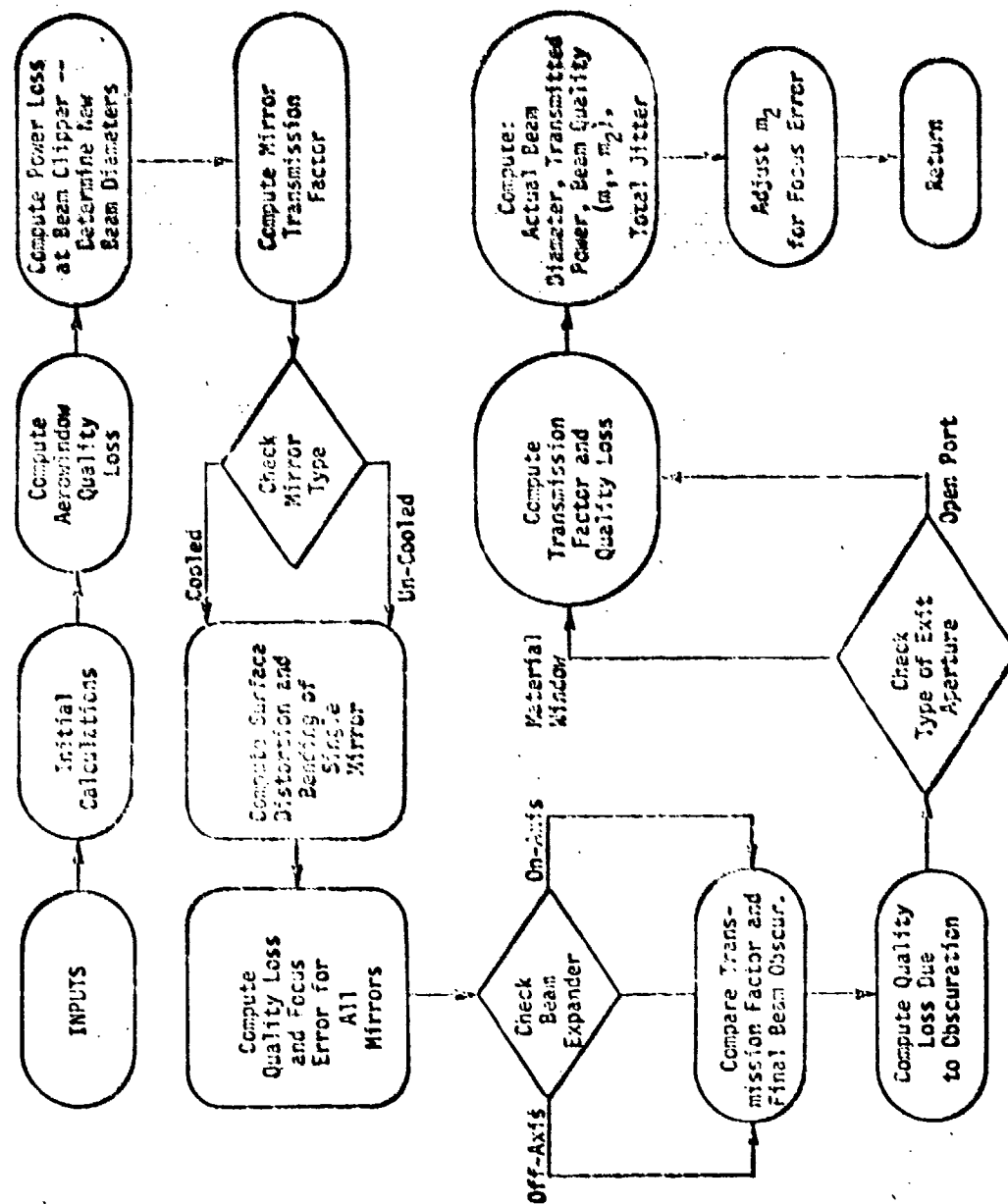


Figure 3.7 OPTRAIN Flow Diagram

two parameters (m_1 and m_2) characterizing the optical quality of the beam. The beam quality parameter m_2 is internally adjusted to account for any defocusing error induced by the high power mirrors in the optical train.

3.2.2 ATM

Part of the initialization process in ATM is to determine if the user has specified a negative wavelength (e.g., $-1.06\text{E}-5$ or $-3.8\text{E}-6$) which means the user is specifying his own single line absorption and scattering coefficients

$$\alpha_A = ABL * EXP (-ABE * R)$$

$$\alpha_S = SCL * EXP (-SCE * R)$$

or his own power ratios for the multi-line $3.8 \mu\text{m}$ propagation (see Figure 3.8). Note that single-line $3.8 \mu\text{m}$ propagation is available only if the user specifies his own coefficients. Also note that if one wishes to alter the power ratio, $PLINE(I)$, $I = 1, 2, 3$ without altering the built-in multi-line coefficients, simply set $LAMDA$ equal to $-3.8\text{E}-6$ and leave the absorption and scattering coefficients off namelist `USPEC`. The three power ratios need not total unity since the program is self-normalizing. The heart of ATM is the call to `AA`, `AB`, `BA`, or `BB` where the intensities for the pathlengths of interest are calculated. If `AB` or `BA` are called, they in turn call `BB` for those portions of the propagation path that lie below 100 km. Following the return to ATM, the beam displacement, eccentricity, contour data, breakdown power, optimum power, and effects of power variations are determined for straight propagation unless the propagation path is totally exo-atmospheric (`AA`), or the blooming parameter `NI` is less

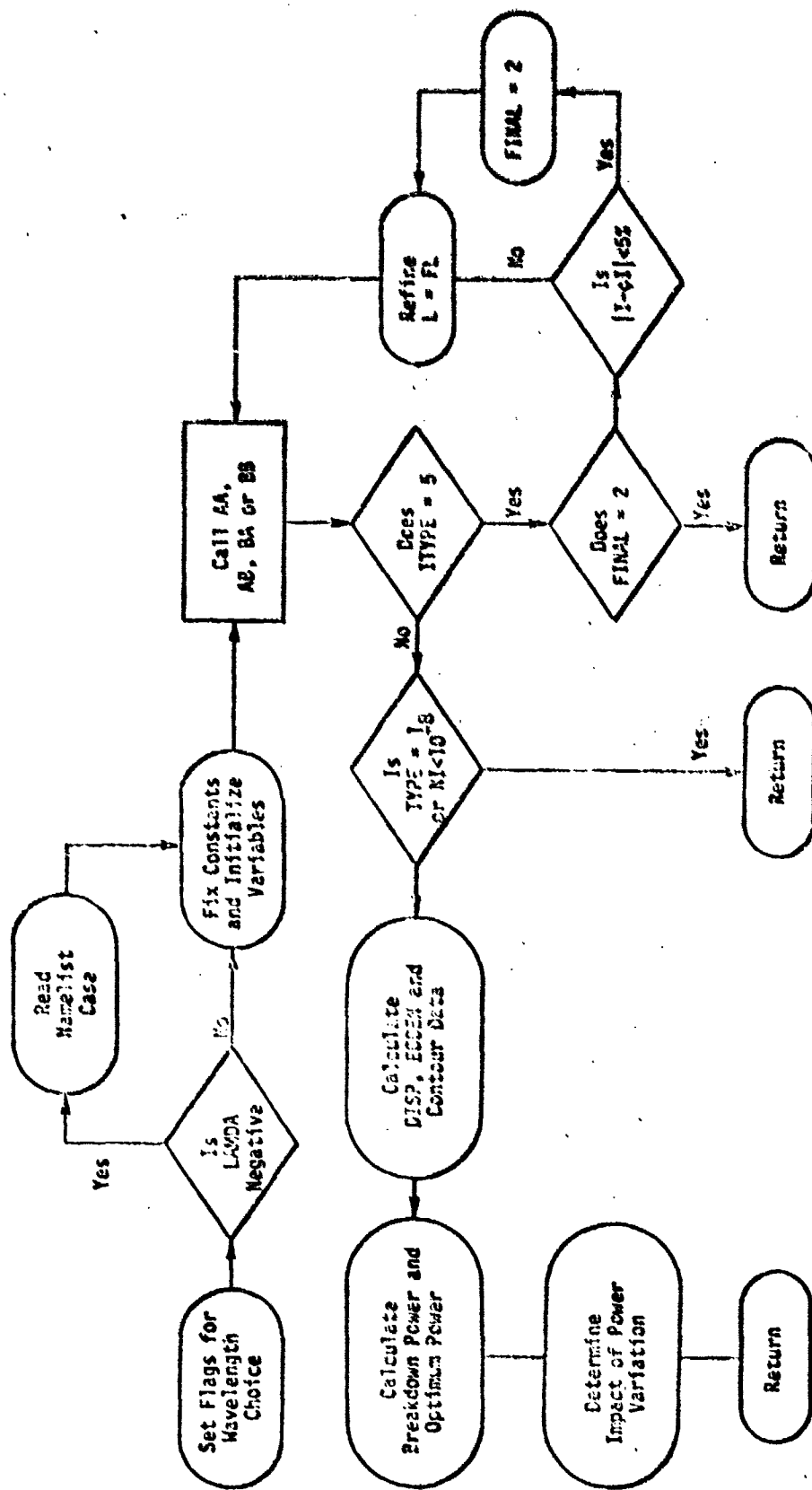


Figure 3.8 ATM Flow Diagram

than 10^{-8} . It should be noted that when the power is varied to compute the impact of propagating a beam that is more or less powerful than the specified level, the beam quality is not altered; this gives some error to the results since beam quality is affected by the total power transmitted through the optical train.

If the reverse propagation option (ITYPE = 5) has been chosen, the calculations are repeated using different target ranges (= focal ranges for ITYPE = 5) until the calculated intensity is within 5% of the desired value. If convergence is not achieved within 20 iterations, the program returns control to SAICOM and goes to the next case.

3.2.3 BB

In Figure 3.9, the logic flow for the BB subroutine is shown. All cases except AA use this subroutine to compute the atmospheric effects on the high-power beam propagation. The subroutine performs calculations at discrete points along the beampath. For calculations of the linear propagation effects, the pathlength intervals are fixed (NSTEP = 30 is the default value) while in the blooming loop the intervals are increased or decreased as required to minimize time and increase accuracy of the calculation. A series of linear or exponential extrapolations for the i^{th} interval based on the $i^{\text{th}} - 1$ interval are made and compared with the actual calculation for the i^{th} interval. If the comparison is unfavorable, the interval is decreased. If the comparison is favorable, the contribution from the interval is incorporated into the integral, if the comparison is unnecessarily good, the interval is increased. This procedure replaces the time-consuming multiple iterations used in CONBO.

3.2.4 Input Data

In Table 3.3 a list of the input parameters and their functions is given. This reference list does not

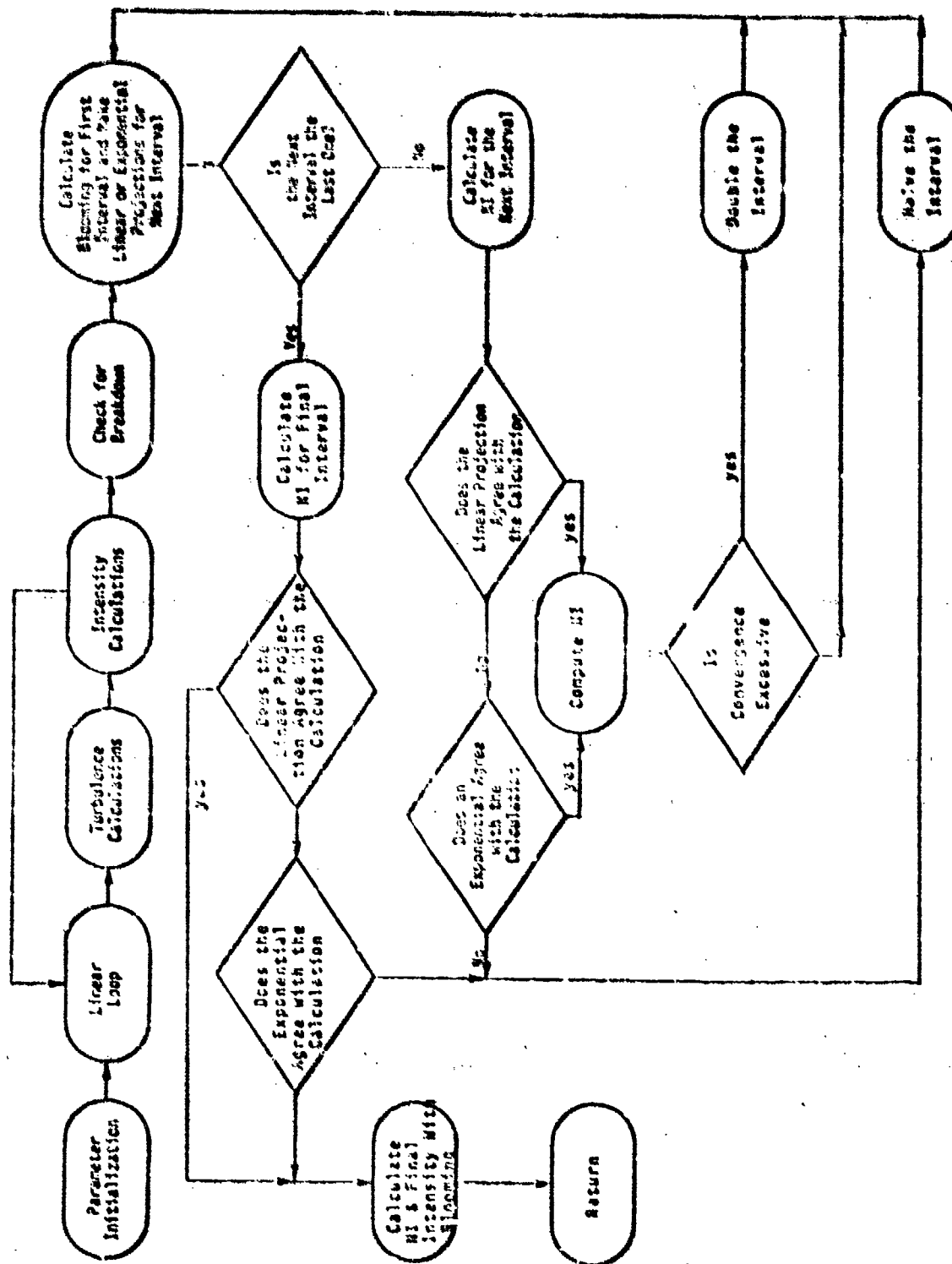


Figure 3.9. BB Flow Diagram

Table 3.3 Input Parameters

REQUIRED

ITYPE	If ITYPE = 5 reverse calculation is called with OI and PD or PT specific. All other entries will result in straight propagation.
PD or PT	User may stipulate either device power or telescope power; if IT is specified OPTIM is bypassed.
OI	Desired intensity of ITYPE = 5; otherwise it is the minimum intensity contour in the variable power calculation.
L	Range from laser to the target if ITYPE \neq 5; if ITYPE = 5, L is a first guess for the range.

OPTIONAL - NAMELIST/INPUT/

Beam	0 \Rightarrow Collimated, 1 \Rightarrow Focused.
CHI	Horizontal projection of beampath with respect to the direction of platform movement.
DEPUG	1 \Rightarrow no extra diagnostic statement, 2 \Rightarrow extra diagnostic statement.
FL	Focal length.
GL	Ground level.
HTM	Target altitude.
HOM	Laser altitude.

Table 3.3 (Continued)

OPTIONAL - NAMELIST/ INPUT/ (Continued)

LANDA	Wavelength 3.8x10 ⁻⁶ , 5.0x10 ⁻⁶ , and 1.06x10 ⁻⁵ are the acceptable values. A negative sign in front is a flag that the user will specify the multi-line power ratios or the single line absorption and scattering coefficients.
M	Beam quality.
NSTEP	Beampath intervals in the linear calculation.
OMEGA	Slowing rate.
OUT	1 ⇒ standard output, 2 ⇒ extra output.
PHI	Firing angle with respect to zenith. If PHI is specified HIM should not be given and vice versa.
PROP	1 ⇒ 1/e ² 2 ⇒ plane wave, truncated Gaussian 3 ⇒ infinite Gaussian.
RH	Relative humidity.
RI	Radius of obscuration.
RO	Outer radius of exit aperture.
SIGHF	High-frequency turbulence.
VP	Platform velocity.
VXB	Total crosswind across beam. If it is specified VP, OMEGA and natural wind are inoperative.
WTHR	-1 ⇒ high turbulence, low natural wind 0 ⇒ nominal turbulence and natural wind 1 ⇒ low turbulence, high natural wind.

Table 3.3 (Continued)

OPTIONAL - NAMELIST/CASE/

DB	Beam diameter coming from the laser.
EPS	Obscuration ratio.
DL	Pulse length.
XRI	Phase front curvature.
DIOVI	Peak-to-peak intensity fluctuation.
DLI	Scale size of fluctuation wrt beam size.
DELTAR	Aerowindow.
RREF	Aerowindow density divided by ambient density.
XLC	Distance from laser exit to beam clipper.
DC	Clipper diameter.
N	Number of mirrors in optical train.
REFL	Reflectivity of each mirror.
SFAB	Mirror fabrication error.
ITYPEI	Mirror type: 1 \Rightarrow cooled, 2 \Rightarrow uncooled.
XMLIR	Distance between mirrors.
XMAG	Telescope magnification.
ITYPEB	Telescope type: 1 \Rightarrow on-axis, 2 \Rightarrow off-axis.
XLEA	Exit aperture width.
BETA	Exit aperture absorption coefficient.
ASAB	Strut area/beam area.
ITYPEA	Type of exit aperture: 1 \Rightarrow material window, 2 \Rightarrow open port.

Table 3.3 (Continued)

OPTIONAL - NAMELIST/CASE/ (Continued)

THTR	Tracker jitter (1σ).
THBS	Boresight jitter (1σ).
THAA	Autoalignment jitter (1σ).
THSV	Servo jitter (1σ).

OPTIONAL - NAMELIST/USPEC/

PLINE (1)	Percent (or actual) power in line 1.
PLINE (2)	Percent (or actual) power in line 2.
PLINE (3)	Percent (or actual) power in line 3.
ABL	User specified linear absorption coefficient.
ABE	User specified exponential absorption coefficient.
SCL	User specified linear scattering coefficient.
SCE	User specified exponential scattering coefficient.

include the first two cards which must precede each set of runs. The first uses I2 format in columns 1 and 2 to state the number of cases (NRUN) which will be run, the second uses free-field format to allow the user to title each of the runs. The first card appears only once while the title card must precede each new case. Hence, the data stream is as follows:

NRUN CARD		
Title		
Required Inputs	}	Case 1
Namelist INPUT		
Namelist CASE		
Namelist USPEC (if required)		
Title	}	Case 2
Required Inputs		
Namelist INPUT		
Namelist CASE		
Namelist USPEC (if required)		

Table 3.4 provides a convenient work sheet format that may be used to specify each case. It includes a list of the default values and units. Those familiar with COMBO will recognize a change in some of the default values; the default statements now reflect sea level applications. Note that either PHI or HTM may be specified, but that PHI should always be given as a positive angle (measured from the zenith). A negative PHI is a flag that HTM was specified.

For additional convenience, Table 3.5 lists several of the important program flags which may be of interest to the user. A complete program listing and sample run is supplied along with a sample problem output in Appendix B.

Table 3.4 Sample Input Form with Default Values

Required	Type	Position	Units	Case 1	Case 2	Case 3
ITYPE ✓	(3,5)	12				
PD ² or PT	(3,5) (3,5)	11-20 21-30	w w			
OI ⁵ L	(3,5) (3)	31-40 41-50	w/m ² m			
Header						
Header Namelist "INPUT" Optional	Default		Units	Case 1	Case 2	Case 3
BEAM ✓	1 (focused)					
CHI	0.52		rad			
FL	L		m			
GL	0.		m			
HOM	50.		m			
HTN	10.		m			
LAMDA	3.E-6		m			
M	1.5					
NSTEP ✓	30					
OMEGA	0.		rad/sec			
OUT ✓	1 (short)					
PHI ³	-1.E-6		rad			
PROP ✓	1 (Gaussian)					
RH	0.5					
RI	.08		m			
RO	.35		m			
SIGHF	5.E-6					
SIGLF	5.E-6					
VP	15.		m/sec			
VXB	0.		m/sec			
WTHR ✓	0 (normal)					

Table 3.4 (Continued)

Namelist "CASE" Optional	Default	Units	Case 1	Case 2	Case 3
ASAB	0.05				
BETA	0.01	m ⁻¹			
DD	.16	m			
DC	0.166	m			
DELT	1.0	°K			
DELTAR	0.1				
DIOVI	0.5				
DLI	0.1	L/WT			
DI	2.0	seconds			
EPS	.35				
ITYPAW ✓	1 (focused)				
ITYPEA ✓	2 (open)				
ITYPEB ✓	1 (on-axis)				
ITYPEM ✓	1 (cooled)				
N	5				
RETL	0.985				
R1	1.170	m			
RR1F	2.5				
STAB	1./8.	vis lambda			
THAA	5.E-6	rad			
THBS	5.E-6	rad			
THSV	5.E-6	rad			
THTR	5.E-6	rad			
XLC	50.	m			
XLEA	0.05	m			
XMLIR	.15	m			
XMAC	4.375				
Namelist "USPEC" Optional	Default	Units	Case 1	Case 2	Case 3
Pline (1)	.338				
Pline (2)	.32				
Pline (3)	.342				
ADE	0.	m ⁻¹			
ABL	0.	m ⁻¹			
SCE	0.	m ⁻¹			
SCL	0.	m ⁻¹			

NOTES:

1. Check mark (✓) indicates "I" format is required.
2. User may specify either power exiting the device or telescope.
3. PHI need not be specified if HIM is given.
4. Although data on \$INPUT\$ card are optional, the card must be present even when all default values are to be used. The same applies to data card \$CASE\$. The namelist card \$USPEC\$ is only read when a negative lambda has been inserted on data card \$INPUT\$ as a flag.
5. If ITYPE = 5, OI is the desired intensity for the reverse calculation; otherwise it is the minimum useful intensity for the variable power tabulation (default value of 10^7 w/m²).

Table 3.5 Flags

<u>FORM</u>	<u>MEANING</u>
<u>Inputs</u>	
Negative LAMDA	The users will specify the multi-line power ratios or the single-line absorption and scattering coefficients.
Negative PHI	HTM is specified (Default).
<u>Internal</u>	
CNVRGD	TRUE => the last blooming interval passed over the end point.
ENDED	TRUE => this is the last blooming interval.
ERR	TRUE => the reverse calculations have not converged in 20 iterations.
FINAL	= 1, the reverse calculations have not converged yet; = 2, last pass through the propagation calculation.
FRACT	Tells the fraction of the last blooming interval that is within L.
LAM	= 1, 10.6 μm = 2, 3.8 μm (multi-line) = 3, 5 μm (single-line at present) = 4, user will specify single-line absorption and scattering coefficients.
OK	TRUE => save previous values for multi-line absorption and scattering calculations.

Table 3.5 (Continued)

<u>FORM</u>	<u>MEANING</u>
<u>Internal</u> (Continued)	
TYPE	= 1, AA = 2, BB = 3, AB = 4, BA.
UNIFRM	TRUE => last two blooming intervals were the same.

Section 4

SUMMARY OF TASKS I-IV

The purpose of this section is to briefly review the objectives and results of the original four tasks. Specific details may be found in the first and second interim reports (References 1 and 2). The primary objective here is to highlight some of the issues which arose during the course of the work and to indicate some of their implications as they relate to propagation modeling in general.

4.1 REVIEW OF TASK I. CODE COMPARISONS

The objective of Task I was to quantitatively compare the results obtained from three propagation codes over a parameter space representative of realistic engagement conditions. The codes were: NOLEC (Naval Surface Weapons Center); COMBO (Air Force Weapons Laboratory); ESP-I (United Aircraft Research Laboratories). The comparisons were presented at the First DOD Conference on High Energy Laser Technology on 3 October 1974 in San Diego (Reference 14). An unclassified version of this paper is included as an appendix in the first interim report (Reference 1). The major conclusions from these comparisons were that all three codes give comparable results for situations in which thermal blooming is not severe, but that ESP-I gives intensities up to an order of magnitude or more higher than the other two codes when blooming is significant. NOLEC and COMBO agree reasonably well under most conditions.

A secondary objective of Task I was to ascertain the reasons for major discrepancies between the codes. The effort was concentrated on COMBO and ESP-I since there is considerable disparity in their results even though they both use essentially the same approach for calculating thermal blooming. NOLEC uses an entirely different approach. In reviewing the theoretical basis of the codes, several issues were raised whose significance goes beyond the immediate objectives of the present work.

The blooming subroutines in both COMBO and ESP-I are based on the theoretical and experimental work of Gebhardt and Smith (Reference 20). The essence of the basic approach is the representation of the ratio of the bloomed and unbloomed focal plane peak intensities, I_{REL} , as a function of a single "blooming parameter," N . N is a theoretically derived, dimensionless, similarity parameter. However, the relationship between I_{REL} and N was obtained experimentally. Both COMBO and ESP-I use the same empirical relationship for $I_{REL}(N)$. They yield different results in blooming calculations because they compute N differently. The differences in the recipes for calculating N were identified explicitly in the First Interim Report (Reference 1). The question as to which method is more "correct" could not be resolved on theoretical grounds for several reasons.

1. An approximation to the theoretically derived expression for N was used in correlating the experimental data. The approximation was not generally valid even for the conditions of the experiments. It is even more questionable for realistic engagement-scale conditions such as those for which the simplified propagation codes are used.

2. COMBO uses the theoretical expression for N except for a relatively minor ad hoc correction. In principle, this has some important advantages, such as an inherent capability to treat non-coaltitude engagements. Unfortunately, it is not consistent with the empirical relationship used to correlate the experimental data.

3. ESP-I uses the same expression for N as was used for the empirical correlation. In that sense, it is at least consistent. However, it does not engender much confidence in the extrapolation from small scale laboratory experiments to realistic engagement conditions.

To summarize the situation, both COMBO and ESP-I use a semi-empirical blooming model which is flawed by a basic inconsistency between its theoretical and empirical components. The First Interim Report implies a preference for COMBO simply because it was in closer agreement with NOLEC. It should be emphasized, however, that this may be, at least to some extent, fortuitous. Furthermore, there does not exist sufficient data to provide convincing validation of any of the codes.

Evaluation of the codes on theoretical grounds in any kind of absolute sense was beyond the scope of the study, but two observations are in order. First, the consistency problem with the Gebhardt and Smith blooming model does not necessarily reflect adversely on its basic approach; the deficiencies are primarily associated with its implementation. Secondly, there are no clear and obvious theoretical reasons why either of the basic approaches should be superior in accuracy to the other. All of the codes incorporate numerous simplifying assumptions and approximations, both explicit and implied, and rely to some extent on heuristic arguments.

4.2 REVIEW OF TASK II. BEAM SHAPE AND DISPLACEMENT

The objective of this task was to develop empirical models for predicting beam shape distortion and displacement in the focal plane due to thermal lensing. Results from the NRL non-linear propagation code were used as the data base for the analysis.

Since beam distortion and displacement both are closely related to thermal blooming, I_{REL} (the reduction in peak intensity due to blooming) was used as the primary correlation parameter. This automatically accounts for much of the dependence on the independent parameters and has the further advantage of being readily computed from the NRL scaling law.

The beam displacement model is represented by

$$\left(\frac{d}{a_f}\right)^{\eta, 29} = \frac{-0.519 + \sqrt{(0.519)^2 + 1.500 \ln(1/I_{REL})}}{0.750}$$

where d is the displacement of the peak intensity into the wind, a_f is the e^{-1} beam radius (without blooming) in the focal plane, a_i is the e^{-1} beam radius in the source plane, and $\eta = a_f / a_i$.

The beam shape model represents the constant intensity contours as ellipses and the intensity distribution as

$$I(x,y) = I_{PEAK} \exp \left\{ -SD \left[\left(\frac{x}{a_f}\right)^2 + \left(\frac{y-d}{Da_f}\right)^2 \right] \right\}$$

where

$$D = 0.3 + 0.7 I_{REL}$$

$$S = I_{REL}$$

$$I_{PEAK} = \frac{P e^{-\alpha R} I_{REL}}{\pi a_f^2}$$

This model automatically gives the correct peak intensity and conserves total power. It also provides an excellent representation of the data in terms of the area within a given constant intensity contour and the eccentricity of the constant intensity contours.

These models, of course, are subject to the same limitations as the data from which they were derived. For example, they do not apply (unless suitably modified) in the presence of jitter or turbulence or when slewing is not in the same plane as the wind. Actually, the most significant result of this task is that both distortion and deflection are probably too minor to have a significant impact on system effectiveness.

4.3 REVIEW OF TASK III. BEAM QUALITY

The objective of this task was to develop an approach to modeling the effect of phase and amplitude aberrations in the aperture plane on the far-field beam profile. In more general terms, it was desired to obtain a rational approach to representing beam quality.

The recommended approach involves approximating the far-field intensity profile (neglecting blooming) as a Gaussian distribution of the form

$$I(R) = \frac{m_1 P_T e^{-\alpha_e R} \exp \left\{ - \frac{r^2}{2R^2 \left(\frac{m_2^2 \sigma_{DL}^2}{I_{REL}} + \sigma_J^2 + \sigma_T^2 \right)} \right\}}{2\pi R^2 \left(\frac{m_2^2 \sigma_{DL}^2}{m_1 I_{REL}} + \sigma_J^2 + \sigma_T^2 \right)}.$$

The parameters m_1 and m_2 are the proposed beam quality parameters and are determined so that the integrated power distribution corresponding to the above expression matches the actual distribution at two specified points, e.g., $r = w_f$ and $r = 2w_f$, where w_f is the beam waist.

This two parameter representation of beam quality is a significant advance over the usual "m x diffraction limited" concept. It can account both for power loss due to wide angle scattering and for beam spreading. It should be fully adequate to represent all situations in which the far-field beam profile is dominated by a central lobe. Furthermore, the general approach is sufficiently flexible that it can include effects associated with beam truncation and obscuration (see following section) as well as with other amplitude perturbations and with phase aberrations. For example, the simplified optical train model (OPTRAIN) described in Section 2 provides a method of estimating m_1 and m_2 for a wide range of system parameters.

4.4 REVIEW OF TASK IV. BEAM TRUNCATION AND OBSCURATION

The effect of truncation and obscuration were investigated both analytically and within the empirical framework of the beam quality model developed in Task III,

i.e., the results were presented in terms of the parameters m_1 and m_2 . Detailed results of the analysis are presented in Reference 2. Since the degree of truncation and obscuration is determined by the optical train, the model itself has been incorporated into the optical train model (Section 2).

Section 5

CONCLUSIONS

In any high technology program, like the DOD laser program, it is important that technologists and analysts work together to resolve the issues and support the efforts of the other group. During the early phases of a new program the technologists severely bound the problem under study to facilitate modeling of complicated processes. On the other hand, the analysts use extremely simplistic models for the elements of the system under study because they must address every aspect of the problem albeit in a naive manner. As time passes these two groups move closer together with the theoreticians studying ever increasing segments of the problem and the systems analysts improving their models and studying the issues in greater depth.

The atmospheric propagation coding studied under this contract is really second generation modeling. Improving the speed and accuracy of a program, adding multi-line propagation, and studying beam shape are exemplary of the movement of HEL system analysts toward increasingly complex modeling. One of the other areas investigated -- the optical train analysis -- is less well developed. The detailed tools for modeling the beam propagation through the optical train have been operational only recently. Hence, the simplified codings developed under this contract are first generation models. The authors hope that both of these modeling tasks will contribute to the continuing convergence of laser technology and systems analysis.

APPENDIX A

Molecular Absorption of DF Laser Radiation

A.1 INTRODUCTION

This appendix was written by Dr. T. Tuer of the Ann Arbor SAI office. This work was undertaken to provide better values for the molecular absorption coefficients used in the thermal blooming code. These coefficients are required as a function of both altitude and of atmospheric water vapor content for several "typical" DF laser line groups. Here, "typical" means a characteristic laser propagation-altitude function (this will be clarified in Section A.3). For convenience in the thermal blooming code, the coefficients are given as a simple analytical function of altitude and water content, with different sets of coefficients (i.e., one for each typical group).

A.2 APPROACH

Due to time constraints, it was decided to use McClatchey's DF absorption coefficients (Reference A.1) rather than re-calculating them with our own line-by-line codes. The ten BDL laser lines that McClatchey considered were selected for this study (see Table A-1). However, since McClatchey did not include the water continuum absorption in his calculations, it was necessary to add this component. A simple computer program DAFT (DF Altitude Fitting Code), was written to: (1) evaluate this continuum component for the frequencies, altitudes and model atmospheres desired, (2) add this to McClatchey's

results, and (3) plot the total absorption coefficient as a function of altitude.

Table A-1. List of DF-BDL Lines

DF Laser Line	Frequency (cm^{-1})	Relative Power	Considered by McClatchey and Here
P ₃ (8)	2546.37	10.7	yes
P ₃ (7)	2570.51	10.2	yes
P ₂ (10)	2580.16	6.2	yes
P ₃ (6)	2594.23	7.7	yes
P ₂ (9)	2605.87	9.7	yes
P ₃ (5)	2617.41	1.8	yes
P ₂ (8)	2631.09	12.9	yes
P ₂ (7)	2655.97	10.0	yes
P ₁ (10)	2665.20	3.9	yes
P ₂ (6)	2680.28	6.2	yes
P ₁ (9)	2691.41	9.1	no
P ₁ (8)	2717.54	6.6	no
P ₁ (7)	2743.03	3.5	no
P ₁ (6)	2767.91	2.0	no

The water continuum absorption coefficient is given by (Reference A.2).

$$n = c_S^0 \cdot w p_w^* + c_N^0 \cdot w p^*$$

where p_w is the partial pressure of water vapor, P is the total pressure and the $*$ indicates the density-equivalent-

pressures¹. This reference also gives measured values of $c_{s,w}^0$ as a function of frequency at 294° K², and recommends value of $c_{N,w}^0 = 0.12 c_{s,w}$. The absorption coefficient n differs from the usual coefficient k by:

$$k = nU/L$$

where U is the absorber thickness and L is the path length. Values for p^* , P^* and U were calculated as a function of altitude using data given by the Handbook of Geophysics and Space Environment (Reference A.3).

The attenuation of most of the DF laser lines is dominated by atmospheric water absorption (i.e., H₂O or HDO line absorption, or H₂O continuum absorption). In order to account for different atmospheric water content, the calculated absorption coefficient was normalized by:

$$k^* = k/\rho^*$$

Here ρ^* is a normalized water density-altitude profile which varies between a value of ρ_0^* at sea level, to unity as $h \rightarrow \infty$. The quantity ρ_0^* is the sea level density of the model atmosphere under consideration, normalized to that of the midlatitude summer model atmosphere. The form of ρ^* was arbitrarily taken to be:

$$\rho^* = 1 + (\rho_0^* - 1)10^{R/2}$$

1. Since the pressures are generally less than one atmosphere, we used the usual pressure in place of the density-equivalent-pressure.
2. Since the temperature dependency of this quantity is uncertain, its value at 294°K was used throughout.

where R is the normalized water density profile based on the data in Reference A.3 (see Figure A-1). An example of the effect of this scaling is shown in Figure A-2, where the absorption coefficient profiles for the five different model atmospheres are seen to collapse nicely into a narrow band.

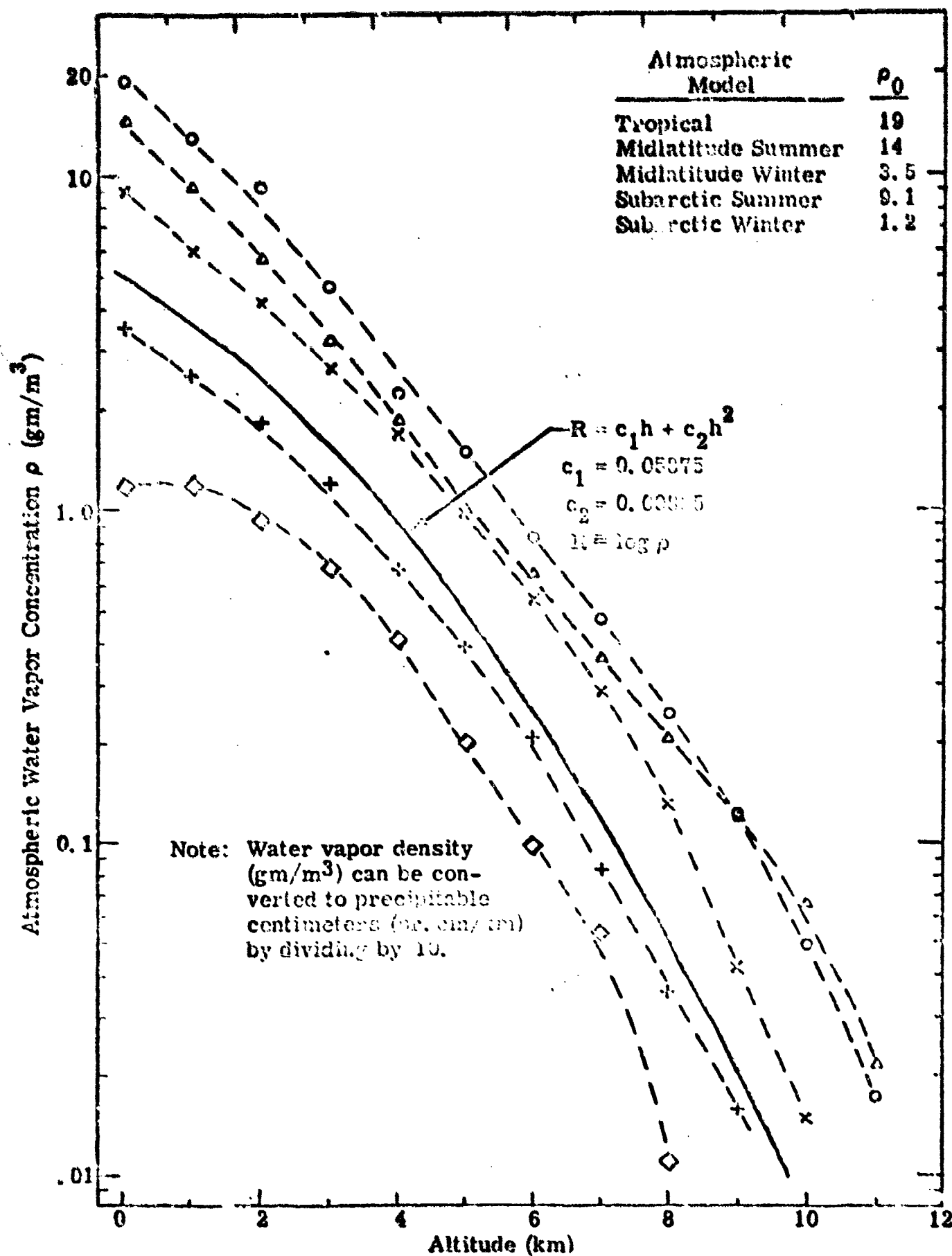


Figure A-1. Water Concentration Profiles for Five Model Atmospheres and Analytic Fit.

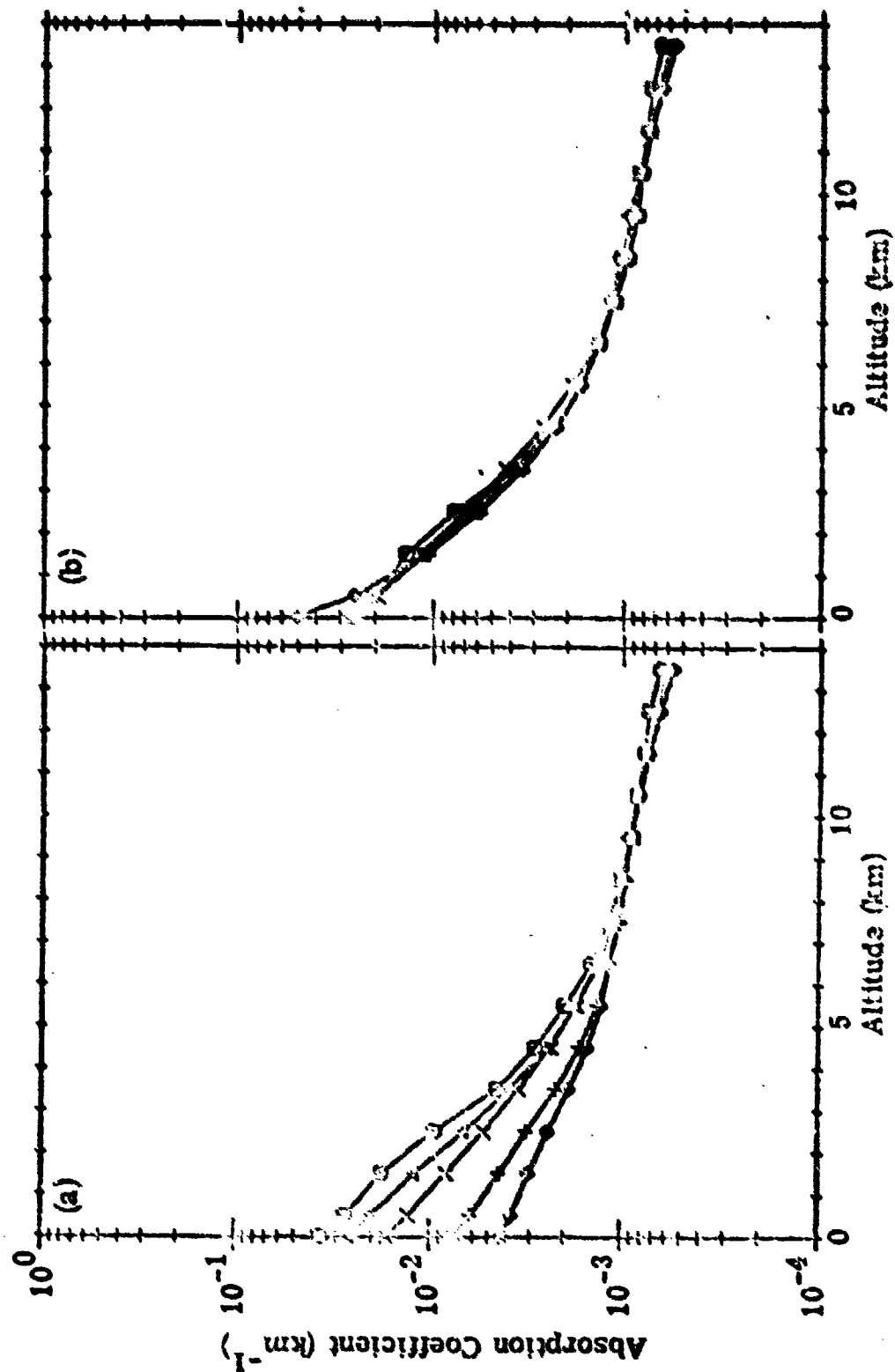


Figure A-2. Demonstration of the Effect of Scaling to Account for Various Atmospheric Water Concentrations - $P_2(8)$ DF Laser.
 (a) No Scaling
 (b) With Scaling

A.3 DETERMINING TYPICAL GROUPS

Normalized profiles for all the water dominated laser lines were plotted on a common scale. Of course the lines which are dominated by other species (e.g., N_2O line absorption), were not normalized in this fashion but simply plotted. These plots tend to collect in three general groups. Those laser lines which are dominated by water at low altitudes, but happen to fall on underlying absorption lines (Type A), have a knee in their profile (see Figure A-3). Those that do not have underlying lines (Type B), do not have a pronounced knee but continue to decrease with altitude, at least for the altitude range considered here (see Figure A-4). Lines which are not dominated by water (Type C), have no knee but fall off less rapidly with altitude (see Figure A-5).

The mechanism for each type can be elucidated by examining the details of the absorbing lines and continuum. Figure A-6 shows components of the absorption coefficient of a Type A laser line at sea level. Notice the underlying CH_4 absorption line (M2), which will become important at higher altitude as the absorption by water diminishes. Figure A-7 shows a Type B laser line where there is no important underlying absorption lines. Finally, a Type C laser line is shown in Figure A-8, which is dominated by N_2O absorption even at sea level, and is affected little by water.

A.4 RESULTS

A least squares fit was applied to each group of laser lines (i.e., Types A, B and C). The analytic form used was:

$$\ln k^* = A_0 + A_1 h + A_2 h^2$$

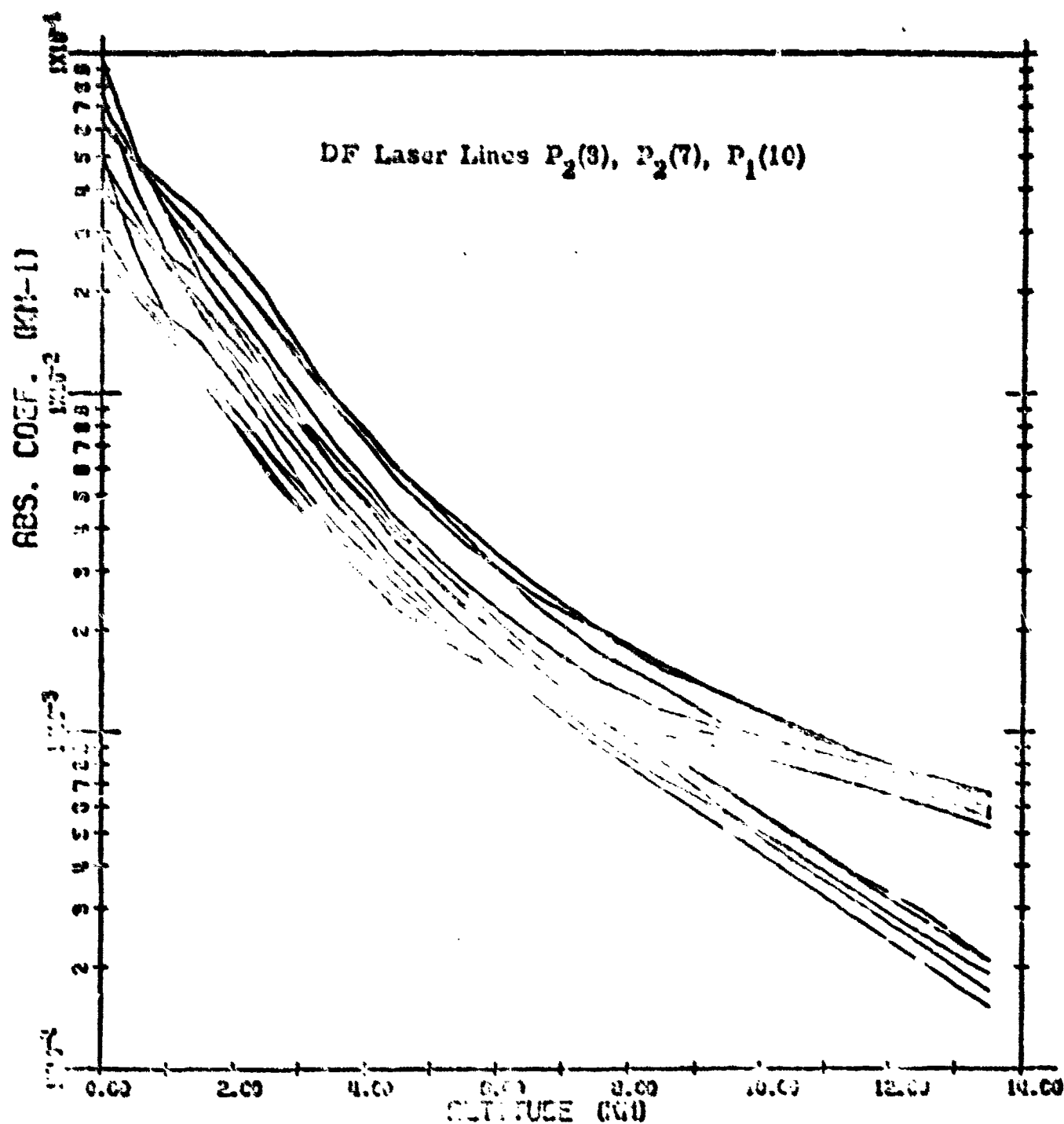


Figure A-3. Laser Propagation-Altitude Function Type A: Dominated by Water at Low Altitudes but with Underlying Absorption Lines which become Important at High Altitudes.

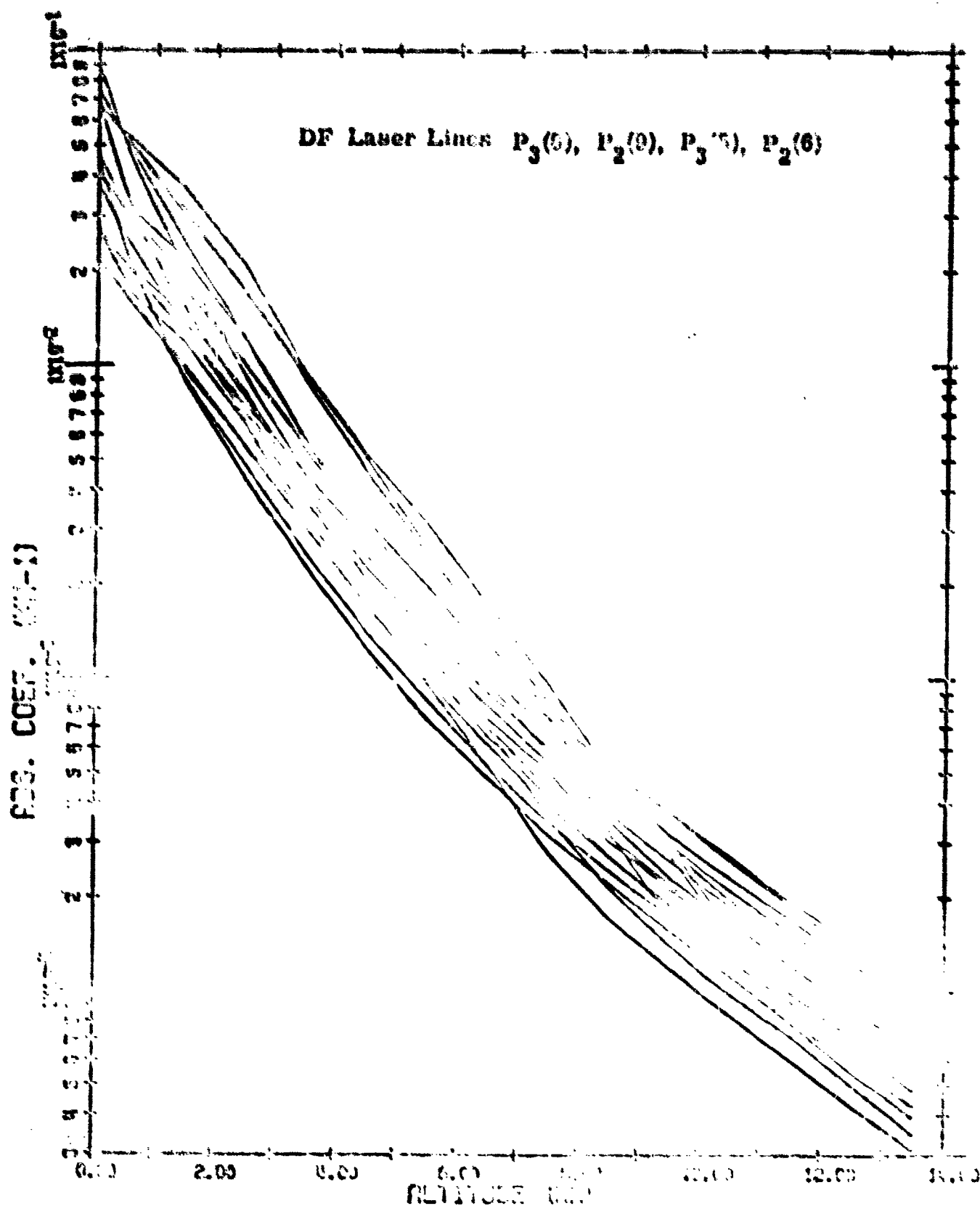


Figure A-4. Laser Propagation-Altitude Function Type B: Dominated by Water at Low Altitudes but with Underlying Absorption Lines which become Important at High Altitudes.

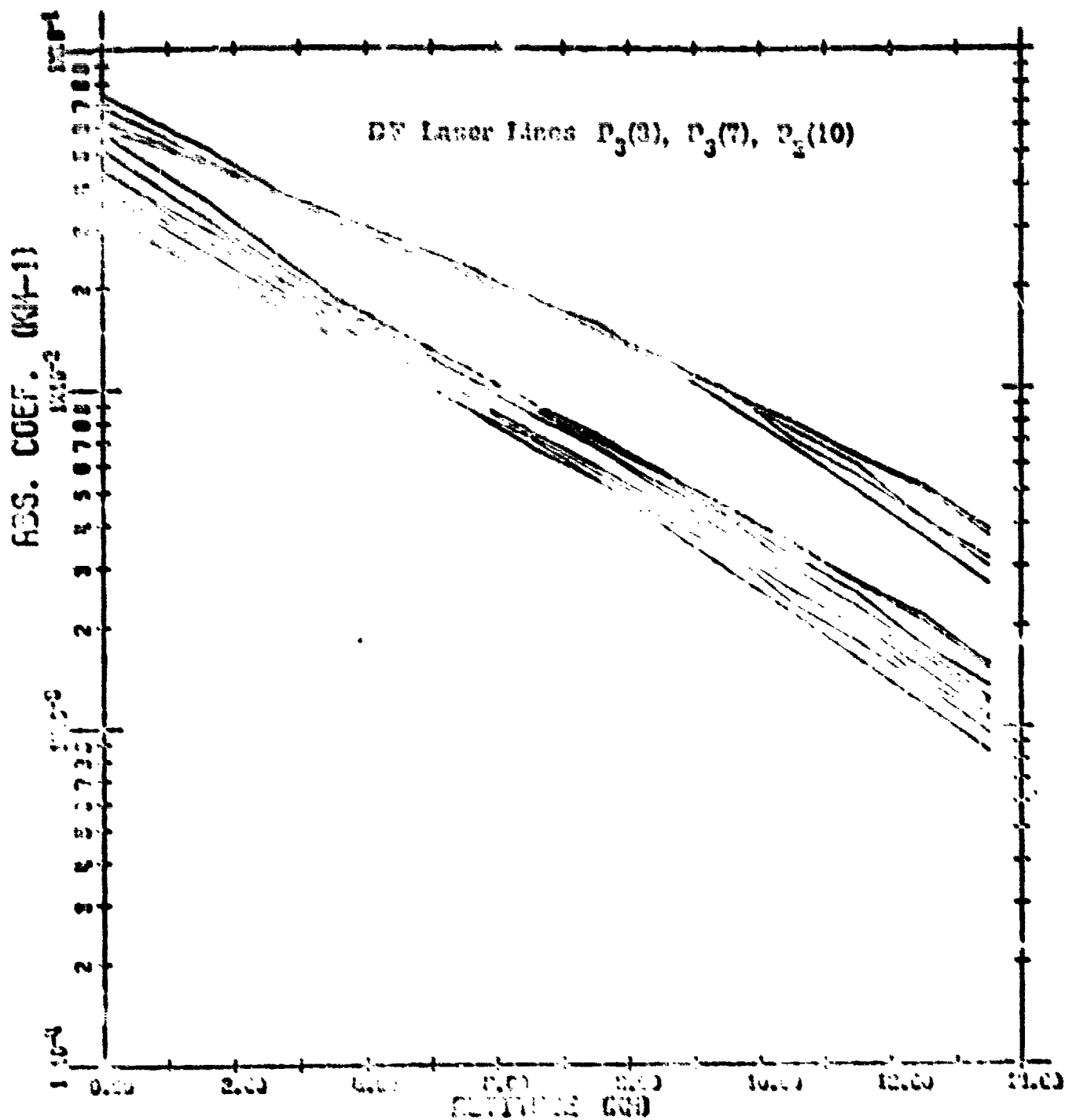


Figure A-5. Laser Prevention-Altitude Function Type C: Dominated by Water at Low Altitudes but with Underlying Absorption Lines which become important at High Altitudes.

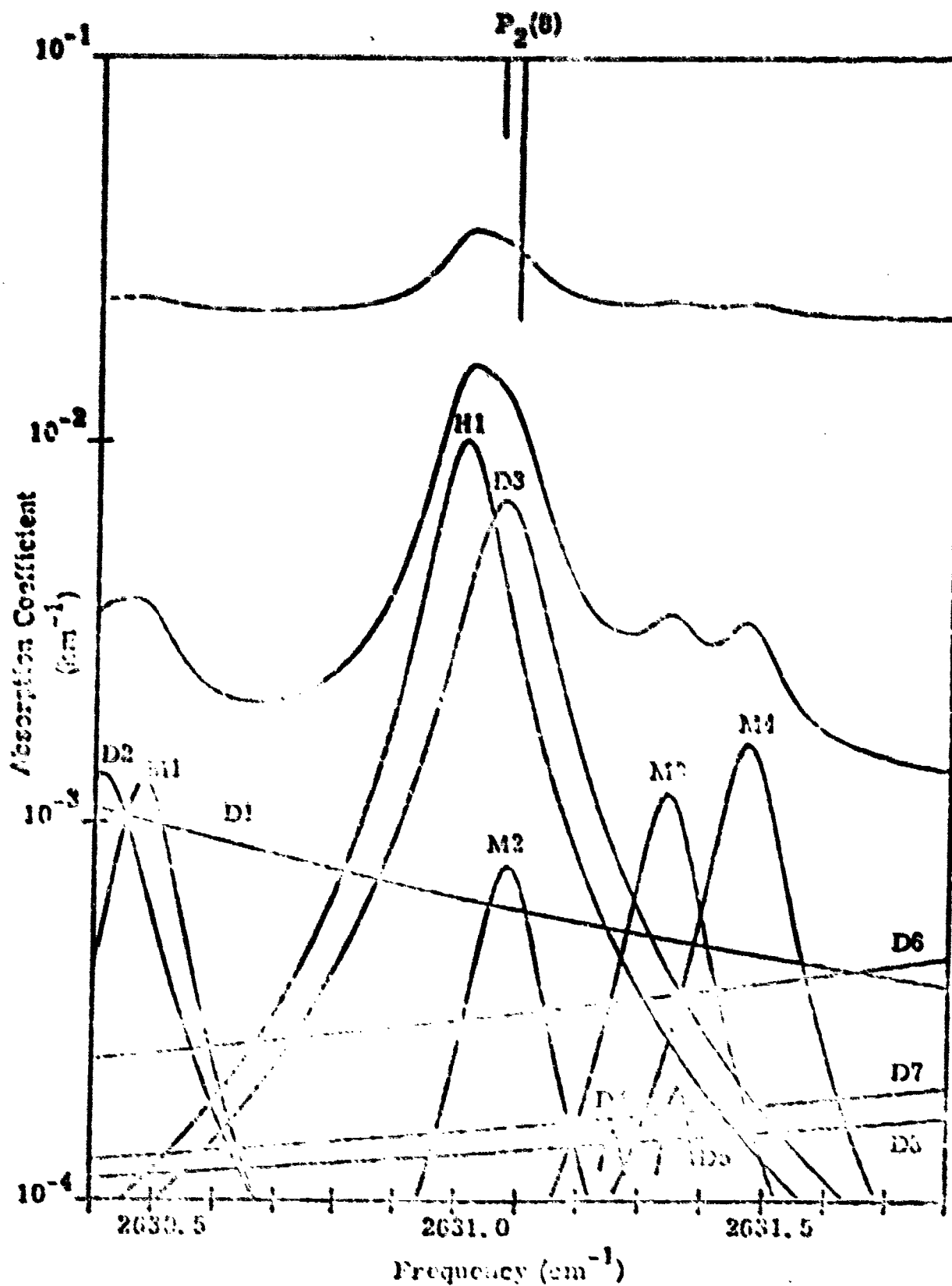


Figure A-6. Contributors to the Molecular Absorption of the $P_2(8)$ DF Line (Midlatitude Summer, Sea Level).

Example of Type A Absorption, Extracted from Ref. A.4.

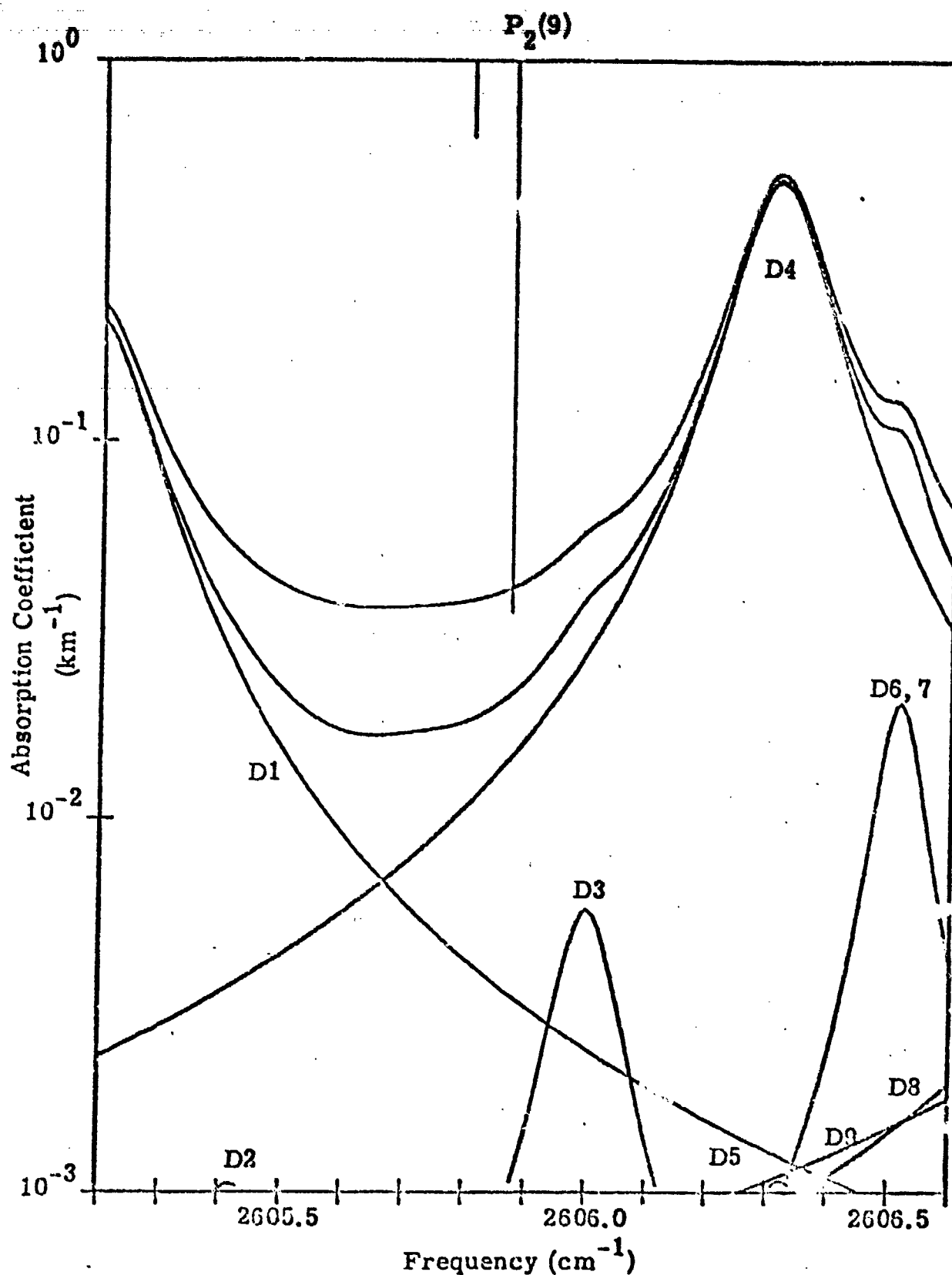


Figure A-7. Contributors to the Molecular Absorption of the P₂(9) DF Line (Midlatitude Summer, Sea Level).

Example of Type B Absorption, Extracted from Ref. A.4

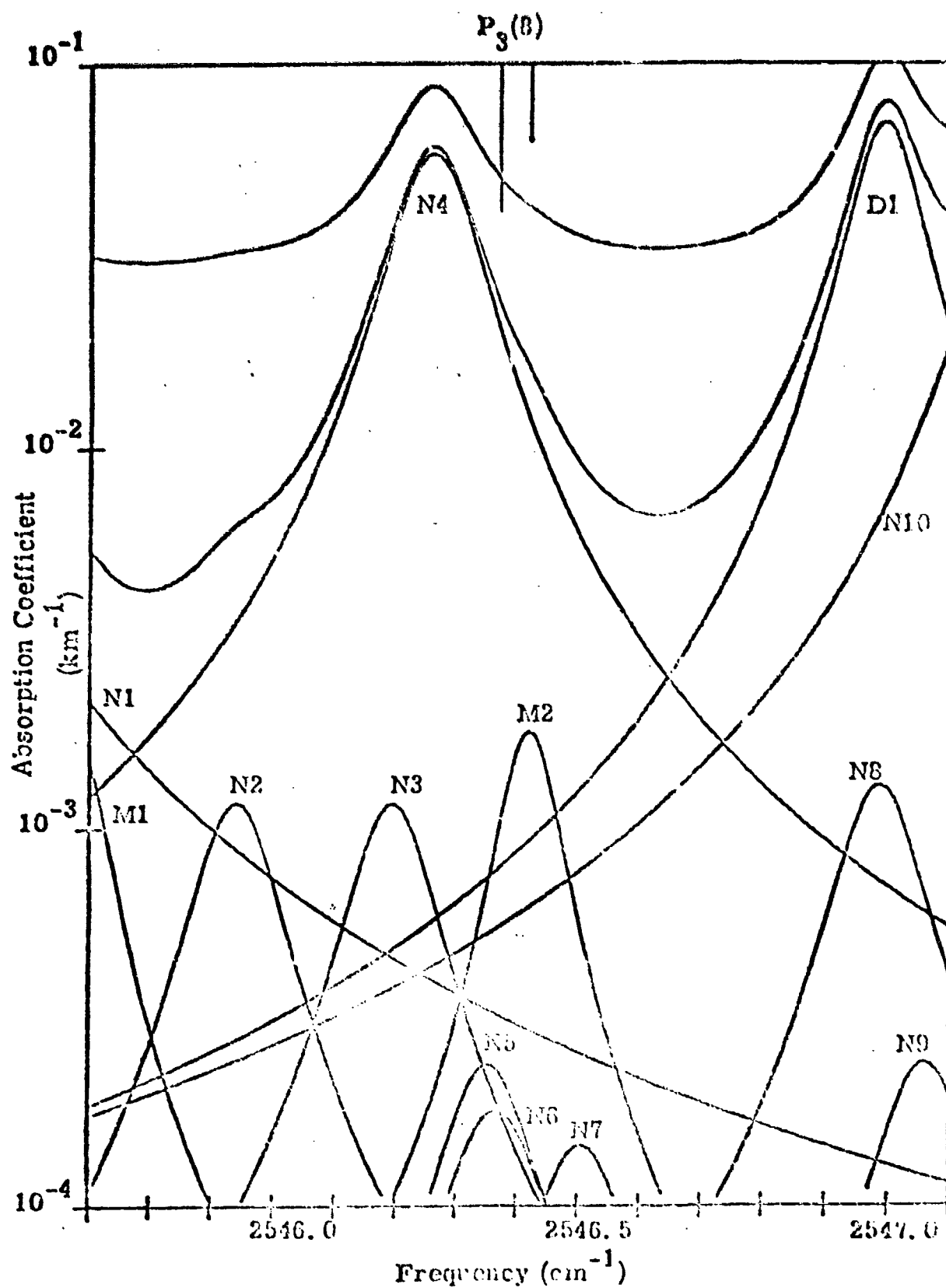


Figure A-8. Contributors to the Molecular Absorption of the $P_3(8)$ DF Line (Midlatitude Summer, Sea Level).

Example of Type C Absorption, Extracted from Ref. A.4

where k^* is the normalized absorption coefficient (km^{-1}) and h is the altitude (km). The results of this fit for each group are shown in Figures A-9 through A-11, and the determined coefficients (i.e., A_0 , A_1 , A_2) given in Table A-2.

Table A-2. Coefficients of Least Squares Fit

Type	DF Laser Lines	A_0	A_1	A_2
A	$P_2(8)$, $P_2(7)$, $P_1(10)$	-3.138	-0.6388	0.0225
B	$P_3(6)$, $P_2(9)$, $P_3(5)$, $P_2(6)$	-3.173	-0.6952	0.0155
C	$P_3(8)$, $P_3(7)$, $P_2(10)$	-3.039	-0.2199	-0.00196

For Type C laser lines this normalized coefficient k^* is identical to the un-normalized coefficient k (since water absorption is insignificant):

$$k = k^* \quad (\text{for Type C})$$

Type A and B lines must be un-normalized by:

$$k = \rho^* k^* \quad (\text{for Types A \& B})$$

where $\rho^* = 1 + (\rho_0^* - 1) 10^{R/2}$ and: $\rho_0^* = 1 + ((\rho_0^* - 1) 10^{R/2})$ and:

$$R = C_1 h + C_2 h^2$$

with $C_1 = 0.05375$ and $C_2 = 0.00835$.

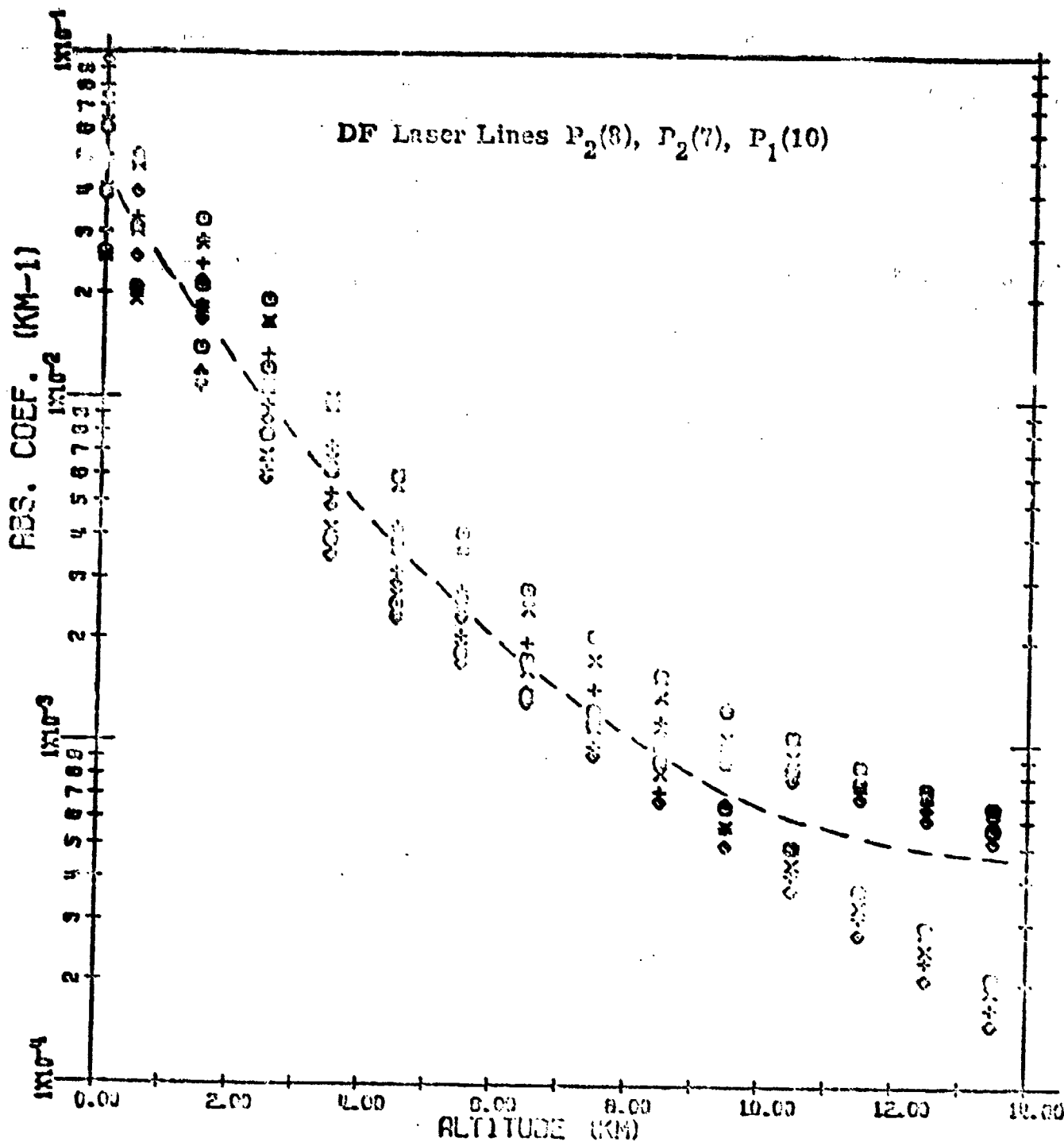


Figure A-9. Least Squares Fit to Type A Laser Lines

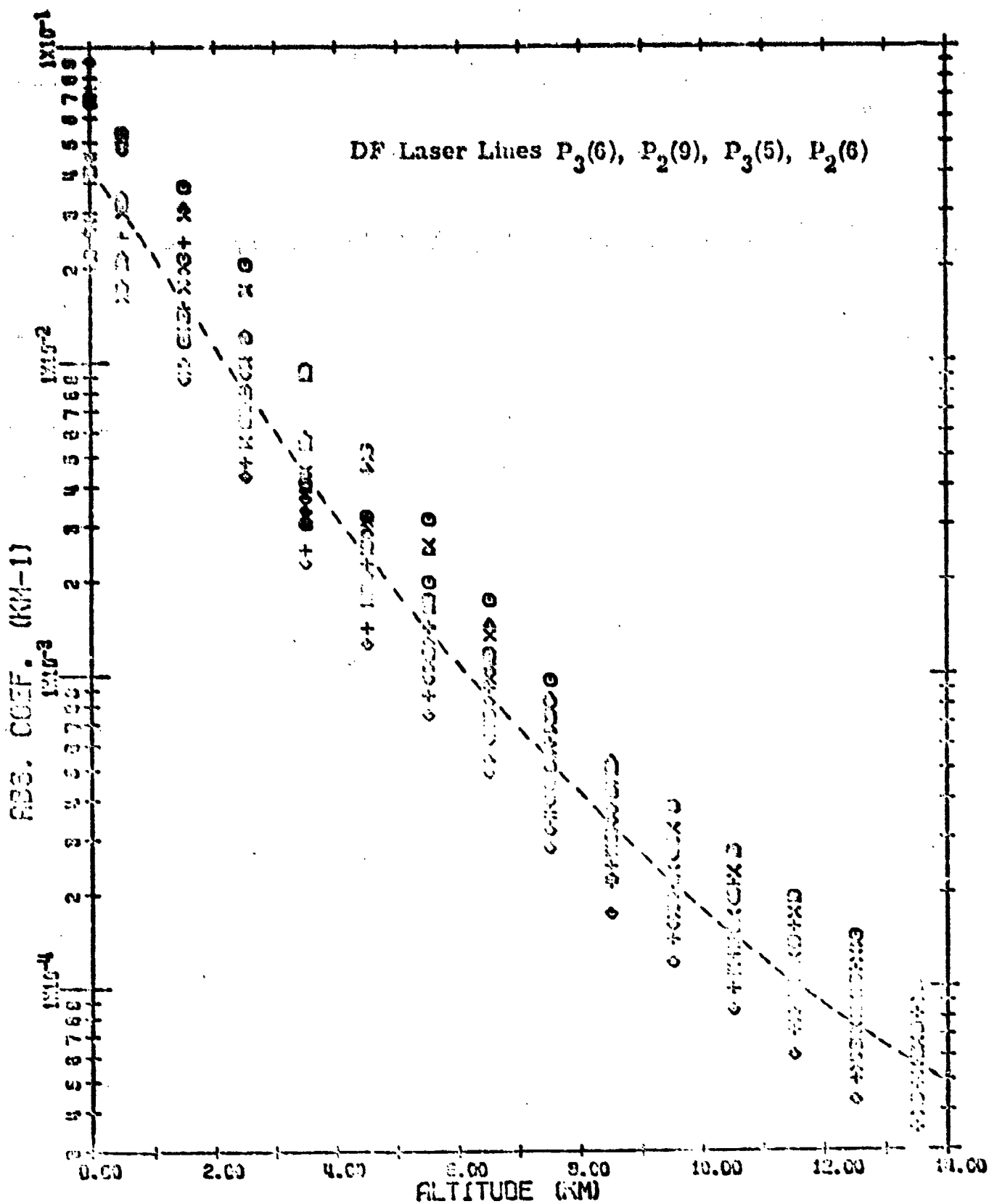


Figure A-10. Least Squares Fit to Type B Laser Lines

Reproduced from
best available copy.

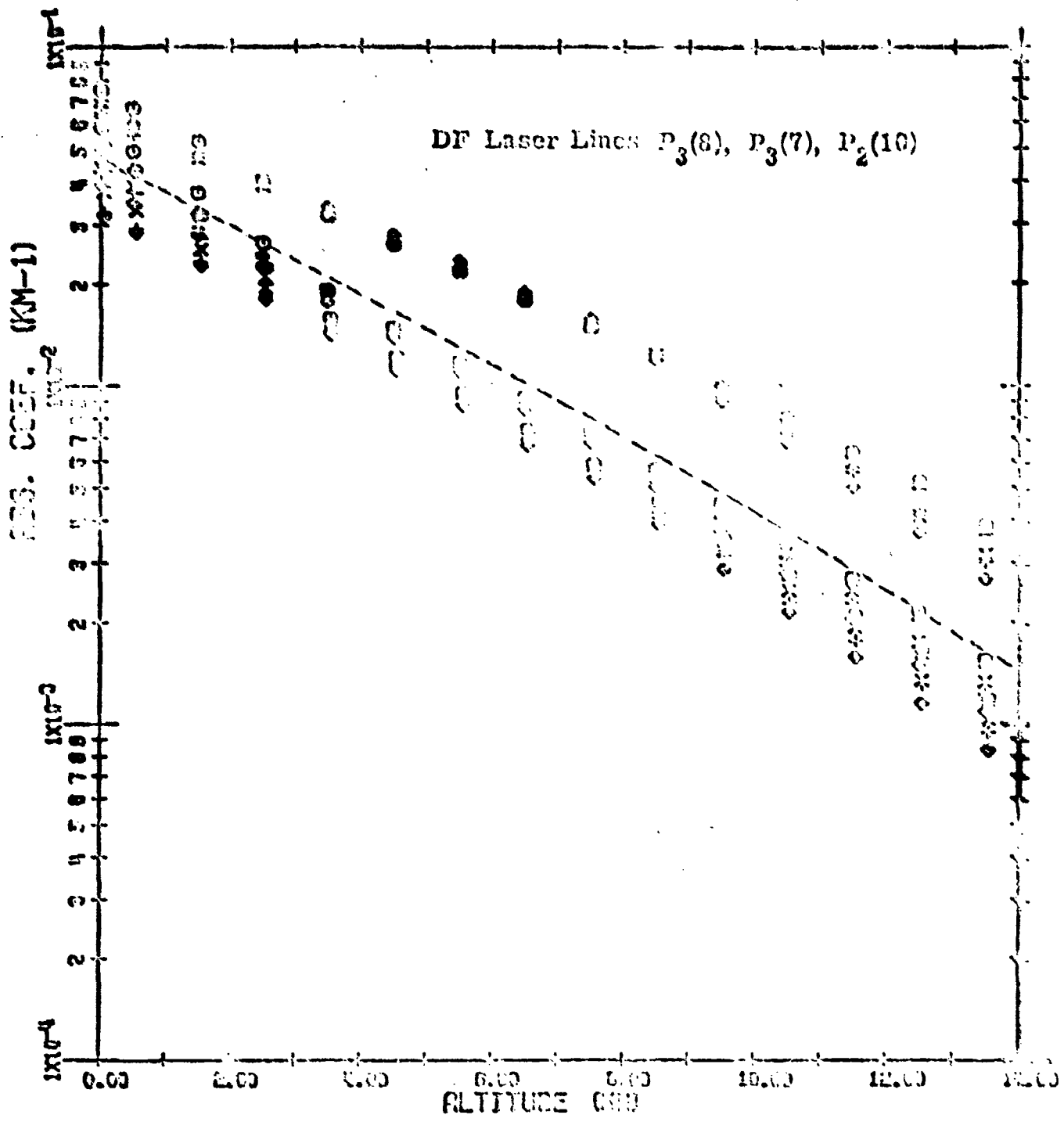


Figure A-11. Least Squares Fit to Type C Laser Lines

APPENDIX B

SECRET

175
180
185
190
195
200
205

171
172
173
174
175
176
177
178
179
180
181
182
183
184
185
186
187
188
189
190
191
192
193
194
195
196
197
198
199
200
201
202
203
204
205
206
207

C
7
8
9
10
11
12
13
14
15

FORMAT (I2)
FORMAT (7A10)
FORMAT (I2,AX,6E10.0)
FORMAT (I4I,30A,7A10/)
FORMAT (///,10X,A5,20H OUTPUT FORMAT, WITH, A10, //, 10X, 40H TARGET RAN
1GE (L) -----, 1PE10.3, 0 METERS, 5A, 34H DEVICE POWER SIC
2 (PD) -----, E10.3, 0 WATTS, //, 10X, 40H FOCAL DISTANCE (FL) SIC
3 -----, E10.3, 0 METERS, 5A, 34H POWER OUT OF THE TELESCO SIC
4PE (PT) ---, 1PE10.3, 0 WATTS, //)
FORMAT (///, 10X, A5, 20H OUTPUT FORMAT, WITH, A10, //, 10X, 40H DESIRED I SIC
INTERSTITY (OI) -----, 1PE9.2, 0 WATTS, //, 10X, 40H 2A24H DEVICE SIC
2 POWER (PD) -----, E10.3, 0 WATTS, //, 10X, 40H FOCAL DISTANCE SIC
3E (FL) -----, 0PE9.0, 0 METERS, 5A, 34H POWER OUT OF TM SIC
4E TELESCOPE (PT) ---, 1PE10.3, 0 WATTS, //)
FORMAT (10A, 40H GROUND LEVEL (GL) -----, 0PE5.0, 0 SIC
1 METERS, 5A, 34H WAVELENGTH (LWDA) -----, 1PE9.2, 0 METERS SIC
2, // 10A, 40H DEVICE ALTITUDE (HGM) -----, E9.2, 0 METERS, SIC
3A, 40H INPUT JITTER (HIGH FREQUENCY) ---, 1PE9.2, //, 50H, 1PE9.2, 0 FE SIC
4E10.21A, 0 (LOW FREQUENCY) ---, 1PE9.2, //, 10X, 40H TARGET ALTITU SIC
5DE (MI) -----, E9.2, 0 METERS, 5A, 34H HACKING RATE 1CM SIC
6E10A) -----, 0PE5.2, 0 PADIANS/SEC, //, 50A, 1PE9.2, 0 FEET, 0A, SIC
8 OPTICS RADIUS (R0) -----, 0PE6.2, 0 METERS, //, 10X, 0H VENTICA SIC
7L ANGLE (PM) -----, E7.3, SIC
8 0 RADIANS, 0A, 0H OSCILLATION RADIUS (RI) -----, 0, F6.2, SIC
9 0 METERS, //)
FORMAT (10A, 0H AZIMUTH ANGLE (CM) -----, 0, F7.3, SIC
10 RADIANS, 0A, 0H FEAM TYPE (PROM) -----, 0, A10, //, 10A, SIC
20 PLAZFORM VELOCITY (VP) -----, 0, F7.0, 0H (EIMS/SEC, 5A, SIC
30 TYPE OF PROPAGATION (BEAM) -----, 0, A10, //, 10X, 0H SPECIFIED CROSS SIC
4 WIND (VAM) -----, 0, F6.2, 10A, 0H AREA QUALITY (M) -----, 0, SIC
5 -----, 0, F6.2, //, 10A, 0H SEVERITY OF TURBULENCE (WIR) -----, 0, SIC
6A6-15A, 0H NUMBER OF BEAMPATH INCREMENTS -----, SIC
612, //, 10A, 0H RELATIVE HUMIDITY (RH) -----, 0, F4.2, // SIC
FORMAT (10A, 0H RESULTANT BEAM QUALITY, 5A, 0A) = 0, F5.3, 5A, 0A2 = 0, SIC
1F5.3)
END


```
167 OPT
168 OPT
169 OPT
170 OPT
171 OPT
172 OPT
173 OPT
174 OPT
175 OPT
176 OPT
177 OPT
178 TCP
179 OPT
180 OPT
181 OPT
182 OPT
183 OPT
184 TCP
185 OPT
186 OPT
187 OPT
188 OPT
189 OPT
190 OPT
191 OPT
192 OPT
193 OPT
194 OPT
195 OPT
196 OPT
197 OPT
198 OPT
199 OPT
200 OPT
201 TCP
202 OPT
203 OPT
204 OPT
205 OPT
206 OPT
207 OPT
208 OPT
209 OPT
210 OPT
211 OPT
212 OPT
213 OPT
214 OPT
215 OPT
216 TCP
217 OPT
218 OPT
219 OPT
220 OPT

T6=(T2/T4-Y)/T5
X=X-T6
IF (ABS(T6)-GT.1.E-5) GO TO 17
M2=SQRT(X)
M1=M1/T2

TRANSMISSION
T=TC+TM+TBE+TEA
P=I*PI

C
C
C
C
JITTER
TH=SQRT((THTR**2+THSV**2+THBS**2+THE**2+(THI**2+THAA**2)/(MAG**2)))
WRITE (6,23)
WRITE (6,24)
WRITE (6,25) BLK,ONE,SI,ZR,BLK,ONE,SAW,ZR,BLK,TC,ZR,ZR,MM(ITYPEM),
1TH,SM,LM,MM(ITYPEM),TRE,SBE,LBE,HEA(ITYPEA),TEA,SEA,DLI,BLK,T,S,LT
WR=1.0*(3.14159*DB*DB/(4.0*WL*R2))**2
WR=SQRT(WR)
XM2=M2
M2=WR*M2
WRITE (6,26) DB,P,M1,XM2,WR,M2
WRITE (6,27) TH,R2
RETURN

C
18
19
FORMAT(10X,30(1H*),*INPUT TO OPTICAL TRAIN*,30(1H*))
FORMAT(20X,*LASER BEAM DIAMETER
1 20X,*LASER POWER
2 20X,*WAVELENGTH
3 20X,*OBSCURATION
4 20X,*BEAM QUALITY
5 20X,*PULSE LENGTH
6 20X,*PHASE FRONT CURVATURE
7 20X,*JITTER
8 20X,*INTENSITY FLUCTUATIONS
FORMAT(20X,*SCALE SIZE OF FLUCTUATIONS
X 20X,*TYPE OF AEROWINDOW
1 20X,*AEROWINDOW DELTA RHO/RHO
2 20X,*RHO/RHO REF
3 20X,*DISTANCE TO CLIPPER
4 20X,*CLIPPER DIAMETER
5 20X,*NUMBER OF MIRRORS
6 20X,*REFLECTIVITY
7 20X,*FABRICATION ERROR
8 20X,*TYPE OF MIRRORS
21
FORMAT(20X,*DISTANCE BETWEEN MIRRORS
1 20X,*TELESCOPE MAGNIFICATION
3 20X,*TELESCOPE DIAMETER
4 20X,*TELESCOPE TYPE
2 20X,*TYPE OF EXIT APERTURE
5 20X,*EXIT APERTURE LENGTH
6 20X,*ABSORPTION COEFFICIENT
X 20X,*TEMPERATURE FLUCTUATION
7 20X,*STIPUT AREA/ BEAM AREA
22
FORMAT(20X,*TRACKER JITTER
1 20X,*HOME-SIGHT JITTER
2 20X,*SERVO JITTER
3 20X,*STIPUT IGNITION JITTER

*G12.4,* METERS*/
*OPG12.4,* WATTS
*E12.4,* METERS*/
*OPG12.4,*
*G12.4,*
*G12.4,* SECONDS
*G12.4,* METERS*/
*OPG12.4,* RADIANS
*G12.4,* PEAK-TO-PEAK*
*G12.4,* L/WT
*G12.4,*
*G12.4,*
*G12.4,*
*G12.4,* METERS*/
*OPG12.4,*
*G12.4,* METERS*/
*G12.4,*
*G12.4,*
*G12.4,* VIS. LAMBDAS*/
*G12.4,* METERS*/
*OPG12.4,*
*G12.4,* METERS*/
*G12.4,*
*G12.4,* METERS
*OPG12.4,* METERS-1
*G12.4,* DEG K
*G12.4,*
*G12.4,* RADIANS
*G12.4,* RADIANS
*G12.4,* RADIANS
*G12.4,* RADIANS
```

04/06/73 13.10.03.

FTN 4-0-P357

TRACE

097-9

73/76

SUBROUTINE OPTRAIN

[illegible]

IF (REAM.EQ.1) GO TO 4
(COLLIMATED)

GS=0.
G4=1.

SET CONSTANTS AND VARIABLES

G3=1.-.865*H1
COFF2=PI/PI
COFF3=.865*H1*PI
EXPXAS=1.

FINAL=2

FIVE3=5./3.

FIVE9=5./9.

HOM=HOM*GL

HTM=HTM*GL

IFLAG=1

IW=ATHR*2

KAS=0.

KOUNT=0

LCOUNT=0

M=M2

MSQ=M*4

OM=1.05*O1

OIL=.95*O1

PO=1

R0SQ=R0*R0

R1G=R0*10.

SIGSO=SIGLF**2+SIGMF**2

ZPHEV=0.

SIGMAH=0.3183*M2*LAMDA/(R0*2.)

SIGMAR=SIGMAR*SIGMAR

SIGMA=SQRT(SIGRSQ+SIGSO)

SIGASQ=SIGMA*SIGMA

SIGMAT=0.

Z=0.

IF (ITYPE.NE.5) GO TO 5

C CALCULATE L FOR REVERSE PROPAGATION--O1 AND PT KNOWN

FL=L

IF (L.GY.0.) GO TO 5

NU=.865*PI*M1-PI*G4*R0SQ*O1

L=SQRT(-NU/(4.*PI*O1*SIGASQ))

IF (DEHUG.EQ.2) WRITE (6,33) NU*L

IF (L.LT.R10) L=100.

FL=L

C CALCULATE PHI OR HTM

CPHI=.FALSE.

IF (PHI.LT.0.) GO TO 6

COSPHI=COS(PHI)

HTM=HOM*L*COSPHI

GO TO 7

CPHI=.TRUE.

HO=HTM-HOM

HOP=ABS(HO)

NHD=1

IF (HOP.NE.HO) NHD=-1

ATM 59
ATM 60
ATM 61
ATM 62
ATM 63
ATM 64
ATM 65
ATM 66
ATM 67
ATM 68
ATM 69
ATM 70
ATM 71
ATM 72
ATM 73
ATM 74
ATM 75
ATM 76
ATM 77
ATM 78
ATM 79
ATM 80
ATM 81
ATM 82
ATM 83
ATM 84
ATM 85
ATM 86
ATM 87
ATM 88
ATM 89
ATM 90
ATM 91
ATM 92
ATM 93
ATM 94
ATM 95
ATM 96
ATM 97
ATM 98
ATM 99
ATM 100
ATM 101
ATM 102
ATM 103
ATM 104
ATM 105
ATM 106
ATM 107
ATM 108
ATM 109
ATM 110
ATM 111
ATM 112
ATM 113
ATM 114
ATM 115

Line	Code	Statement	Label
115		IF (L.LT.HDP) HD=L*HND	
116	ATM	COSPHI=HD/L	
117	ATM	PHI=ACOS(COSPHI)	
118	ATM	VPSC=VP*((SIN(PHI)*SIN(CHI))**2+COSPHI**2)	
119	ATM	IF (DEBUG.EQ.2) WRITE (6,36) HDM,HTM,PHI	
120	ATM	HTF=3.281*HTM	
121	ATM	LT2=L**2	
122	ATM	LT250=LT2*LT2	
123	ATM	IF (HDM.GT.1.E5.AND.HTM.GT.1.E5) NSTEP=1	
124	ATM	NSM1=NSTEP-1	
125	C		
126	ATM	GAUSSIAN OR PLANE WAVE	
127	ATM	G2=6.54	
128	ATM	IF (PROP.EQ.2) G2=3.54	
129	ATM	IF (PROP.EQ.3) G2=6.9	
130	ATM	IF (OUT.EQ.2) WRITE (6,49)	
131	TCP		
132	ATM	DECIDE WHICH TYPE OF CALCULATIONS TO DO	
133	ATM	IF (HDM.LT.1.E5) GO TO 9	
134	ATM	IF (HTM.LT.1.E5) GO TO 8	
135	ATM	TYPE=1	
136	ATM	GO TO 11	
137	ATM	TYPE=3	
138	ATM	GO TO 11	
139	ATM	IF (HTM.LT.1.E5) GO TO 10	
140	ATM	TYPE=4	
141	ATM	GO TO 11	
142	ATM	TYPE=2	
143	ATM	WRITE (6,35) TYPED(TYPE),TYPEE(TYPE)	
144	ATM		
145	ATM	PROPAGATION OR REVERSE PROPAGATION	
146	ATM	IF (ITYPE.NE.5) GO TO 12	
147	ATM	REVERSE PROPAGATION--OI AND PI KNOWN	
148	ATM	FINAL=1	
149	ATM		
150	C	REGULAR PROPAGATION	
151	ATM		
152	ATM	COMPUTE STARTING VALUES OF AREA AND INTENSITY	
153	ATM	AREA=PI*R0SQ	
154	ATM	I=PI/AREA	
155	ATM	IP=2.312*I	
156	ATM	EXPKAS=1.	
157	ATM	KAS=0.	
158	ATM	SIGMAT=0.	
159	ATM	PRINT=.FALSE.	
160	ATM	IF (OUT.EQ.2.AND.(FINAL.EQ.2.OR.DERUG.EQ.2)) PRINT=.TRUE.	
161	ATM	IF (PRINT) WRITE (6,36) Z,HDM,SIGMAT,SIGTST,EXPKAS,AREA,I,IP	
162	ATM		
163	ATM	GO TO (13,14,15,16), TYPE	
164	ATM	CALL AA (HDM)	
165	ATM	GO TO 4A	
166	ATM	CALL HM (HDM)	
167	ATM	GO TO 4B	
168	ATM	CALL AH (HDM)	
169	ATM	GO TO 4B	
170	ATM	CALL HA (HDM)	
171	ATM		

```

175      C
176      4A
177      C
178      IF (XN.LT.1.E-8) RETURN
179      IF (TYPE.EQ.1) RETURN
180      IF (ITYPE.EQ.5) GO TO 22
181
182      COMPUTE AND PRINT DISPLACEMENT, ECCENTRICITY AND ISO-INTENSITY
183      CONTOUR DATA.
184
185      AF=.70710678*ROLO
186      PTOTAL=PI*XPXKAS*(1.-G3)
187      ETA=ROLD/MO
188      ANOM=3.1415926*AF*AF/KIP
189      ECC=0.3*0.7*KIP
190      CISP=(1.-0.692)*SORT(0.478864-2.6666667*ALOG(KIP))
191      DISP=AF*(ETA*(-.29))*.01SP
192      IF (PD.EQ.0.) WRITE (6,49)
193      WRITE (6,42) DISP,ECC
194      GAMMA=1.0
195      OGAM=0.1
196      DO 17 KGAM=1,9
197      GAMMA=GAMMA-OGAM
198      AREA=(-ANOM)*ALOG(GAMMA)
199      POWER=PTOTAL*(1.-GAMMA)
200      AVGI=POWER/AREA
201      WRITE (6,43) GAMMA,AREA,POWER,AVGI
202      CONTINUE
203
204      BREAKDOWN POWER AND OPTIMUM POWER CALCULATIONS
205
206      IF (PD.NE.0.)WRITE (6,49)
207      PRD = PRD + PT * KIP / (2.312 * I)
208      PRINT 45, PRD,PHD
209      PMAX=PT*5.54/XN
210      XI=1.205/(XN*KIP)
211      IF (PMAX.LE.PHD) GO TO 18
212      PMAX=PHD
213      XI=PHD
214      PRINT 32, XI,PMAX
215
216      EFFECT OF POWER VARIATIONS
217
218      DP=PI*0.1
219      DN=XN*0.1
220      PP=0.
221      YN=0.
222      PTOT=1/(KIP*PT)
223      DO 20 III=1,20
224      PP=PP+DP
225      IF (PP.GT.PHD) GO TO 21
226      YN=YN+DN
227      ZZ=XI*(HEAM,YN)
228      ZN=1+ZZ*YI/(XN*KIP)
229      ZXXX=ZN*2.312
230      FACTDN=XI/ZXXX
231      IF ((FACTOR*IT.1).AND.(FACTOR.GT.0.)) GO TO 19

```



```

230 PUSE=0.
    AUSE=0.
    GO TO 20
    19 PUSE=PI*OT*PP*(1.-FACTOR)
    AUSE=-0.5*AREA*ALOG(FACTOR)/ZZ
    20 PRINT 46, PP,ZN,PUSE,AUSE
    21 PRINT 47, OI
    RETURN
    C
    C
    C
    22 LCOUNT=LCOUNT+1
    IF (LCOUNT.GT.20) GO TO 31
    IF (FINAL.EQ.2) RETURN
    C
    C
    C
    23 SELECTION OF NEXT FOCAL LENGTH
    XK=0.7
    RAT=1/OI
    IF (RAT.LT.0.45.OR.RAT.GT.2.22) GO TO 26
    IF (RAT.LT.0.62.OR.RAT.GT.1.6) GO TO 25
    IF (RAT.LT.0.8.OR.RAT.GT.1.25) GO TO 24
    IF (RAT.LT.0.91.OR.RAT.GT.1.1) GO TO 23
    XK=1.0
    GO TO 26
    23 XK=0.95
    GO TO 26
    24 XK=0.9
    GO TO 26
    25 XK=0.8
    FL=FL*XK*SORT(RAT)
    IF (FL.GE.R10) GO TO 27
    KOUNT=KOUNT+1
    IF (KOUNT.GT.2) GO TO 30
    FL=100.
    L=FL
    LT2=L*2
    LT250=LT2*LT2
    C
    C
    26 RECALCULATE PHI OR MTM
    IF (CPHI) GO TO 28
    MTM=HGM*L*COSPHI
    MTM=MTM*GL
    GO TO 29
    27 L=FL
    LT2=L*2
    LT250=LT2*LT2
    C
    C
    28 HDP=HGM*HGM
    HMD=HDS(HDI)
    HMD=1
    IF (HDP.NE.HMD) HMD=-1
    IF (L.LT.HDP) HMD=L*HMD
    COSPHI=HDI/L
    PHI=ACOS(COSPHI)
    29 IF (DEHUG.EQ.2) WRITE (6,37) FL,MTM,PHI
    IF (L.LT.OIL.OR.I.GI.OIM) GO TO 12
    WRITE (6,38) L
    FINAL=2
    GO TO 12
    C
    C
    25 RANGE FOR CPHI

```

ATM 227
ATM 228
ATM 229
ATM 230
ATM 231
ATM 232
ATM 233
ATM 234
ATM 235
ATM 236
ATM 237
ATM 238
ATM 239
ATM 240
ATM 241
ATM 242
ATM 243
ATM 244
ATM 245
ATM 246
ATM 247
ATM 248
ATM 249
ATM 250
ATM 251
ATM 252
ATM 253
ATM 254
ATM 255
ATM 256
ATM 257
ATM 258
ATM 259
ATM 260
ATM 261
ATM 262
ATM 263
ATM 264
ATM 265
ATM 266
ATM 267
ATM 268
ATM 269
ATM 270
ATM 271
ATM 272
ATM 273
ATM 274
ATM 275
ATM 276
ATM 277
ATM 278
ATM 279
ATM 280
ATM 281
ATM 282
ATM 283

03/05/75 18.20.27.

FTM 4.0-P357

73/74 OPT=0 TRACE

SURROUTINE AA

```

2  AA
3  AA
4  AA
5  AA
6  AA
7  AA
8  AA
9  AA
10 AA
11 AA
12 AA
13 AA
14 AA
15 AA
16 AA
17 AA
18 AA
19 AA
20 AA
21 AA
22 AA
23 AA
24 AA
25 AA
26 AA
27 AA
28 AA
29 AA
30 AA
31 AA
32 AA
33 AA
34 AA
35 AA
36 AA
37 AA
38 AA
39 AA
40 AA
41 AA
42 AA
43 AA

SURROUTINE AA (HOM)
CALCULATIONS FOR ORIGIN AND TARGET ABOVE 100 KM
LOGICAL EQUAL=EMP.PRINT
INTEGER PEAM=DEHUG.FINAL.OUT.PO
REAL I=IRU.KAS.KIP.L.LAMDA.LI2.LI250.MSO
COMMON /MESH/ XTRA(3).AREA
COMMON /ERROR/ ERR
COMMON /ATMS/ BEAM.FL.GL.MTM.IRU.L.LAMDA.NSTEP.PMI
COMMON /INS/ DEHUG.ITYPE.OUT.PI.PO
COMMON /SAIM/ COEF1.COE2.COE3.CUSPH.EQUAL.FINAL.FIVE3.FIVE9.G2.
103.64.G5.MTF.I.IFLAG.KAS.KIP.LI2.LI250.MSO.NSM1.PI.PO.PRINT.N650.R
210.SIGASO.SIGASO.SIGMAT.SIGSO.NOLD
CALCULATE RADIUS. AREA. AND INTENSITY
RSO=LI250*SIGASO
RESORT(RSO)
AREA=PI*RSO
I=COEF3/AREA
IF (FINAL.NE.2.AND.DERUG.EQ.1) RETURN
WRITE RESULTS
ROLD=R
IF (OUT.EQ.1) GO TO 1
WRITE (6,2) L.HOW.I.AREA.R
RETURN
WRITE (6,3) MTM.MTF.L.R.AREA.I
RETURN
FORMAT (10X,12HABOVE 100 KM/1X,1P2E15.4,5X,2M0.0X,3E15.4,5X,10M1.
1000E-0C/)
FORMAT (/10X,23HTARGET ALTITUDE (MTM) =,1PE10.3,9M METERS (,E10.3
1,5M FEET)/10X,42HTARGET RANGE (L)
2M METERS,12X,29RADIUS WITHOUT BLOOMING (R) =,CP7.2,7M METERS/10X
3,42AREA WITHOUT BLOOMING (AREA)
4,2,8X,29HTARGET PLANE INTENSITY (I) =,E11.4,11M WATTS/M**2/)
END

```

03/09/75 18.29.29.

FTM 4.0.257

TRACE

73/74 OPT=0

SUBROUTINE AB

```

SUBROUTINE AB (MOM)
C
C
C
  S      REAL I-L-L1-L2
        REAL IP
        LOGICAL PRINT
        COMMON /ATMS/ HEAV,FL,GL,HTM,IPD,L,LAND,NSTEP,PHI
        COMMON /INS/ DEHUG,ITYPE,OUT,PI,R0
        COMMON /SATM/ COEF1,COEF2,COEF3,COSPHI,EQUAL,FINAL,FIVE3,FIVE9,G2,
        IC3,G4,G5,HTF,I,IFLAG,KAS,KIP,L12,LT250,MSO,NSM1,PI,PO,PRINT,R050,R
        19      IC3,G4,G5,HTF,I,IFLAG,KAS,KIP,L12,LT250,MSO,NSM1,PI,PO,PRINT,R050,R
        210,SIGASQ,SIGBSQ,SIGMAT,SIGSQ,OLD
        COMMON /MESM/ EXPRES,L1,NI,AREA
        L1=(IES-HOM)/COSPHI
        L2=L-L1
        15      ABOVE 100 KM
        C
        C
        C
        RSQ=R050
        IF (HEAV.EQ.1) RSQ=(R0*L2/L)**2
        20      RSQ=RSQ*4.*L1*L1*SIGASQ
        RSQ=RSQ*(R050)
        AREA=PI*HMSQ
        L1=(IES-HOM)/COSPHI
        L2=L-L1
        25      ABOVE 100 KM
        C
        C
        C
        RSQ=R050
        IF (HEAV.EQ.1) RSQ=(R0*L2/L)**2
        30      RSQ=RSQ*4.*L1*L1*SIGASQ
        RSQ=RSQ*(R050)
        AREA=PI*HMSQ
        35      IP=1+2.*I2
        IF (OP1.NE.1) WRITE (6,1) L1,AREA,I,IP
        HOLD1=FL
        HOLD2=R050
        HOLD3=L
        FL=L2
        L=L2
        R050=RSQ
        40
        C
        45      CALL BR (1.E5)
        FL=HOLD1
        R050=HOLD2
        L=HOLD3
        RETURN
        50
        C
        C
        C
        55      FORMAT (4X,'ABOVE 100 KM',/.1X,1PE15.4,5X,/.1X,0000E-05,5X,00,0.13X
        100,0.13X,/.1X,0000E-00,3E15.4,/)
        END

```



```

40 RADIANSE./10X*LINEAR EFFECTS ON TRANSMISSION (EXPAS) -- BA
50 PF6.3.19X*RAIDING 411-OUT BLOWING (R) -- PF7.3.
50 METERSE./10X*
50 DON TRANSMISSION (KIP) -- PF6.3.19X*RAVERAGE INTENSITY (I)
400 1PE11.4.0 WATTS/0.34002/10X*AREA WITHOUT BLOWING (AREA)
5 -- E10.3.0 METERSE./10X*2.5X*PEAK INTENSITY (IP)
5 -- E11.4.0 WATTS/0.34002/10X*AREA WITH BLOWING (BLAREA)
7 -- E10.3.0 METERSE./10X*2.5X*
END

```

39
40
41
42
43
44
45
46
47

BA
BA
BA
BA
BA
BA
BA
BA
BA

```

2  SUBROUTINE 88 (MOM)
3
4  CALCULATIONS FOR ORIGIN AND TARGET BELOW 100 KM
5
6  LOGICAL CNV-GE-EMED-UNIFRM
7  LOGICAL EQUAL-EM-LESS-PRINT
8
9  INTEGER MEAN-DE-UG-FINAL-OUT-PO-ST
10 REAL I-IMU-KAS-0-1-KIP-L-LAMDA-LT2-LT250-MSO-W-NAJ-MI-IP-MI-M2-M
11
12 COMMON /MESM/ FAPKAS-ZPHEV-MI-AREA
13 COMMON /EM-UG/ EPM
14 COMMON /ATMS/ MEAN-FL-GL-MTM-IMD-L-LAMDA-MSICP-PME
15 COMMON /IMS/ DEMOS-ITYPE-OUT-PI-EO
16 COMMON /SATM/ COEF2-COEF3-COSPHI-EQUAL-FINAL-FIVE3-FIVE9-62-
17 173-64-95-MF-I-IFLAG-KAS-KIP-LT2-LT250-MSO-MSI-MI-PI-PC-PRINT-R050-R
18 210-SIGASO-SIGASO-SIGASO-SIGASO-SIGASO-SIGASO-SIGASO-SIGASO-SIGASO-SIGASO
19 COMMON /ATM1/ W-01-PROP-SIGLF-SIGMF-NTM3-M1-M2
20 COMMON /AT/ SIGST
21
22 LOGICAL OK
23
24 DIMENSION UG10(15), OG10(15)
25 DIMENSION SVS10(150)
26
27 DATA UG10/.499533,.4325317,.3397068,.216677,.07443717/
28 DATA OG10/.9133567,.07472567,.1095432,.1346334,.14773717/
29 DELTAZ=L/MSIEP
30
31 COMPARE STARTING Z WITH R0=10
32 DO 1 K=1,MSM1
33   KJ=K
34   Z=DELTAZ*K
35   IF (Z-GE-P10) GO TO 2
36   CONTINUE
37   WRITE (K,22) Z,R10
38   EXX=TRUE
39   RETURN
40
41 LESS=.FALSE.
42 IF (MTM-LT-MOM) LESS=.TRUE.
43 Y=0.
44 R=0.01M=0.
45 OK=.TRUE.
46 CALL ALFSET (NLAM-LAM)
47 DZ=DELTAZ*0.1
48 DMS=ZCOSPHI
49 MMS=0.99-0.99*0.5
50 TEMP2=1./FLOAT(MNSTEP)
51 TEMPAS=6.494/LAMDA*0.6
52 TEMP7=1.434/(LAMDA/6.20319)*0.1.2
53
54 LINEAR LOOP
55
56 DO 4 K=KJ,MSIEP
57   KJ=FLOAT(MNSTEP-J)*TEMP2
58   TEMP1=KJ*0.5*TEMP2

```

```

60      Z=DELTAZ*J
61      Z1=DELTAZ*(J-1)
62      IF (LESS) GO TO 3
63
64      SHOOTING UP
65      ML=Z1+COSPHI*HOM
66      MU=Z1+COSPHI*HOM
67      MU=Z1+COSPHI*HOM
68      MU=Z1+COSPHI*HOM
69      MU=Z1+COSPHI*HOM
70      MU=Z1+COSPHI*HOM
71      MU=Z1+COSPHI*HOM
72      MU=Z1+COSPHI*HOM
73      MU=Z1+COSPHI*HOM
74      MU=Z1+COSPHI*HOM
75      MU=Z1+COSPHI*HOM
76      MU=Z1+COSPHI*HOM
77      MU=Z1+COSPHI*HOM
78      MU=Z1+COSPHI*HOM
79      MU=Z1+COSPHI*HOM
80      MU=Z1+COSPHI*HOM
81      MU=Z1+COSPHI*HOM
82      MU=Z1+COSPHI*HOM
83      MU=Z1+COSPHI*HOM
84      MU=Z1+COSPHI*HOM
85      MU=Z1+COSPHI*HOM
86      MU=Z1+COSPHI*HOM
87      MU=Z1+COSPHI*HOM
88      MU=Z1+COSPHI*HOM
89      MU=Z1+COSPHI*HOM
90      MU=Z1+COSPHI*HOM
91      MU=Z1+COSPHI*HOM
92      MU=Z1+COSPHI*HOM
93      MU=Z1+COSPHI*HOM
94      MU=Z1+COSPHI*HOM
95      MU=Z1+COSPHI*HOM
96      MU=Z1+COSPHI*HOM
97      MU=Z1+COSPHI*HOM
98      MU=Z1+COSPHI*HOM
99      MU=Z1+COSPHI*HOM
100      MU=Z1+COSPHI*HOM
101      MU=Z1+COSPHI*HOM
102      MU=Z1+COSPHI*HOM
103      MU=Z1+COSPHI*HOM
104      MU=Z1+COSPHI*HOM
105      MU=Z1+COSPHI*HOM
106      MU=Z1+COSPHI*HOM
107      MU=Z1+COSPHI*HOM
108      MU=Z1+COSPHI*HOM
109      MU=Z1+COSPHI*HOM
110      MU=Z1+COSPHI*HOM
111      MU=Z1+COSPHI*HOM
112      MU=Z1+COSPHI*HOM
113      MU=Z1+COSPHI*HOM
114      MU=Z1+COSPHI*HOM
115      MU=Z1+COSPHI*HOM

```

TURBULENCE CALCULATIONS

```

76      ZL=Z/L
77      CG10A=0.5*(ML*HOM)-GL
78      CG10B=ML*HOM
79      CG10C=1.5
80      TEM=3*CG10A*(CG10B)
81      CG10C=TEM*CG10A
82      TEM=3*TEM*CG10A
83      TEM=3*TEM*CG10A
84      TEM=3*TEM*CG10A
85      TEM=3*TEM*CG10A
86      TEM=3*TEM*CG10A
87      TEM=3*TEM*CG10A
88      TEM=3*TEM*CG10A
89      TEM=3*TEM*CG10A
90      TEM=3*TEM*CG10A
91      TEM=3*TEM*CG10A
92      TEM=3*TEM*CG10A
93      TEM=3*TEM*CG10A
94      TEM=3*TEM*CG10A
95      TEM=3*TEM*CG10A
96      TEM=3*TEM*CG10A
97      TEM=3*TEM*CG10A
98      TEM=3*TEM*CG10A
99      TEM=3*TEM*CG10A
100      TEM=3*TEM*CG10A
101      TEM=3*TEM*CG10A
102      TEM=3*TEM*CG10A
103      TEM=3*TEM*CG10A
104      TEM=3*TEM*CG10A
105      TEM=3*TEM*CG10A
106      TEM=3*TEM*CG10A
107      TEM=3*TEM*CG10A
108      TEM=3*TEM*CG10A
109      TEM=3*TEM*CG10A
110      TEM=3*TEM*CG10A
111      TEM=3*TEM*CG10A
112      TEM=3*TEM*CG10A
113      TEM=3*TEM*CG10A
114      TEM=3*TEM*CG10A
115      TEM=3*TEM*CG10A

```

IF (MIN) SIGNAL=SIGN(SIGTISO)

```

95      RCS=5*(FL-Z1)/FL
96      RCS=5*(FL-Z1)/FL
97      ZL=0.5*(Z1+HOM)*2
98      P=5*(HOM*CG10C*CG10C*ZL*(SIGTISO-SIGTISO))
99      P=5*(HOM*CG10C*CG10C*ZL*(SIGTISO-SIGTISO))
100      P=5*(HOM*CG10C*CG10C*ZL*(SIGTISO-SIGTISO))
101      P=5*(HOM*CG10C*CG10C*ZL*(SIGTISO-SIGTISO))
102      P=5*(HOM*CG10C*CG10C*ZL*(SIGTISO-SIGTISO))
103      P=5*(HOM*CG10C*CG10C*ZL*(SIGTISO-SIGTISO))
104      P=5*(HOM*CG10C*CG10C*ZL*(SIGTISO-SIGTISO))
105      P=5*(HOM*CG10C*CG10C*ZL*(SIGTISO-SIGTISO))
106      P=5*(HOM*CG10C*CG10C*ZL*(SIGTISO-SIGTISO))
107      P=5*(HOM*CG10C*CG10C*ZL*(SIGTISO-SIGTISO))
108      P=5*(HOM*CG10C*CG10C*ZL*(SIGTISO-SIGTISO))
109      P=5*(HOM*CG10C*CG10C*ZL*(SIGTISO-SIGTISO))
110      P=5*(HOM*CG10C*CG10C*ZL*(SIGTISO-SIGTISO))
111      P=5*(HOM*CG10C*CG10C*ZL*(SIGTISO-SIGTISO))
112      P=5*(HOM*CG10C*CG10C*ZL*(SIGTISO-SIGTISO))
113      P=5*(HOM*CG10C*CG10C*ZL*(SIGTISO-SIGTISO))
114      P=5*(HOM*CG10C*CG10C*ZL*(SIGTISO-SIGTISO))
115      P=5*(HOM*CG10C*CG10C*ZL*(SIGTISO-SIGTISO))

```

IF (IP.LI.LI) GO TO 7

```

105      I GREATER THAN I BREAKDOWN WRITE AND RETURN
106      WRITE (A,23) Z,IP
107      END=.TRUE.
108      RETURN
109      AMEL=PI*HOM
110      WRITE OUTPUT

```



```

115      IF (PRINT) WRITE (6,24) Z,H0,SIGMAT,SIGTST,EXPKAS,AREA,I,IP
116      CONTINUE
117
118      ROLD=R
119      FINDIO=1./DELTAZ
120
121      START COMPUTATION OF BLOOMING LOSSES
122
123      ENDED=.FALSE.
124      CNVRGD=.FALSE.
125      HQM=HQM
126
127      SIGMAT=SQRT(SIGTST)
128      CALL ALFSET (NLAM,LAM)
129      TEMP3=ISIGHF-SIGHF)**2+4.*SIGTST
130      TEMP4=GA*ROSO
131      TEMP5=GS*WOSO
132      UNIFORM=.FALSE.
133      RSQ=TEMP4+TEMP5+TEMP3*ZPREV**2
134
135      CALCULATIONS FOR Z = R * 10
136
137      DZ=R/10
138      HDZ=DZ*0.5
139      TFDZ=DZ*0.0416666666667
140      DZFL=DZ/FL
141      TEMP1=DZ*COSPHI
142      DZSQ=DZ*0Z
143      TEMP6=G3*0Z/L
144      GPREV=GALTIM(HQM)*ALFFAC(0.,HQM,OK)/(VX(GL,HQM,HQM,PHI,0.,) *RSQ)
145      Z=DZ
146      L=HQM+TEMP1
147      G3TRM=1.-TEMP6
148      RC=1.-DZFL
149      RSQ=TEMP4+TEMP5*PC**2+(TEMP3+SVSTSQ(KJ))*(Z+ZPREV)**2
150      GCURR=GALTIM(H)*ALFFAC(DZ,H,OK)*G3TRM/(VX(GL,H,HQM,PHI,Z)*RSQ)
151      XCURR=DZSQ*(-0.5*GPREV-(GPREV-GCURR)*0.0416666666667)/SQRT(RSQ)
152      NI=XCURR
153      G=(GCURR+GPREV)*HDZ
154      GUESS=GCURR+GCURR-GPREV
155
156      CALCULATIONS FOR NEXT INTERVAL
157
158      Z=Z+DZ
159      IF (Z.GE.L) GO TO 16
160      H=H+TEMP1
161      G3TRM=G3TRM-TEMP6
162      RC=RC-DZFL
163      TGINO=Z*FINDIO+1.
164      INDO=TGINO
165      IF (INDO.GE.NSTEP) INDO=NSTEP-1
166      SVSTSQ=SVSTSQ(INDO)
167      SVSTSQ=SVSTSQ+(TGINO-FLOAT(INDO))*(SVSTSQ(INDO+1)-SVSTSQ)
168      WSO=TEMP4+TEMP5*PC**2+(TEMP3+SIGTST)*(Z+ZPREV)**2
169      GNEW=GALTIM(H)*ALFFAC(DZ,H,OK)*G3TRM/(VX(GL,H,HQM,PHI,Z)*RSQ)
170      IF (ABS(GNEW)-L1.1E-4) GO TO 12
171      OK=.FALSE.
172

```

CHECK ACCURACY OF LINEAR EXTRAPOLATION

```

DEVIAT=ABS((GNEW-GUESS)/GUESS)
IF (DEVIAT.GT.0.05) GO TO 15
OK=.TRUE.

```

175

```

RSHOLD=RSU
G=G+GNEW*OZ
XPREV=XCURR
XCURR=DZ*((HOZ*GNEW-G)-(GCURR-GNEW)*TFDZ)/SORT(RSQ)
NI=NI+XCURR
IF (EMDEN) GO TO 17
IF (DEVIAT.LT.0.01) GO TO 12
GPREV=GNEW
GCURR=GNEW
GUESS=GCURR+GCURR-GPREV
UNIFORM=.TRUE.
GO TO 9
IF (CNVSGD) GO TO 11

```

11

185

```

GO TO 9
IF (CNVSGD) GO TO 11

```

190

```

INCREASE SIZE OF INTERVAL

```

```

CONTINUE

```

195

```

HOZ=DZ
DZ=DZ*OZ
UNIFORM=.FALSE.
IF ((OZ*OZ).GE.1) GO TO 14
TFDZ=TFDZ+TFDZ
OZFL=DZFL*OZFL
TEMP1=TEMP1+TEMP1
TEMP6=TEMP6+TEMP6
GCURR=GNEW
GUESS=GCURR+GCURR-GPREV
GO TO 9

```

200

```

GO TO 9

```

205

```

FINAL INTERVAL

```

14

```

CNVSGD=.TRUE.
FRACT=(1-Z)/OZ
IF (FRACT.LT.5.E-4) GO TO 17
DZ=(1-Z)*0.5
HOZ=DZ*0.5
TFDZ=DZ*0.0416666666667
OZFL=DZFL*FRACT
TEMP1=TEMP1*FRACT
TEMP6=TEMP6*FRACT
GUESS=(GNEW-GCURR)*FRACT+GNEW
GPREV=GNEW-GUESS
GCURR=GNEW
GO TO 9

```

210

215

220

```

TRY EXPONENTIAL EXTRAPOLATION

```

C

C

15

```

DEVIAT=ABS(GCURR*2/(GPREV-GNEW)-1.)
IF (DEVIAT.LT.0.05) GO TO 19
IF (OZ.LT.0.01) GO TO 19
CNVSGD=.FALSE.
UNIFORM=.FALSE.

```

225

```

88 173
88 174
88 175
88 176
88 177
88 178
88 179
88 180
88 181
88 182
88 183
88 184
88 185
88 186
88 187
88 188
88 189
88 190
88 191
88 192
88 193
88 194
88 195
88 196
88 197
88 198
88 199
88 200
88 201
88 202
88 203
88 204
88 205
88 206
88 207
88 208
88 209
88 210
88 211
88 212
88 213
88 214
88 215
88 216
88 217
88 218
88 219
88 220
88 221
88 222
88 223
88 224
88 225
88 226
88 227
88 228
88 229

```


04/08/75 13.10.17.

FTN 4.0-P357

73/74 OPT=0 TRACE

SUBROUTINE 88

```

290      XPREV=XCURR
      XCURR=D7*(GOLD-TEMP)/ALOG(TEMP/GOLD)
      NI=NI+XCURR
      IF (ENDED) GO TO 17
      IF (DEVIAT.LT.0.01) GO TO 21
      GPREV=GCURR
      GCURR=GNEW
      GUES=GCURR+GCURR-GPREV
      GO TO 9
      IF (CNVRGD) GO TO 20
      GO TO 13

295      C
      C
      C
300      FORMAT (59H THE LENGTH OF THE BEAM PATH IS LESS THAN 10 TIMES R0,
      1Z=1PE10.3,7H R10 = E10.3)
      FORMAT (/10X*INTENSITY HAS REACHED BREAKDOWN, Z(J) = *,1PE10.3,* 18
      10 = *,E10.3)
      FORMAT (1X,1PE15.4)
      FORMAT (///,* NI = *,1PE12.5,8X,* KIP = *,E12.5,8X,* SLAREA = *,
      1E12.5,8X,* IAVL = *,E12.5,8X,* IPEAK = *,E12.5,/)
      FORMAT (///,10X,* TARGET ALTITUDE (HTM) = *,1PE10.3,* METERS (*,
      1E10.3,* FEET)*,9X,* LONG-TERM TURBULENCE (SIGMAT) = *,E10.3,
      2* PAULANS*,/,10X,* TARGET RANGE (L)
      3E9.2,* METERS*,9X,* SHORT-TERM TURBULENCE (SIGIST)=*, E10.3,
      4* RADIANS*,/,10X,* LINEAR EFFECTS ON TRANSMISSION (EXPKAS) =*, 88
      50PF6.3,19X,* RADIUS WITHOUT BLOOMING (R) = *,F7.3,
      5* METERS*,/,10X,
      3 ON TRANSMISSION (KIP) =*,F6.3,19X,* AVERAGE INTENSITY (I)
      4=*,1PE11.4,* WATTS/M*,3H*2/10X,* AREA WITHOUT BLOOMING (AREA)
      5 =*,E10.3,* METERS*,3H*2,5X,* PEAK INTENSITY (IP)
      6 =*,E11.4,* WATTS/M*,3H*2/10X,* AREA WITH BLOOMING (BLAREA)
      7 =*,E10.3,* METERS*,3H*2,/)
      END

```

```

C
C
C
5
10
15

SUBROUTINE ALFSET (NL,IL)
POWER RATIOS FOR MULTILINE PROPAGATION
COMMON /ALFDTA/ P(3),RHOFA,PLINE(3)
COMMON /ALFA/ LAM,RH
IF (LAM.EQ.2) GO TO 1
P(1)=1.
RETURN
DO 2 I=1,3
P(I)=PLINE(I)
IF (RH.EQ.0.) RH=1.E-6
RHOFA=0.9446*RH-1.
RETURN
END
SET 2
SET 3
SET 4
SET 5
SET 6
SET 7
SET 8
SET 9
SET 10
SET 11
SET 12
SET 13
SET 14
SET 15
SET 16
SET 17

```

```
5      C      FUNCTION ALFFAC (Z,M,OK)
      C      MULTI-LINE POWER LOSSES
      C      LOGICAL OK
      COMMON /ALFDIA/ P(3),RMOFAC
      COMMON /ALFA/ LAM,RH
      DIMENSION POLD(3)
      IF (LAM.EQ.2) GO TO 3
      IF (OK) GO TO 1
      P(1)=POLD(1)
      GO TO 2
      1      POLD(1)=P(1)
      2      TEMP=P(1)*EXP(-ALFAEX(M)*OZ)
      P(1)=TEMP
      ALFFAC=ALFAAB(M)*TEMP
      RETURN
20      C      IF (OK) GO TO 5
      DO 4 I=1,3
      4      P(I)=POLD(I)
      GO TO 7
      5      DO 6 I=1,3
      6      POLD(I)=P(I)
      7      ASSIGN 17 TO J1
      ASSIGN 20 TO J2
      ASSIGN 23 TO J3
      ASSIGN 12 TO J4
      SUM=0.
      8      C      IF (M.GT.13500.) GO TO 11
      IF (M.GT.9500.) GO TO 10
      IF (M.GT.5000.) GO TO 9
      ALFAS=3.6E-06*EXP(4.1056*RH-M*0.833333333333333E-3)
      GO TO 14
      9      ALFAS=9.3998E-6*EXP(4.1056*RH-M*1.031E-3)
      GO TO 16
      10     ALFAS=4.32E-10*EXP(4.1056*RH)
      GO TO 15
      C      CALCULATIONS FOR M GREATER THAN 13500 METERS
      11     XTRA=EXP(-ALFAEX(M)*OZ)
      GO TO J4(12,14)
      12     AS=ALFAAB(M)
      DO 13 I=1,3
      13     TEMP=P(I)*XTRA
      P(I)=TEMP
      SUM=SUM+TEMP*AS
      ALFFAC=SUM
      RETURN
      14     DO 15 I=1,3
      15     TEMP=P(I)*XTRA
      P(I)=TEMP
      SUM=SUM+TEMP
```

04/08/75 13.10.24.

FTW 4.0-P357

TRACE

OPT=0

73/74

FUNCTION ALFFAC

```

59  FAC
60  FAC
61  FAC
62  FAC
63  FAC
32  TCP
33  TCP
34  TCP
35  TCP
64  FAC
65  FAC
66  FAC
67  FAC
68  FAC
69  FAC
70  FAC
71  FAC
36  TCP
37  TCP
38  TCP
39  TCP
72  FAC
73  FAC
74  FAC
75  FAC
76  FAC
77  FAC
78  FAC
79  FAC
40  TCP
41  TCP
42  TCP
43  TCP
60  FAC
81  FAC
82  FAC
83  FAC
84  FAC
85  FAC
86  FAC
87  FAC
88  FAC
89  FAC
90  FAC
91  FAC
92  FAC
93  FAC
94  FAC
95  FAC
96  FAC
97  FAC
98  FAC
99  FAC
100 FAC
101 FAC
102 FAC
103 FAC

ALFFAC=SUM
RETURN
C
16  RHOSTR=1-RHOFAC*EXP(-H*(6.738E-5+9.61E-9*M))
    AS=RHOSTR*EXP(-10.047+H*(-6.38HE-4+H*2.25E-8))
    IF (H.GT. 8000) AS = EXP(-((RH*.9471)+ 10.37917)+((4.6303E-4-(RH
    1+1.6251E-4))*H)))
    AH1 = AS
    AS3 = ALFAS
    TEMP=P(1)*EXP(-(AS+ALFAS)*DZ)
    P(1)=TEMP
C
GO TO J1(17.1F)
SUM=SUM+AS*TEMP
GO TO 19
SUM=SUM+TEMP
AS=RHOSTR*EXP(-10.082+H*(-6.952E-4+H*1.55E-8))
19  IF (H.GT. 8000) AS = EXP (-((RH*.9474)+12.6721)+((2.9317E-4-(RH
    1+1.6251E-4))*H)))
    AH4 = AS
    AS4 = ALFAS
    TEMP=P(2)*EXP(-(AS+ALFAS)*DZ)
    P(2)=TEMP
C
GO TO J2(20.21)
SUM=SUM+AS*TEMP
GO TO 22
SUM=SUM+TEMP
AS=EXP(-9.948+H*(-2.199E-4+H*1.96E-9))
22  IF (H.GT. 8000) AS=EXP(-((RH*1.813)+4.8547)+((8.7225E-4-(R
    1+1.6251E-4))*H)))
    AH2 = AS
    AS2 = ALFAS
    TEMP=P(3)*EXP(-(AS+ALFAS)*DZ)
    P(3)=TEMP
C
GO TO J3(23.24)
ALFFAC=SUM+AS*TEMP
RETURN
ALFFAC=SUM+TEMP
RETURN
C
ENTRY ALFAS
C
IF (LAM.EQ.2) GO TO 25
TEMP=P(1)*EXP(-ALFAEX(H)*DZ)
P(1)=TEMP
ALFFAC=TEMP
RETURN
C
25  ASSIGN 14 TO J1
    ASSIGN 21 TO J2
    ASSIGN 24 TO J3
    ASSIGN 14 TO J4
    GO TO 6
C
END

```

5	C	FUNCTION ALFAAB (H)	AAH	2
	C	SINGLE LINE ABSORPTION COEFFICIENTS IN 1/M	AAH	3
	C	COMMON /ALFA/ LAM.24	AAH	4
	C	COMMON /ALFCOA/ DUM4Y(73).ARL.ARE	AAH	5
		MF=1.241*H	AAH	6
10		CALL MEGAIR (MF,TR,PMP,MS)	AAH	7
		P=0.359*PMP/0.474502502	AAH	8
		T=19*5.0/4.0	AAH	9
		PM=6.0724E-10*PM*P*EXP(0.0546*P)	AAH	10
		GO TO (1.5*8.11), LAM	AAH	11
15	C	LAMDA IS 10.6	AAH	12
	C		AAH	13
	C		AAH	14
	1	IF (MGT.16000.0) GO TO 3	AAH	15
20		ALFCO2=7.94577416E-5-2.10562795E-9*H-3.57576007E-12*H*H-1.07366914	AAH	16
		1E-15*H**3-1.69645494E-19*H**4+1.50364450F-23*H**5-7.16578722E-28*H	AAH	17
		2*H**1.61585924E-32*H**7-1.13662124E-37*H**8	AAH	18
		GO TO 4	AAH	19
25	C	IF (MGT.55000.0) GO TO 3	AAH	20
	2	ALFCO2=7.67462668E-5-1.89713935E-7*H-1.98650379E-11*H*H-1.14976017	AAH	21
		1E-15*H**3-1.04716134E-20*H**4-2.90401506E-25*H**5+1.19826061E-29*H	AAH	22
		2*H**9.03345045E-35*H**7-2.92529072E-40*H**8	AAH	23
		GO TO 4	AAH	24
30	C	ALFCO2=1.0E-7*EXP(-1.74E-4*H+12.18)	AAH	25
	C	ALFH20=4.32E-9*PW*(P+193.0*PW)	AAH	26
	4	ALFAAB=ALFCO2+ALFH20	AAH	27
		RETURN	AAH	28
35	C	LAMDA IS 3.6	AAH	29
	C	ALFH20=5.4E-6*PW	AAH	30
	5	IF (P1.GE.0.2) ALFH20=-5.923E-7+8.3633E-6*PW-3.1184E-8*PW*PW	AAH	31
40	C	IF (MGT.7500.0) GO TO 4	AAH	32
		ALFCO2=1.84E-6*EXP(-2.272E-4*H)	AAH	33
		GO TO 7	AAH	34
45	C	ALFCO2=4.25E-6*EXP(-3.36E-4*H)	AAH	35
	C	ALFAAB=ALFH20+ALFCO2	AAH	36
	7	RETURN	AAH	37
50	C	LAMDA IS 5.0	AAH	38
	C	IF (PW.GT.4.5E-4) GO TO 9	AAH	39
	8	AAA=1.9222	AAH	40
		BBB=1.4032	AAH	41
		GO TO 10	AAH	42
55	9	AAA=1.14256	AAH	43
		BBB=4.6052	AAH	44
	10	ALFAAB=(1.E-3)*EXP(AAA*ALOG(PW)+BBB)	AAH	45


```

60
C
C
C
RETURN
INSERT EQUATIONS FOR OTHER WAVELENGTHS HERE
ALFAAB=ABL*EXP(-ABE*H)
RETURN
END
AAB
AAB
AAB
AAB
AAB
AAB
AAB
59
60
61
62
63
64
65

```

04/08/75 13.10.27.

FTN 4.0-P357

TRACE

73/74

FUNCTION ALFAEX

```

      FUNCTION ALFAEX (M)
      THIS ROUTINE CALCULATES THE EXTINCTION COEFFICIENT IN 1/M
      COMMON /ALFOT/ DUMMY(7),ARL,ABE,SCL,SCE
      GO TO (1,2,3,10), LAM
      LAMDA IS 10.6
      ALFAS0=1.0E-6*EXP(4.75*RM)
      GO TO 4
      LAMDA IS 3.8
      ALFAS0=3.6E-6*EXP(4.1056*RM)
      GO TO 4
      INSERT EQUATIONS FOR OTHER WAVELENGTHS HERE
      LAMDA IS 5.0
      ALFAS0=3.E-6*EXP(4.2*RM)
      THE REST OF THE FUNCTION IS INDEPENDENT OF LAMDA
      IF (M.GT.13500.0) GO TO 7
      IF (M.GT.9500.0) GO TO 6
      IF (M.GT.5000.0) GO TO 5
      ALFAS=ALFAS0*EXP(-M/1.2E+3)
      GO TO 9
      ALFAS=ALFAS0*2.586*EXP(-M*1.031E-3)
      GO TO 9
      ALFAS=ALFAS0*1.2E-4
      GO TO 9
      IF (M.GT.25000.0) GO TO 8
      ALFAS=ALFAS0*(-3.251E-3+3.738E-7*M-9.6557E-12*M*M)
      GO TO 9
      ALFAS=ALFAS0*1.8E-3*EXP(-1.535E-4*(M-25000.))
      ALFAS = ALFAS/9.7725
      ALFAEX=ALFAS*ALFAR(M)
      RETURN
      USER SPECIFIED COMPUTATION
      ALFAEX=ARL*EXP(-ABE*M)-SCL*EXP(-SCE*M)
      RETURN
      END

```


FUNCTION CNSO 73/74 OPT=0 TRACE

59
60
61
62
63
64

RETURN

IF 14.GY.1.5241 GO TO 4
CNSO=3.0E-12
RETURN
END

69
C
12

03/05/75 10:2:19.

FTN 4.0-P357

FUNCTION KI 73/74 OPT=0 TRACE

```

REAL FUNCTION IREFAM(X)
  C
  C COMPUTES THE INTENSITY RATIO
  C
  S      IF (X.GT.0.1) GO TO 1
  KI=1.0
  RETURN
  C
  C      X2=X*X
  C      IF (X.EQ.0.0) GO TO 5
  C
  C      FOCUSED BEAM
  C
  C      X32=X**1.5
  C      X15=X**0.2
  C      IF (X.GT.1.0) GO TO 2
  C      X1=.174*X32-.164/X15+.733*EXP(-X2)
  C      RETURN
  C
  C      IF (X.GT.2.0) GO TO 3
  C      X1=-.176*X+.793
  C      RETURN
  C
  C      IF (X.GT.100.0) GO TO 4
  C      X2=X**2.5
  C      X36=X**0.75
  C      X12=1.57/X5+.6.3/X32+2.42/X34-12.9/(X2+.1)-1.71*ALOG(X)/X
  C      RETURN
  C
  C      X1=EXP21-2.445*ALOG(X)+5.378)
  C      RETURN
  C
  C      COLLIMATED BEAM
  C
  C      X4=X2**2
  C      IF (X.GE.5.0) GO TO 6
  C      X12=X**0.5
  C      X13=X**(.1./3.1
  C      X26=X**0.75
  C      X1=-4.14E-4*X4-2.99E-5/X4+.598*X13-.384/X12+.6/X34
  C      RETURN
  C
  C      X1=EXP(-2.183*ALOG(X)+3.145)
  C      RETURN
  C
  END

```


[illegible]

03/05/75 18.23.18.

FTN 4.0P357

TRACE

OPT=0

73/74

SUBROUTINE MEGAIR

```

115      G=50*(RO/(PO+H))**2
      RETURN
      C
120      PERFORM CALCULATIONS FOR H GREATER THAN 30000 FEET.
      C
      C
      C      SINCE MOLECULAR WEIGHT IS NO LONGER CONSTANT, MOLECULAR SCALE
      C      TEMPERATURE IS NO LONGER EQUAL TO KINETIC TEMPERATURE.
      C      THREE INDEX EQUATIONS ARE REQUIRED IN THE REGION ABOVE 30000 FEET
      C      MAKE AN INDEX APPROXIMATION FOR VALUES OF H GREATER THAN 30000
      C      FEET BUT LESS THAN 492126 FEET.
      C
125      IF (H.GT.492126.) GO TO 7
      I=.000257344*H*1.88
      IF (I.GT.12) I=12
      IF (H.GE.DELTAH(I)) GO TO 6
      IF (H.GE.DELTAH(I-1)) I=I-1
      C
130      ESTABLISH BASE VALUES OF TEMPERATURE, PRESSURE, AND GRADIENT.
      H=DELTAH(I)
      TH=DELTAH(I)
      PR=DELTAH(I)
      L=DELTAH(I)
      C
135      CALCULATE MOLECULAR WEIGHTS FROM EMPIRICAL, GRAPHICALLY DERIVED,
      EQUATIONS.
      MW=COEFF1(I)-COEFF2(I)*H+COEFF3(I)*H*H
      HP=H/(1.+H/RO)
      C
140      CALCULATE MOLECULAR SCALE TEMPERATURE AND CONVERT TO KINETIC
      TEMPERATURE.
      TH=((TH*L*(H-HB))**4)/MW
      C
145      PRESSURE (P), IN LB/FT**2.
      X=50*HP-TB/L
      Y=1./((X*(RO+H))-1./((X*(RO+HB)))+(1./((X*X)))*ALOG(((H-HB+TB/L)*(RO+HB
      150      1)*L)/((RO+H)*TH))
      B=(50*MW*RO*RO)/(L*R)
      P=EXP(PH-B*Y)
      PMR=P*X*H
      C
155      DENSITY
      D=(M*P*GO)/(R*TH)
      C
160      GRAVITATIONAL ACCELERATION
      G=GO*(RO/(RO+H))**2
      RETURN
      C
      C      MAKE AN INDEX APPROXIMATION FOR VALUES OF H GREATER THAN 492126
      C      FEET BUT LESS THAN 984252 FEET.
      C
165      IF (H.GT.984252.) GO TO 8
      Z=(H-740000.)/50000.
      I=17.5+.50*Z-.04348*Z*Z
      IF (H.GE.DELTAH(I)) GO TO 6
      IF (H.GE.DELTAH(I-1)) I=I-1
      GO TO 6
      C
170      C

```

SUBROUTINE MEGAIR

73/74 OPT=0 TRACE

FTN 4.0-P357

03/05/75 18.23.18.

PAGE

MAKE AN INDEX APPROXIMATION FOR VALUES OF H GREATER THAN 984252
FEET.

175

C
C
C

IF (H.GT.2320000.) GO TO 9
I=.000003048*H+15.
IF (H.GE.DELTAH(1)) GO TO 6
IF (H.GE.DELTAH(I-1)) I=I-1
GO TO 6

180

C
C

WRITE (6,10) H
RETURN

185

C
C
C

FORMAT (1H ,20X,22H**ERROR FROM MEGAIR2**5H H = ,E12.5)
END

MEG 173
MEG 174
MEG 175
MEG 176
MEG 177
MEG 178
MEG 179
MEG 180
MEG 181
MEG 182
MEG 183
MEG 184
MEG 185
MEG 186
MEG 187
MEG 188

5	C	FUNCTION VX (GL,H,HOM,PHI,ZJ)	VX	2
	C	CROSS WIND VELOCITY PLUS SLEW VELOCITY IN METERS/SECOND	VX	3
	C	COMMON /MESH/ XTRA,ZPREV	VX	4
		COMMON /CNVM/ IN	VX	5
	C	COMMON /X/ CHI,OMEGA,VP,VPSC,VXB	VX	6
10		VX=VXB	VX	7
		IF (VXB.NE.0.) RETURN	VX	8
	C	VS=OMEGA*(ZJ-ZPREV)	VX	9
		VX=VS	VX	10
15		IF (H.GE.5.E4) GO TO 6	VX	11
		IF (H.GE.2.44E4) GO TO 2	VX	12
		IF (H.GE.1.22E4) GO TO 1	VX	13
		VX=3.42E-3*H+.75	VX	14
		GO TO 3	VX	15
20	1	VX=H2.4-2.53E-3*H	VX	16
		GO TO 3	VX	17
	2	VX=27.2-2.72E-4*H	VX	18
	3	IF (1A-2) 4,5,6	VX	19
	4	VX=VX*.27	VX	20
		GO TO 6	VX	21
25	5	VX=VX*.5	VX	22
	6	IF (H04-GL).GT.10.) VX=VX*.2	VX	23
		IF (VPSC-GE.VX) VX=VPSC	VX	24
		VX=VX*.VS	VX	25
		RETURN	VX	26
30		END	VX	27
			VX	28
			VX	29
			VX	30
			VX	31

CASE 1 BELOW-BELOW.PD

SHORT OUTPUT FORMAT, WITHOUT CEBUG

TARGET RANGE (L)	1.000E+03 METERS	DEVICE POWER (PD)	1.000E+06 WATTS
FOCAL DISTANCE (FL)	1.000E+03 METERS	POWER OUT OF THE TELESCOPE (PT)	0.
GROUND LEVEL (GL)	0.	WAVELENGTH (LAM, A)	3.00E-06 METERS
DEVICE ALTITUDE (HOM)	1.00E+02 METERS	INPUT JITTER (LOW FREQ)	5.00E-06
TARGET ALTITUDE (HTM)	3.28E+02 FEET	TRACKING RATE (CMER)	5.00E-06
VERTICAL ANGLE (PHI)	0.	OPTICS RADIUS (RO)	0.00 RADIAN/SEC
	0.	OBSCURATION RADIUS	.35 METERS
	0.00 RADIAN		.00 METERS
AZIMUTH ANGLE (CHI)	.520 RADIAN	BEAM TYPE (PROP)	GAUSSIAN
PLATFORM VELOCITY (VP)	0. METERS/SEC	TYPE OF PROPAGATION (BEAM)	FOCUSED
SPECIFIED CROSS WIND (VIB)	10.00	BEAM QUALITY (M)	1.50
SEVERITY OF TURBULENCE (WTHR)	NORMAL	NUMBER OF BEAMPATH INCREMENTS	30
RELATIVE HUMIDITY (RH)	.50		

*****INPUT TO OPTICAL TRAIN*****

LASER BEAM DIAMETER	.1600 METERS
LASER POWER	.1000E+07 WATTS
WAVELENGTH	.3000E-05 METERS
OBSCURATION	.3600
BEAM QUALITY	1.500
PULSE LENGTH	2.000 SECONDS
PHASE FRONT CURVATURE	.1000E+71 METERS
JITTER	.7071E-05 RADIAN
INTENSITY FLUCTUATIONS	.5000 PEAK-TO-PEAK
SCALE SIZE OF FLUCTUATIONS	.1000 L/λ
TYPE OF AEROWIND	FOCUSED
AEROWIND Δ K/ρ/ρ	.1000
ρ/ρ/ρ REF	2.500
DISTANCE TO CLIPPER	50.00 METERS
CLIPPER DIAMETER	.1600 METERS
NUMBER OF MIRRORS	7
REFLECTIVITY	.9160
FABRICATION ERROR	.1250
TYPE OF MIRRORS	COOLED
DISTANCE BETWEEN MIRRORS	.1500 METERS
TELESCOPE MAGNIFICATION	6.375
TELESCOPE DIAMETER	.7000 METERS
TELESCOPE TYPE	ON-AXIS
TYPE OF EXIT APERTURE	WINDOW
EXIT APERTURE LENGTH	.5000E-01 METERS
ABSORPTION COEFFICIENT	.1000E-01 METERS-1
TEMPERATURE FLUCTUATION	1.000 DEG K
SPOT AREA/ BEAM AREA	.5000E-01
TRACKER JITTER	.5000E-05 RADIAN
BORE-SIGHT JITTER	.5000E-05 RADIAN
SERVO JITTER	.5000E-05 RADIAN
AUTOALIGNMENT JITTER	.5000E-05 RADIAN

*****OPTICAL TRAIN OUTPUT*****

SOURCE
 INPUT BEAM
 AERODYNAMIC WINDOW
 BEAM CLIPPER
 MIRRORS
 COOLED
 BEAM EXPANDER
 ON-AXIS
 EXIT APERTURE
 WINDOW
 TOTALS
 TRANSMISSION SIGMA L/W
 1.0000 .333 0.000
 1.0000 0.000 0.000
 1.0000 0.000 0.000
 .9050 .3028 .0007
 .9570 .3413 .0001
 .9495 .0593 .1000
 .8233 .6979 .1573
 TRANSMITTED BEAM DIAMETER .7000 METERS
 TRANSMITTED POWER .8233E+05 WATTS
 BEAM QUALITY BEFORE ACCOUNTING FOR DIVERGENCE
 M1 = .497 M2 = 1.1130
 EFFECT OF BEAM DIVERGENCE ON WAIST 1.090
 FINAL BEAM SPREAD PARAMETER M2 1.113
 TOTAL BEAM JITTER .8884E-05 RADIAN
 PHASE FRONT CURVATURE .4375E+71 METERS

RESULTANT BEAM QUALITY M1 = .560 M2 = 1.215

CALCULATIONS FOR ORIGIN BELOW 100 KM AND TARGET BELOW 100 KM.

TARGET ALTITUDE (HTM) = 0. METERS (0. FEET)
 TARGET RANGE (L) = 1.00E+03 METERS
 LINEAR EFFECTS ON TRANSMISSION (EAPKAS) = .946
 NON-LINEAR EFFECTS ON TRANSMISSION (KIP) = .500
 AREA WITHOUT BLOOMING (AREA) = 1.065E-03 METERS**2
 AREA WITH BLOOMING (BLAREA) = 2.131E-03 METERS**2

DISPLACEMENT = .025 METERS ECCENTRICITY = .650

1/2 PEAK CONTOUR	AREA (METER**2)	CUMULATIVE POWER	AVERAGE INTENSITY
.9	1.122E-04	3.714E-04	3.265E+08
.8	2.377E-04	7.547E-04	3.175E+08
.7	3.800E-04	1.112E-03	2.979E+08
.6	5.442E-04	1.519E-03	2.774E+08
.5	7.384E-04	1.817E-03	2.555E+08
.4	9.761E-04	2.264E-03	2.320E+08
.3	1.263E-03	2.642E-03	2.040E+08
.2	1.715E-03	3.015E-03	1.761E+08
.1	2.450E-03	3.390E-03	1.500E+08

LONG-TERM TURBULENCE (SIGMAT) = 1.159E-06 RADIAN
 SHORT-TERM TURBULENCE (SIGST) = 8.633E-07 RADIAN
 RADIUS WITHOUT BLOOMING (R) = .010 METERS
 AVERAGE INTENSITY (I) = 1.7712E+08 WATTS/M**2
 PEAK INTENSITY (IP) = 4.0950E+08 WATTS/M**2

BREAKDOWN INTENSITY = 1.00E+12
 MAXIMUM INTENSITY ON TARGET = 2.56E+18
 ACHIEVED AT TELESCOPE POWER = 1.01E+09
 ACHIEVED AT TELESCOPE POWER = 2.74E+06

POWER RANGE AVAILABLE

TELESCOPE POWER (WATTS)	INTENSITY (WATTS/M**2)	USEFUL POWER (WATTS)	OVER AREA (M**2)
8.23E+04	3.426E+07	3.542E+07	1.139E-02
1.647E+05	6.383E+07	7.085E+07	1.307E-02
2.470E+05	8.602E+07	1.063E+08	1.469E-02
3.293E+05	1.063E+08	1.417E+08	1.652E-02
4.116E+05	1.194E+08	1.771E+08	1.853E-02
4.949E+05	1.311E+08	2.125E+08	2.051E-02
5.763E+05	1.454E+08	2.478E+08	2.175E-02
6.586E+05	1.573E+08	2.831E+08	2.307E-02
7.409E+05	1.687E+08	3.184E+08	2.450E-02
8.233E+05	1.771E+08	3.543E+08	2.605E-02
9.056E+05	1.834E+08	3.897E+08	2.777E-02
9.879E+05	1.874E+08	4.251E+08	2.967E-02
1.070E+06	1.936E+08	4.605E+08	3.126E-02
1.153E+06	1.998E+08	4.960E+08	3.270E-02
1.235E+06	2.062E+08	5.314E+08	3.405E-02
1.317E+06	2.128E+08	5.668E+08	3.534E-02
1.400E+06	2.194E+08	6.022E+08	3.662E-02
1.482E+06	2.259E+08	6.377E+08	3.791E-02
1.564E+06	2.290E+08	6.731E+08	3.922E-02
1.647E+06	2.335E+08	7.085E+08	4.055E-02

USEFUL INTENSITY = 1.000E+04WATTS/M**2

REFERENCES

1. P.R. Carlson, R.T. Liner, and L. Peckham, Propagation Modeling and Analysis for High Energy Lasers - First Interim Report, SAI-74-587-WA, Science Applications, Inc., October 1974.
2. R.T. Liner, P.R. Carlson, and L.N. Peckham, Propagation Modeling and Analysis for High Energy Lasers - Second Interim Report, SAI-74-622-WA, Science Applications, Inc., 31 January 1975.
3. E.A. Sziklas, et al. System Optical Quality Study, Phase I - Problem Definition, AFWL-TR-73-231, Air Force Weapons Laboratory, Kirtland AFB, New Mexico 87117, June 1974.
4. K.R. Vogelsang and S.H. Brewer, System Optical Quality Study, Phase I - Final Report, Report No. P73-401, Hughes Aircraft Company, Culver City, California, October 1973.
5. D.A. Holmes and P.V. Avizonis, "An Approximate Optical System Model," Laser Digest, Spring 1974, AFWL-TR-74-100, Air Force Weapons Laboratory, Kirtland Air Force Base, New Mexico, 1974.
6. C.B. Hogge, R.R. Butts, and M. Burlakoff, "Characteristics of Phase-Aberrated Nondiffraction-Limited Laser Beams," Appl. Optics, Vol. 13, No. 5, p. 1065, May 1974.
7. B.D. O'Neil, Laser Digest, Fall 1974, p.54, AFWL-TR-74-344, Air Force Weapons Laboratory, Kirtland Air Force Base, N.M. 87117.
8. B. Skehan, et al., NPT/Chemical Laser Compatibility Study (U), Report No. P74-29, Hughes Aircraft Company, Culver City, California, January 1974 (Confidential).
9. SAI Memorandum, "Cooled/Uncooled Mirrors in the NPT," R.E. Hodder and R.A. Greenberg to J. Bachkosky, 4 June 1974.
10. A.E. Siegman, An Introduction to Lasers and Masers, McGraw-Hill Book Company, 1971.

11. L.N. Peckham and R.W. David, A Simplified Propagation Model for Laser System Studies, AFWL-TR-72-95, Revised, Air Force Weapons Laboratory, Kirtland AFB, New Mexico, April 1973.
12. L.N. Peckham and R.W. Davis, High Power Gas Laser Technology Forecast (U), AFWL-TR-72-154, Air Force Weapons Laboratory, Kirtland AFB, New Mexico, November 1972 (SECRET).
13. F.G. Gebhardt, and D.C. Smith, Investigation of Self-Induced Thermal Effects of CO₂ Laser Radiation Propagation in Absorbing Gases, United Aircraft Research Laboratories, Report L-921004-8, April 1972.
14. R.W. Davis, et al., "Comparative Analysis of HEL Simplified Propagation Codes (U)," First DOD Conference on High Energy Laser Technology, San Diego, California, October 1974. (This paper is included as an appendix in Reference 1) (SECRET)
15. L.N. Peckham, Laser Analysis Codes Review and Recommendations for the Naval Ordnance Laboratory, SAI-74-5.1-WA, January 1974.
16. H.T. Yura, "Short-Term Average Optical-Beam Spread in a Turbulent Medium," J. Opt. Soc. Am., 63, No. 5 pp. 567-572, May 1973.
17. D.L. Fried, "Limiting Resolution Looking Down through the Atmosphere," J. Opt. Soc. Am., Vol 56, No. 10, pp.1360-1389, October 1966.
18. W.P. Brown and J.E. Pearson, "Multidither Coat Compensation for Thermal Blooming and Turbulence," First DOD Conference on High Energy Laser Technology, San Diego, California, October 1974.
19. R.W. Davis and L.N. Peckham, A Simplified Propagation Model for Laser System Studies, Supplement, AFWL-TR-72-95 Supplement, Air Force Weapons Laboratory, Kirtland AFB, New Mexico, November 1974.
20. F.G. Gebhardt, and D.C. Smith, Investigation of Self-Induced Thermal Effects of CO₂ Laser Radiation Propagation in Absorbing Gases, United Aircraft Research Laboratories, Report K-921004-4, April 1971.

- A-1. R. A. McClatchey and J. E. A. Selby, Atmospheric Attenuation of HF and DF Laser Radiation, AFCRL-72-0312, 23 May 1972.
- A-2. D. E. Burch, D. A. Gryvnak and J. D. Pembroke, Investigation of the Absorption of Infrared Radiation by Atmospheric Gases: Water, Nitrogen, Nitros Oxide, AFCRL-71-0124, January 1971.
- A-3. S. L. Valley (ed.), Handbook of Geophysics and Space Environments, AFCRL, 1965.
- A-4. R. E. Meridith, T. W. Tuer and D. R. Woods, Investigation of DF Laser Propagation, SAI-74-001-AA, Science Applications, Inc., Ann Arbor, July 1974.